Characterization of the molecular causes of neurodegeneration in a *Drosophila* model of Ataxia-telangiectasia

by

Andrew J. Petersen

A dissertation submitted in partial fulfillment of

the requirements for the degree of

Doctor of Philosophy

(Molecular and Cellular Pharmacology)

at the

UNIVERSITY OF WISCONSIN-MADISON

2012

Date of final oral examination: 12/04/12

The dissertation is approved by the following members of the Final Oral Committee:

Dr. David A. Wassarman, Professor, Cell and Regenerative Biology
Dr. Shigeki Miyamoto, Professor, Oncology
Dr. Barry Ganetzky, Professor, Genetics
Dr. Randy S. Tibbetts, Assistant Professor, Human Oncology
Dr. Grace Boekhoff-Falk, Assistant Professor, Cell and Regenerative Biology

Acknowledgements

First and foremost, I need to thank my mentor, David Wassarman. He has provided a great example for how to conduct science in a thorough manner, and his enthusiasm towards my research has made it enjoyable coming in to work. Additionally, he has been open to learning new ideas and entire fields of study that were previously foreign to both of us and never worried about jumping head-first into a set of experiments without much precedence in the literature. And ultimately, everything worked out great!

I also need to thank the other members of the Wassarman lab for providing a great work environment. Specifically, thanks are due to Becky Katzenberger and Stacey Rimkus for their help and assistance directly on my project, as well as Matt Marengo, Ashley Anderson, and Nicole Haugen for help with statistical questions and for making lab a fun place to work. I also need to thank the various summer students and undergraduates who have passed through the lab for their questions about the basic aspects of experiments and procedures that forced me to learn that information myself. Finally, I need to thank the "grunts" of the lab, whose efforts in cleaning, fly food making, and pipette tip stuffing made my life much easier!

Next, I want to thank the faculty, staff, and students of the Molecular and Cellular Pharmacology program. Their input and critiques at seminar, as well as general enthusiasm about science, has aided my progress throughout graduate school and for that I am very grateful. I also need to thank my committee members (Barry Ganetzky, Randy Tibbetts, Grace Boekhoff-Falk, and Shigeki Miyamoto) for keeping me on course throughout graduate school and providing great experiments to supplement my planned experiments. The members of the UW *Drosophila* community deserve recognition as well. Flies are being used for very diverse, impactful science throughout campus, and this is an inspiration that further solidifies the

relevance of *Drosophila* in the scientific future. Specifically within this group I need to thank Barry Ganetzky for allowing me to attend his lab meeting, where I have learned a lot about the fly nervous system, and for collaborating with me on the study of the innate immune response in glial cells. His expertise and knowledge in the field is a great resource that he has allowed me to utilize. Ben August, Toshi Kinoshita, and the great people at the UW Biotech Center provided support and assistance throughout my research and their abilities in their respective fields is astounding, so thank you all!

Finally, I need to thank my friends and family for their support throughout graduate school. Primarily this means my wife and best friend, Julie, as well as my new daughter Avery. They provide a comfortable home for me to go to every night where I can forget about the failed experiments and the looming deadlines and just focus on the great aspects of my life. My parents and family have been a great support throughout my years of schooling, and their general science questions have allowed me to share my knowledge and expertise. And last but not least, I need to thank my friends. Some of my friends are scientists as well, and they have been able to relate to the struggles and joys that graduate school brings. Other friends have no interest in science whatsoever, allowing me to escape work for a few hours while providing laughs and relaxation.

Table of Contents

List of Illustrations

Chapter 1

Chapter 2

Chapter 3

Appendix 1

Appendix 2

Appendix 3

Characterization of the molecular causes of neurodegeneration in a *Drosophila* model of Ataxia-telangiectasia

Andrew J. Petersen

Under the supervision of Professor David A. Wassarman

At the University of Wisconsin-Madison

Ataxia-telangiectasia (A-T) is a multifaceted disorder caused by mutations in the *ataxia-telangiectasia mutated* (*ATM*) gene. *ATM* encodes a serine-threonine protein kinase that functions in the DNA damage response. ATM is recruited to sites of DNA damage, where it is activated and phosphorylates numerous proteins that promote DNA repair, cell cycle checkpoints, and apoptosis. Common characteristics of A-T include susceptibility to leukemia and lymphoma, radiosensitivity, immunodeficiency, and progressive neurodegeneration. Neurodegeneration primarily affects the Purkinje and granule neurons in the cerebellum, causing loss of coordinated movements (ataxia) in A-T patients.

Animal models have been used to study effects of ATM loss on neurodegeneration. Mouse models of A-T have provided insight into cancer and immunodeficiency in A-T but do not exhibit overt neurodegeneration. The prevailing belief is that the mice succumb to other phenotypes prior to development of detectable neuronal loss. However, previous work in our lab revealed that loss of ATM function in the *Drosophila* compound eye causes photoreceptor neurodegeneration, providing a model system for studying neurodegeneration in this disease (Rimkus *et al*. 2008). Using an endogenous loss-of-function allele of *ATM*, I discovered that ubiquitous loss of ATM causes neurodegeneration in the *Drosophila* brain. Furthermore, specific reduction of *ATM* levels via RNA interference in glial cells, but not neurons,

recapitulates these neurodegenerative phenotypes. Thus, loss of ATM function in glial cells may cause the neurodegeneration observed in A-T.

Gene expression analysis revealed upregulation of an innate immune response in glial cells of ATM-deficient flies. Genetic manipulations showed that this response occurs via the NF-κB protein Relish, a central factor in the innate immune response in both *Drosophila* and mammalian systems. Blocking activation of the innate immune response was sufficient to block neurodegeneration, and aberrant activation of the innate immune response was sufficient to cause neurodegeneration. Other *Drosophila* models of neurodegeneration, as well as human diseases themselves, exhibit activation of the innate immune response, suggesting that this is a common mechanism in neurodegeneration (González-Scarano and Baltuch 1999; Greene *et al*. 2005; Chinchore *et al*. 2012). Thus, *Drosophila* provides a tool for studying a phenomenon that underlies neurodegeneration in multiple human diseases, including A-T.

Chapter 1

Background information

Part of this work was published in:

Petersen AJ and Wassarman DA. (2012) *Drosophila* innate immune response pathways moonlight in neurodegeneration. *Fly* 6: 169-172.

A.J.P. wrote the text (Section 1.3) and designed the figure (Figure 1.5). D.A.W. provided revisions.

1.1 Mutations in the ATM kinase result in the disease Ataxia-telangiectasia

The disease Ataxia-telangiectasia (A-T) is an autosomal recessive disease that was first described in 1926 and clinically defined in 1957 (Syllaba and Henner 1926; Boder and Sedgwick 1957). In 1988, the gene responsible for A-T was localized to chromosomal locus 11q22-23 in humans and ultimately characterized as *ataxia-telangiectasia mutated* (*ATM*) in 1995 (Gatti *et al*. 1988; Savitsky *et al*. 1995). This gene encodes the serine-threonine protein kinase ATM, a member of the phosphoinositide-3 kinase (PI3K)-related kinase (PIKK) family whose structure and function is described later.

A-T is generally caused by truncation mutants in *ATM* resulting in complete loss of the ATM protein. As such, these mutations do not target specific regions of the *ATM* gene (Gilad *et al*. 1996; McConville *et al*. 1996; Telatar *et al*. 1998; Lavin *et al*. 2007). Some A-T patients harbor missense mutations that do not affect ATM levels but severely reduce ATM function (McConville *et al*. 1996). Furthermore, analysis of A-T patients with no detectable ATM protein reveals a wide range of disease severity (Hassin-Baer *et al*. 1999; Lavin *et al*. 2006; Alterman *et al*. 2007). These findings suggest that secondary genetic differences may alter disease presentation, making the identification of these factors important for treating A-T.

A-T affects numerous tissues and organs

A-T presents with numerous manifestations including ocular telangiectasias (excessively dilated blood vessels in the eyes and face), cancer susceptibility, radiosensitivity, immunodeficiency, progressive neurodegeneration, and others.

A-T patients are susceptible to various types of cancers, most notably leukemia and lymphoma (Gumy-Pause *et al*. 2004; Lavin *et al*. 2007). Furthermore, simply carrying one copy of a null *ATM* allele increases susceptibility to breast cancer (Chen *et al*. 1978; Ahmed and

Rahman 2006). Cancer development in A-T occurs due to the inability of a cell to repair damaged DNA, allowing mutations in oncogenes to accumulate, and defects in cell cycle checkpoint control. Additional aspects of A-T pathogenesis are related to impaired DNA damage response mechanisms, including radiosensitivity and immunodeficiency. In the case of radiosensitivity, DNA damage from radiation sources is unable to be repaired, causing cellular damage and death. Immunodeficiency in A-T arises due to the inability of the body to properly form B- and T-cell populations. The maturation of these cell types is dependent on V(D)J recombination of immunoglobulin and B/T-cell receptor genes. Since this process generates double-strand breaks that are repaired in an ATM-dependent manner, loss of ATM produces dysfunctional B- and T-cells, thereby inhibiting proper immune function.

The major clinical manifestation of A-T is progressive ataxia due to degeneration of Purkinje and granule neurons within the cerebellum (Boder 1985; McKinnon 2004). Other neuronal populations are likely also susceptible to loss of ATM. The primary outcome of cerebellar degeneration is loss of motor function in A-T patients, who become wheelchair bound early in life. As the disease progresses, this degeneration results in difficulties during chewing and swallowing which facilitates pulmonary disorders, a common cause of death in A-T (Lefton-Greif *et al*. 2000; Nowak-Wegrzyn *et al*. 2004). While other hallmarks of A-T can be directly linked to defective DNA damage repair mechanisms, its role in neurodegeneration is unclear. Defects in cell cycle checkpoint maintenance in ATM deficient neurons can facilitate cell cycle reentry, a mechanism known to be fatal in post-mitotic neurons (al-Ubaidi *et al*. 1992; Feddersen *et al*. 1992; Herrup and Busser 1995; Kranenburg *et al*. 1996; Yang and Herrup 2005). However, other mechanisms may promote neurodegeneration as well. A fraction of ATM protein is observed in the cytoplasm, rather than in the nucleus where ATM is required for the

DNA damage response (Oka and Takashima 1998; Kuljis *et al*. 1999; Barlow *et al*. 2000). This suggests an unknown, alternative role for ATM, the loss of which may play a role in neurodegeneration. An intriguing possibility is that cytoplasmic ATM regulates NF-κB activation, a feature of ATM during the DNA damage response which is also implicated in neurodegeneration (Chapter 3; Miyamoto 2011).

The DNA damage response functions through the ATM kinase

ATM belongs to the PIKK class of kinases that are primarily serine/threonine protein kinases. Members of this class contain a conserved C-terminal PI3K kinase domain and variable N-terminal sequences (Abraham 2004). Flanking the PI3K kinase domain are two loosely conserved domains termed FAT domains for their conservation in the FRAP, ATM, and TRAPP kinases (Bosotti *et al*. 2000). Four PIKK members function within the DNA damage response: ATM, ATR (Ataxia-Telangiectasia and Rad3-related kinase), ATX/SMG1, and DNA-PKcs (DNA-dependent Protein Kinase catalytic subunit) (Shiloh 2003). Within the DNA damage response, however, the function of these kinases vary. For example, ATM monitors the genome for double strand breaks (DSBs), whereas ATR primarily responds to ultraviolet radiation-induced DNA damage and stalled replication forks (Abraham 2001).

When DSBs occur in a cell, a cascade of events is triggered to repair the lesion (Figure 1.1). The Mre11-Rad50-NBS1 (MRN) complex is recruited to the site of the damage and becomes tethered to the DNA via Rad50 (Jackson 2002; Carson *et al*. 2003; Lee and Paull 2004; Lee and Paull 2005). Underscoring the necessity of the MRN complex in DNA damage repair are the diseases Nijmegen breakage syndrome (NBS) and A-T-like disease (ATLD). Caused by mutations in NBS1 and Mre11, respectively, these diseases exhibit many of the clinical manifestations of A-T including immunodeficiency, radiosensitivity, and genomic instability

(Stewart *et al*. 1999; Tauchi *et al*. 2002; Shiloh 2003). Once the MRN complex reaches the DSB, NBS1 binds ATM and facilitates its activation from an inactive dimer to active monomers, a process dependent on ATM autophosphorylation at S1981 in humans (Bakkenist and Kastan 2003; van der Bosch *et al*. 2003; Falck *et al*. 2005; Lee and Paull 2005; You *et al*. 2005; Dupre *et al*. 2006). Active ATM can phosphorylate hundreds of protein substrates that facilitate DNA repair mechanisms, initiate cell cycle checkpoints, and cause apoptosis including the histone variant H2AX, the cell cycle regulators CHK1 and CHK2, and the tumor suppressor p53 (Banin *et al*. 1998; Canman *et al*. 1998; Rogakou *et al*. 1998; Chebab *et al*. 1999; Matsuoka *et al*. 2000; Matsuoka *et al*. 2007). These ATM-dependent responses function in concert to prevent cellular replication that would pass genomic instability on to daughter cells, giving the cells time to repair the damage. If the damage is deemed irreparable, apoptosis is induced and the cell is eliminated.

Model systems have been used to study the molecular causes of A-T phenotypes

Due to the conservation of ATM between species, many aspects of A-T have been studied using model organisms. The DNA damage response and specific functions of ATM are conserved in both mouse (*Mus musculus*) and fly (*Drosophila melanogaster*) models. Thus, these models can be used to determine not only the role of ATM in normal conditions but also how ATM loss produces the phenotypes in A-T.

ATM deficiency in mice has been studied using two basic strategies. *ATM* knock-out mice were generated either by homologous recombination or by introducing a premature stop codon via gene targeting, thus generating mice lacking any ATM protein (Barlow *et al*. 1996; Xu *et al*. 1996). Additionally, kinase-dead ATM mice ($ATM^{\Delta SRI/\Delta SRI}$) were generated that contain full-length ATM protein but lack kinase function (Spring *et al*. 2001). Cumulatively, these mice

show many phenotypes similar to those observed in A-T patients, including defects in T-cell development, radiosensitivity, and susceptibility to lymphomas (Barlow *et al*. 1996; Elson *et al*. 1996; Xu *et al*. 1996; Spring *et al*. 2001). Recent studies looking at ATM kinase-dead mice suggest that loss of ATM kinase function, but not ATM protein, causes phenotypes more severe than complete loss of protein levels. In these studies, flies expressing kinase-dead ATM exhibited increased genomic instability when compared to *ATM* null mice, and when homozygous, *ATM* kinase-dead alleles were embryonic lethal (Daniel *et al*. 2012; Yamamoto *et al*. 2012). This suggests that inactive ATM may prevent another PIKK family member like DNA-PKcs or ATR from assuming some of the repair capacity of ATM.

ATM function can be studied in *Drosophila* since ATM and other components of the DNA damage response are conserved in flies (Brodsky *et al*. 2000; Ollmann *et al*. 2000; Brodsky *et al*. 2004; Song *et al*. 2004) Initial reports in *Drosophila* mischaracterized ATM as a product of the *mei-41* gene, but later analysis revealed that *mei-41* encodes the ATR homolog and the *tefu* gene (*CG6535*) encodes the true ATM homolog (Hari *et al*. 1995; Sekelsky *et al*. 2000; Song *et al*. 2004). In flies, ATM interacts with the MRN complex in the DNA damage response and phosphorylates the *Drosophila* homologs of H2AX (H2Av), CHK2, and p53, thus facilitating DNA repair, cell cycle checkpoint initiation, and apoptosis via mechanisms analogous to those in mammalian systems (Xu *et al*. 2001; Brodsky *et al*. 2004; Song *et al*. 2004; Bi *et al*. 2005; Joyce *et al*. 2011). Furthermore, ATM has been shown to regulate telomere dynamics in both mammalian and *Drosophila* systems (Pandita *et al*. 1995; Metcalfe *et al*. 1996; Pandita 2002; Oikemus *et al*. 2004; Silva *et al*. 2004).

One unique feature of ATM function in *Drosophila* is that loss of ATM function is developmentally lethal in the fly, whereas *ATM* null mice and humans are still viable. *ATM* null

flies fail to develop past the pupal stage of the *Drosophila* life cycle. Flies lack a homolog of the PIKK kinase DNA-PKcs, which in mammalian systems shows some functional redundancy with ATM (Song *et al*. 2004). It has been hypothesized that this lack of a redundant counterpart in *Drosophila* is what causes loss of ATM to be lethal. Despite this limitation, mechanisms have been generated to study loss of ATM in the fly and will be discussed in detail later.

1.2 *Drosophila* provides a suitable system for studying neurodegeneration in A-T

Despite the ability of A-T mouse models to recapitulate numerous aspects of A-T, their utility in studying neurodegeneration is limited. ATM deficient mice do not exhibit gross neurodegeneration or ataxia similar to that seen in humans. One potential explanation for the lack of overt neurodegeneration is that ATM deficient mice succumb to other disease-related phenotypes like cancer prior to the development of a neurological phenotype, although this hypothesis has not been directly tested. ATM deficient mice do show deficits in motor function, aberrant neuropil morphology, and improper neural progenitor cell differentiation *in vivo* and Purkinje cell branching *in vitro*, indicating that neurological issues do exist (Barlow *et al*. 1996; Kuljis *et al*. 1997; Allen *et al*. 2001; Chen *et al*. 2003). *Drosophila*, on the other hand, represents a suitable model system in which to study the effects of ATM loss on neuronal viability.

The *Drosophila* nervous system faithfully recapitulates most characteristics of mammalian nervous systems

The majority of non-mammalian model organism research for nervous system disorders occurs in *Drosophila* due to the similarities between *Drosophila* and mammalian nervous systems. The fly brain is estimated to have in excess of 300,000 neurons and is organized into complex regions with specific functions (Cauchi and van den Heuvel 2006). When compared to

the estimated $8.5x10^{10}$ neurons in humans, this number seems entirely inadequate; however, contrast this with another invertebrate model organism, the flatworm *Caenorhabditis elegans* which contains only 302 neurons, and *Drosophila* now appears to be much better suited (White *et al*. 1986; Herculano-Houzel 2009). Furthermore, recent work has identified that glial cell populations in *Drosophila* mimic the functions of mammalian glia despite differences in neuron:glia ratios, and trophic interactions between neurons and glial cells appear to be conserved (Doherty *et al*. 2009; Hidalgo *et al*. 2011; Stork *et al*. 2012). Not only is the *Drosophila* nervous system relatively comparable in complexity to mammalian systems, but a high proportion (around 75%) of human disease genes and their functions are conserved in flies (Reiter *et al*. 2001; Pandey and Nichols 2011). These findings suggest that general nervous system function in *Drosophila* can be used to identify specific events that promote neurodegeneration in mammalian systems.

***Drosophila* has been used to model numerous human neurodegenerative diseases**

Based on the rationale described above, numerous groups have used *Drosophila* to study human neurodegenerative diseases. The majority of these models utilize the binary GAL4/UAS expression system modified from yeast to regulate the temporal and spatial expression of human disease genes (Brand and Perrimon 1993). This system utilizes two rounds of P-element transformation to modify the genome of the fly. One transgene contains the coding sequence for the GAL4 transcription factor under the control of a tissue- or cell-type-specific promoter (Rubin and Spradling 1982). A second transgene contains the GAL4 upstream activation sequence (UAS) regulating the expression of a human disease gene. Mating flies with these two transgenes generates progeny that express the human disease protein in a tissue or cell of interest, usually neurons, glial cells, or the cells of the *Drosophila* compound eye (Figure 1.2A). This

method has been used to study Alzheimer's disease (via tau, β-amyloid, Presenilin, or APP overexpression), Parkinson's disease (α-synuclein), Huntington's disease (Huntingtin), and multiple spinocerebellar ataxia diseases (SCA1, SCA2, SCA3, or SCA8) among others (Jackson *et al*. 1998; Warrick *et al*. 1998; Fernandez-Funez *et al*. 2000; Wittmann *et al*. 2001; Auluck *et al*. 2002; Satterfield *et al*. 2002; Finelli *et al*. 2004; Greeve *et al*. 2004; Mutsuddi *et al*. 2004; Celotto and Palladino 2005). Whereas these models utilize misexpression of human genes, endogenous mutation of conserved neurodegenerative disease proteins in the fly can also recapitulate aspects of the human disease. For example, mutation of *parkin* or *Pink1* in the fly, two genes implicated in Parkinson's disease, cause dopaminergic neuron dysfunction and mitochondrial defects analogous to those seen in humans (Greene *et al*. 2003; Greene *et al*. 2005; Yang *et al*. 2006). Similar to this approach, *Drosophila* models of A-T capitalize on the conservation of ATM between flies and humans by studying the loss of endogenous ATM function in the fly.

ATM deficiency in *Drosophila* can be studied using multiple model systems

To study the molecular causes of neurodegeneration in A-T using *Drosophila*, our lab utilizes loss of endogenous ATM function. Three primary methods have been used to accomplish this result: endogenous alleles including a temperature-sensitive allele, RNAi knockdown, and mitotic clones. Loss-of-function alleles of *ATM* have provided insight into effects of ATM loss throughout development but are limited in the adult due to pupal lethality. Developmental effects of ATM loss include improper apoptosis, telomere fusions, chromosomal stability defects, and aberrant sensory structure development (Oikemus *et al*. 2004; Silva *et al*. 2004; Song *et al*. 2004). During the development of *ATM* alleles in the lab of Dr. Shelagh Campbell at the University of Alberta, the serendipitous discovery of a temperature-sensitive

allele of *ATM*, ATM^{8}, changed the future of ATM work in the fly (Pedersen *et al*. 2010). Flies carrying this allele are homozygous viable to the adult stage and retain some ATM kinase function if raised at 18°C, but lose ATM kinase function if cultured at 25°C (Petersen *et al*. 2012). These flies provide a system to study loss of ATM ubiquitously in the adult fly that was used extensively in the experiments for Chapters 2 and 3.

The second system for studying ATM loss in the fly was generated by Dr. Stacey Rimkus in our lab and utilizes the GAL4/UAS system previously described. Instead of using this system to express a human disease gene, however, we use it to express a short hairpin RNA (shRNA) targeting the *ATM* mRNA for degradation via RNAi (Figure 1.2B). A 642 basepair fragment from exon 6 of the *ATM* gene was inserted downstream of a UAS site in the *pWIZ* RNAi vector, resulting in the generation of a double-stranded hairpin structure that is processed by the RNAi machinery and produces a reduction in ATM mRNA levels (Lee and Carthew 2003; Rimkus *et al*. 2008). Transgenic flies were generated and it was discovered that knockdown of ATM in the *Drosophila* eye via the *glass multimer reporter* (*GMR*)-*GAL4* driver or the pan-neuronal driver *embryonic lethal, abnormal vision (Elav)*-*GAL4* was sufficient to cause cell cycle reentry in and neurodegeneration of photoreceptor neurons (Rimkus *et al*. 2008; Rimkus *et al*. 2010). Loss of ATM in mammalian neurons similarly causes cell cycle reentry, providing evidence that neuronal loss of ATM produces similar phenotypes in flies and mammals (Herrup and Busser 1995; Yang and Herrup 2005). I have utilized this UAS-RNAi line to study effects of ATM knockdown in all neurons of the fly via the *Elav*-*GAL4* driver (Chapters 2 and 4), in all glial cells of the fly via the *reversed polarity* (*Repo*)-*GAL4* driver (Chapters 2, 3, and 4), or in the cells of the compound eye via the *GMR*-*GAL4* driver (Appendix 3).

The third system for analyzing loss of ATM in *Drosophila* uses mitotic recombination via the FLP/FRT system (Xu and Rubin 1993). Similar to GAL4/UAS, this system utilizes two transgenes to accomplish its effect. This method is described in detail in Figure 1.3. Using this system and a null allele of *ATM* (*ATM*^{6}), I generated ATM-deficient clones in the *Drosophila* eye disc, a larval precursor tissue of the compound eye. These clones exhibited cell cycle reentry in ATM deficient cells, validating the results of *ATM* knockdown in photoreceptors (Chapter 4; Appendix 2; Rimkus *et al*. 2008). Analysis of *ATM* null clones in the brain of the fly would provide another system for studying effects of ATM loss on neuronal survival. Combined, these systems provide a suitable range of methods to characterize the effects of ATM loss on neuronal survival.

1.3 Activation of the innate immune response in glial cells promotes neurodegeneration in multiple diseases

The research included in the following chapters indicates that, in addition to combating infection, innate immune response activation in glial cells promotes neurodegeneration. Chapter 2 reveals a correlative relationship between the innate immune response and neurodegeneration in *Drosophila* models of A-T (Petersen *et al*. 2012). Subsequent work in these models identified innate immune activation as causative for neurodegeneration (Chapter 3). Publications by Tan *et al.* (2008) and Chinchore *et al.* (2012) support this causative role for the innate immune response in *Drosophila* models of Alzheimer's disease and human retinal degenerative disorders, respectively. Finally, we show that glial cells are responsible for producing the innate immune response in the A-T models, and work by others in *Drosophila* also implicates glial cells in neurodegeneration (Buchanan and Benzer 1993; Kretzschmar *et al*. 1997; Kretzschmar *et al*.

2004; Tamura *et al*. 2007; Petersen *et al*. 2012). Similar observations have been made in human neurodegenerative diseases, although it is difficult to determine if innate immune response activation is causative in these disorders. Collectively, these findings suggest that activation of the innate immune response in glial cells is a common feature, and a possible cause, of neurodegeneration in multiple human diseases.

The innate immune response is a conserved mechanism between *Drosophila* and humans

Multicellular organisms contain an innate immune response whose function is to provide an initial, protective response to infectious pathogens. Simple organisms such as *Drosophila* rely exclusively on an innate immune response for protection from pathogens, and the signaling mechanisms underlying this response is evolutionarily conserved in mammals. Vertebrates, on the other hand, exhibit both an innate immune response and an adaptive immune response to combat pathogens. In the adaptive response, challenge by a particular pathogen produces a long-term response that will quickly combat that pathogen in the future. In the innate immune response, however, no previous exposure to a pathogen is necessary and the response is not tailored to a specific pathogen.

Two primary signaling pathways are responsible for initiating the innate immune response in *Drosophila*. These pathways are typically referred to based on the upstream inclusion of the Toll receptor or immune deficiency (Imd) protein (Figure 1.4). The Toll pathway is responsive to eukaryotic pathogens (yeast and fungi) and gram-positive bacteria. Recognition of pathogens by extracellular peptidoglycan recognition proteins (PGRPs) or Gram-negative binding proteins (GNBPs) stimulates the proteolytic cleavage of the cytokine Spätzle by SPE (Spätzle Processing Enzyme), allowing Spätzle to bind and multimerize the Toll receptor (Weber *et al*. 2003; Hu *et al*. 2004). Multimerized Toll binds to dMyD88 and Tube, which in

turn activate Pelle (Sun *et al*. 2002; Tauszig-Delamasure *et al*. 2002). Pelle is a kinase whose activation facilitates phosphorylation of the Inhibitor of κB (IκB) protein Cactus and stimulates its proteasomal-dependent degradation (Belvin *et al*. 1995; Fernandez *et al*. 2001). This allows translocation of the Rel-type Nuclear Factor κB (NF-κB) transcription factors Dif and Dorsal to the nucleus where they activate innate immunity gene transcription, notably the transcription of antimicrobial peptides (AMPs) which directly combat pathogens (Ip *et al*. 1993; DeGregorio *et al*. 2001; Irving *et al*. 2001; DeGregorio *et al*. 2002; Imler and Bulet 2005).

The Imd-dependent innate immune response pathway primarily responds to gram-negative bacteria. In this pathway, the transmembrane class of PGRP proteins, most notably PGRP-LC, recognizes pathogens and signals through Imd (Georgel *et al*. 2001; Kaneko *et al*. 2006). Imd uses dFADD and TAK1 to activate the IκB Kinase (IKK) complex, consisting of Kenny and Ird5, which phosphorylates Relish (Rel) (Rutschmann *et al*. 2000b; Silverman *et al*. 2000; Lu *et al*. 2001; Silverman *et al*. 2003). Rel is a homolog of mammalian p105-like NF-κB proteins that have an N-terminal NF-κB domain and a C-terminal IκB-like inhibitory domain. Rel phosphorylation directs its proteolytic cleavage by the caspase Dredd, releasing the NF-κB domain from its inhibitor and allowing it to translocate to the nucleus where it activates transcription of innate immunity genes, including AMPs (Leulier *et al*. 2000; Stöven *et al*. 2000; Stöven *et al*. 2003).

All of the identified signaling components of the Toll and Imd pathways are conserved across species, including in other *Drosophila* species and in humans (Lemaitre and Hoffmann 2007; Sackton *et al*. 2007). In the case of humans, however, differences exist in the activation and downstream output of each pathway. In mammalian systems, the homologous pathway to the Toll pathway in *Drosophila* utilizes homologous receptors called Toll-like receptors (TLRs).

However, in mammals TLRs bind directly to pathogenic material like peptidoglycan to become activated, rather than binding an endogenous cytokine (Lemaitre and Hoffmann 2007; Owens 2009). The Imd pathway is conserved in mammals as the tumor necrosis factor (TNF) signaling pathway. In this case, the *Drosophila* pathway responds to pathogenic material whereas the mammalian system responds to an endogenous molecule (TNFα) (Cabal-Hierro and Lazo 2012). For the downstream output, the *Drosophila* innate immune response relies primarily on antimicrobial peptides (AMPs) to combat pathogens. While the mammalian innate immune response also produces AMP molecules, the major output of the response is derived from cytokine production and is comprised of inflammation and phagocytosis of the pathogen (Imler and Bulet 2005; Lehnardt 2010).

Multiple *Drosophila* models of neurodegeneration exhibit innate immune response activation

My recent work identified that loss of ATM function causes an innate immune response in glial cells (Chapter 2). Further analysis revealed that this process is dependent on Rel and potentially its upstream signaling component Imd, but not Dif (Chapter 3). Finally, loss of innate immunity signaling via mutations in Rel suppress the neurodegeneration observed in ATM deficient flies, indicating that glial cell activation of the innate immune response is necessary to cause neurodegeneration (Figure 1.5A).

In addition to our A-T model flies, upregulation of innate immunity gene expression is a feature of other *Drosophila* neurodegenerative disease models (Petersen and Wassarman 2012). AMP gene expression is upregulated in models of Parkinson's disease, CAG-repeat RNA-based neurodegeneration, and retinal degeneration (Greene *et al*. 2005; Shieh and Bonini 2011; Chinchore *et al*. 2012). Thus, a diverse array of triggers of neurodegeneration, including loss of

ATM function, *parkin* mutation, CAG-repeat mRNA misexpression, and *norpA* mutation combined with light, result in activation of the innate immune response. The necessity of the innate immune response for the neurodegeneration found in many of these models was not tested, but evidence from two reports supports a causative role for the innate immune response in neurodegeneration.

Chinchore *et al.* (2012) determined that activation of the NF-κB factor Rel is required for neurodegeneration in a *Drosophila* model of human retinal disorders (Figure 1.5B). This model involves light-induced neurodegeneration of photoreceptor neurons in the eye of *norpA* mutant flies. Neurodegeneration is thought to result from excessive light-dependent endocytosis of rhodopsin, a light sensing protein. The authors found that *rel* mutations almost completely block light-induced photoreceptor degeneration in *norpA* flies. They also found that mutations in *kenny* and *dredd*, genes required for Rel activation, almost completely block photoreceptor degeneration. However, mutations in *imd* and *dFadd*, which function upstream of Dredd activation, have no effect on photoreceptor degeneration. Thus, it appears that in this model a non-canonical innate immune response signal activates Dredd to bring about photoreceptor degeneration.

Tan *et al.* (2008) found that activation of the NF-κB factors Dif and Dorsal (Dl) is required for neurodegeneration in a *Drosophila* model of Alzheimer's disease (Figure 1.5C). This model involves misexpression of Aβ42, a protein associated with the onset of Alzheimer's that accumulates in large aggregates in the brains of Alzheimer's patients. Misexpression of Aβ42 in the eye causes an external rough eye phenotype, the severity of which is likely to report the extent of internal photoreceptor degeneration. In a screen for modifiers of the rough eye phenotype, the authors identified a suppressor deficiency that included the *toll* gene. By

systematically working through mutants of *toll* signaling pathway genes, they determined that *toll*, *pelle*, *tube*, *cactus*, *dif*, and *Dl* mutants also suppress the rough eye phenotype (Figure 1.5C).

These reports support the idea that innate immune response activation functions in causing neurodegeneration. Furthermore, these reports indicate that both the Toll and Imd innate immune response pathways are required in different contexts to promote neurodegeneration. In A-T model flies, activation of the innate immune response is necessary in glial cells to produce neurodegeneration. However, involvement of glial cells in the other models was not characterized. Existing reports in flies indicate that dysfunction of glial cells is sufficient to cause neurodegeneration in multiple contexts. The neurodegenerative mutants *swiss cheese* and *drop-dead* have defective glial cell morphology that may contribute to the observed pathology (Buchanan and Benzer 1993; Kretzschmar *et al*. 1997). Also, overexpression of polyglutamine tracts or the disease-causing polyglutamine proteins Ataxin-1 or Huntingtin exclusively in glial cells induced neurodegeneration (Kretzschmar *et al*. 2004; Tamura *et al*. 2009). However, it remains to be determined in these glial cell systems if the innate immune response is activated and functions in producing the neurodegenerative phenotypes. To date, ATM deficient flies are the only model linking both glial cell dysfunction and the innate immune response during neurodegeneration in *Drosophila*.

Activated glial cells produce an innate immune response in numerous neurodegenerative diseases

Within the human CNS, the primary innate immune response cells are microglia and astrocytes. Microglia are a unique subset of glial cells derived from the myeloid lineage that leave the bone marrow and enter the CNS prior to blood-brain barrier formation during embryonic development (Lucin and Wyss-Coray 2009). Microglia express a majority of the cell

surface receptors responsible for the innate immune response, including all of the TLRs (Owens 2009; Ransohoff and Brown 2012). Astrocytes, a type of glial cell derived from neuroepithelial tissue, express a smaller subset of the innate immune response receptors including TLRs (Owens 2009). TLR activation signals through NF-κB proteins using mechanisms homologous to that of the *Drosophila* Toll pathway to produce pro-peptides of pro-inflammatory interleukin 1 (IL-1) family members such as IL-1β (Ransohoff and Brown 2012). These pro-peptides are sequestered in the cytoplasm until a second class of innate immune receptors, the nucleotide-binding domain leucine-rich repeat-containing receptors (NLRs), stimulates caspase-1 activation. Caspase-1 cleaves the pro-IL-1 peptides and allows their secretion via a mechanism using large protein complexes termed inflammasomes (Martinon and Tschopp 2004; Stutz *et al*. 2009; Chakraborty *et al*. 2010). IL-1 secretion produces an inflammatory environment and induces subsequent rounds of inflammatory cytokine cascades initiated by both microglia and astrocytes in the vicinity of release (Halle *et al*. 2008; Salminen *et al*. 2008; Salminen *et al*. 2009; Chakraborty *et al*. 2010). One of these inflammatory cytokines is TNFα which stimulates a signaling pathway homologous to the *Drosophila* Imd pathway to further initiate inflammatory mechanisms. Additional inflammatory mediators are responsible for stimulating the migration of microglia to the site of inflammation (CCL2) or for actively damaging surrounding cells (nitric oxide and superoxide) (Colton and Gilbert 1987; Liu *et al*. 2002).

The innate immune response is initiated when both TLRs and NLRs bind and respond to pathogen-associated molecular patterns (PAMPs) or danger-associated molecular patterns (DAMPs). PAMPs are molecules released by infectious pathogens such as lipopolysaccharide or peptidoglycan, thus stimulating the classical effects of the innate immune response. DAMPs, on the other hand, are endogenous, "self" molecules secreted or released by injured or dying cells.

They bind specific TLRs, such as the binding of nucleic acids by TLR3, 7, or 9 and the binding of heat shock proteins by TLR2 or 4, to promote either phagocytosis of dying cells or clearance of apoptotic corpses (Asea *et al*. 2002; Zhang *et al*. 2010). Proteins known to be involved in neurodegenerative diseases such as Alzheimer's disease (AD) and Parkinson's disease (PD) also function as DAMPs, thereby initiating microglial activation of the innate immune response.

In AD, TLR2 or 4 found on microglia and astrocytes bind β-amyloid (Aβ) plaques to produce inflammation (Akiyama *et al*. 2000; Landreth and Reed-Geaghan 2009). Mice expressing Aβ and lacking TLR2 or 4 exhibited reduced inflammation and increased scoring on memory tests, indicating that inflammation promotes neurodegenerative phenotypes of AD (Jin *et al*. 2008; Richard *et al*. 2008). In PD, α-synuclein aggregates are either released from dying cells or are actively secreted from cells. Extracellular α-synuclein is phagocytosed by microglial cells and stimulates inflammatory processes and the production of reactive oxygen species (Zhang *et al*. 2005; Lee 2008; Reynolds *et al*. 2008; Roodveldt *et al*. 2008).

While the innate immune response has been best characterized for AD and PD, diseases such as Huntington's disease and amyotrophic lateral sclerosis (ALS) also exhibit signs of microglial cell activation and inflammation although the underlying mechanisms have not been well defined (Möller 2010; Philips and Robberecht 2011). While the protein or process that causes the inflammatory response differs in each of these diseases, activation of the innate immune response in glial cells is a common denominator among them all. This response signals through conserved pathways utilizing TLRs and cytokine receptors to activate NF-κB proteins, the same as is observed in *Drosophila*. With the recent identification that neurodegenerative conditions in the fly produce innate immune responses in glial cells, fundamental experiments to determine the exact role of the innate immune response in neurodegeneration can be performed.

Figure 1.1. Shown is a simplified schematic of the ATM signaling pathway in the DNA damage response. When DNA double-strand breaks occur, such as in response to ionizing radiation (IR) (1), the MRN complex (Mre11, Rad50, NBS1) is recruited to the DSB (2) and binds inactive ATM homodimers. This facilitates ATM autophosphorylation, dissociation, and activation (3). Active ATM phosphorylates numerous substrates that play a role in DNA repair mechanisms (H2AX – 4), cell cycle checkpoints (CHK1/2 – 5), and apoptosis (p53 – 6).

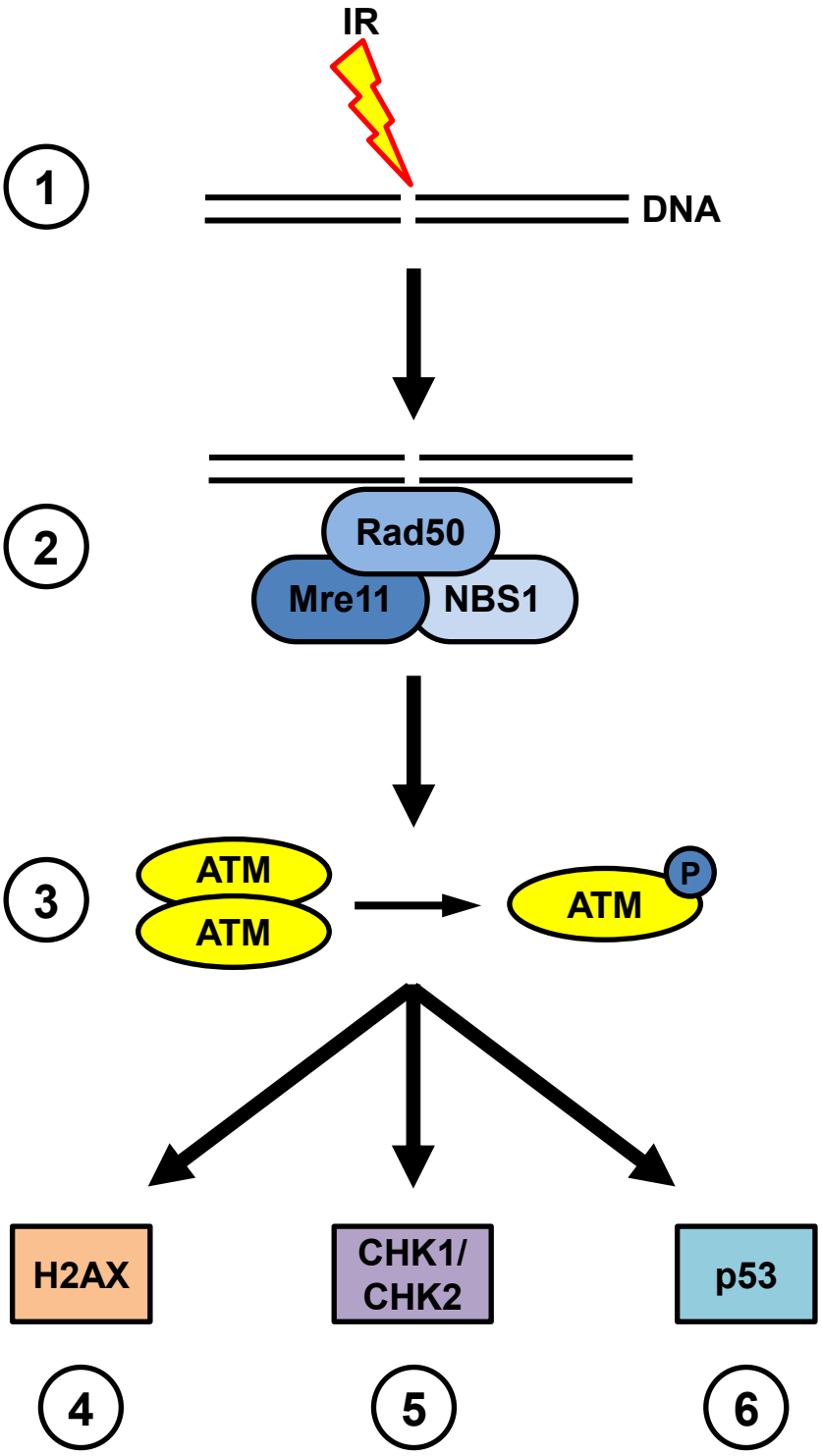
IR
1
DNA
2
Rad50
Mre11
NBS1
3
ATM
ATM
ATM
P
H2AX
CHK1/
CHK2
p53
4
5
6

Figure 1.2. The GAL4/UAS expression system can be used to alter transcription in *Drosophila.* A transgene containing the genomic sequence for the yeast GAL4 transcription factor is inserted into the genome of the fly under the control of a tissue- or cell type-specific promoter. A second transgene contains a target construct downstream of the GAL4 Upstream Activation Sequence (UAS). Spatial expression of GAL4 generates expression of this second transgene in a controlled manner. This system can be used to express (A) human disease genes to determine their effects in the fly or (B) shRNA to a specific gene like *ATM* to generate localized knockdown of protein levels via RNAi.

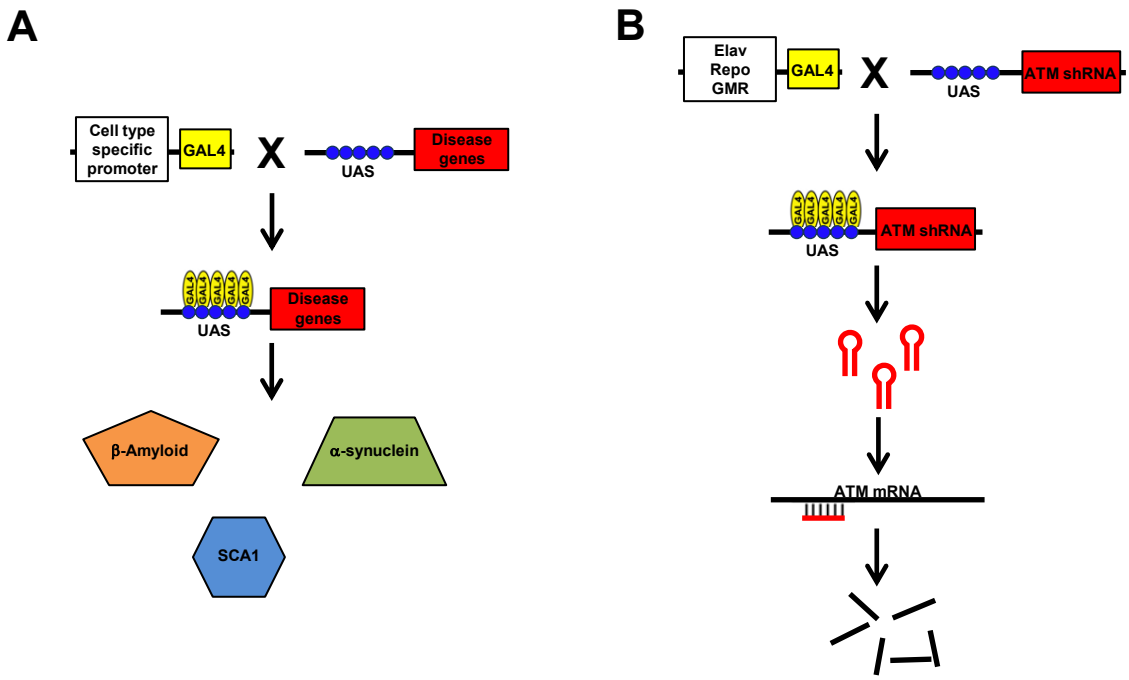
A
Cell type specific promoter
GAL4
X
UAS
Disease genes
UAS
Disease genes
β-Amyloid
α-synuclein
SCA1
B
Elav
Repo
GMR
GAL4
X
UAS
ATM shRNA
UAS
ATM shRNA
ATM mRNA

Figure 1.3. The FLP/FRT system can be used to generate *ATM* null tissue in the adult fly. A transgene is incorporated in two places, and contains a FLP recombination target (FRT) site. This transgene is strategically incorporated into two chromosomes at the same location between the centromere and either the mutant gene of interest (in this case *ATM*) or a cellular marker such as GFP (1). Mating these flies produces flies with one *ATM* null-containing chromosome and one GFP-containing chromosome (2). A third transgene uses a tissue- or cell type-specific promoter to drive expression of the FLP yeast recombinase. FLP activation during the development of the targeted tissue drives mitotic recombination between the *ATM* null and GFP chromosomes (3). Subsequent mitotic events sorts the chromosomes to generate ATM^{-}/ATM^{-} cells that lack GFP expression alongside GFP/GFP cells that have strong GFP expression (4). By monitoring for the presence or absence of GFP expression in a population of cells it is possible to identify and study *ATM* null tissue in the adult fly.

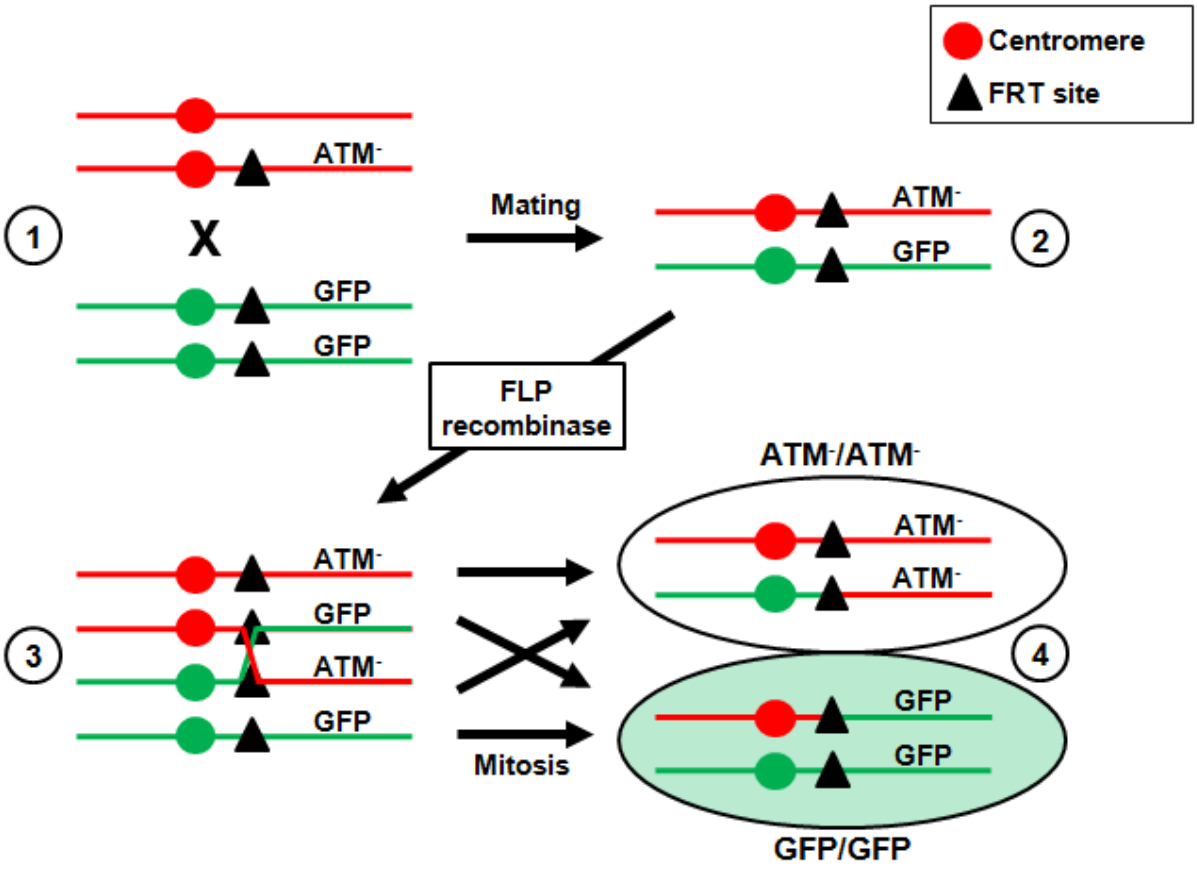
Centromere
FRT site
ATM-
1
X
GFP
GFP
Mating
ATM-
GFP
2
FLP
recombinase
ATM-/ATM-
ATM-
ATM-
3
ATM-
GFP
ATM-
GFP
Mitosis
4
GFP
GFP
GFP/GFP

Figure 1.4. The innate immune response in *Drosophila* primarily signals through the Toll or Imd pathway. Shown is a simplified schematic representing the canonical signaling components required. Both pathways converge on unique NF-κB proteins and stimulate the expression of innate immune response genes including the antimicrobial peptides (AMPs).

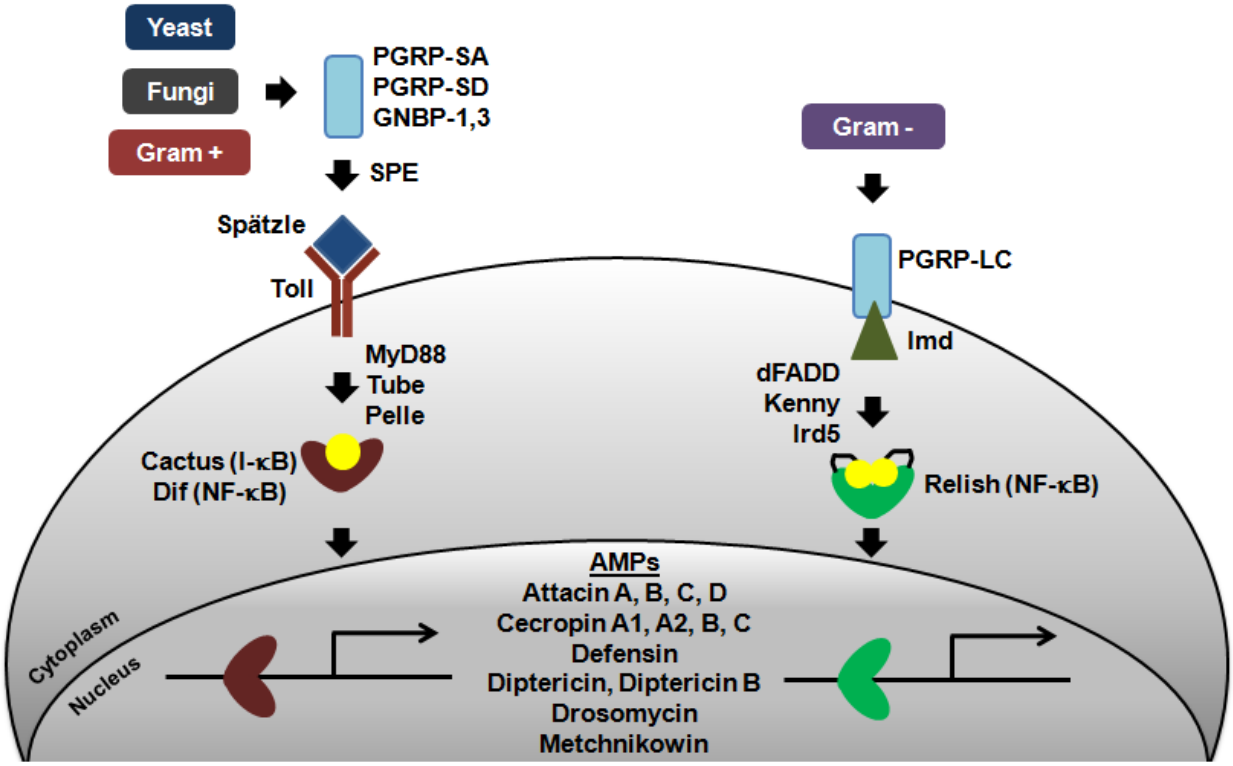
Yeast
Fungi
Gram +
PGRP-SA
PGRP-SD
GNBP-1,3
SPE
Spätzle
Toll
MyD88
Tube
Pelle
Cactus (I-κB)
Dif (NF-κB)
Gram -
PGRP-LC
Imd
dFADD
Kenny
Ird5
Relish (NF-κB)
AMPs
Attacin A, B, C, D
Cecropin A1, A2, B, C
Defensin
Diptericin, Diptericin B
Drosomycin
Metchnikowin
Cytoplasm
Nucleus

Figure 1.5. Activation of the innate immune response via NF-κB proteins functions in neurodegeneration in *Drosophila*. The diagrams summarize the work of Petersen *et al.* (2012) and subsequent research, Chinchore *et al.* (2012), and Tan *et al.* (2008) that examined the role of the innate immune response in Drosophila models of human neurodegenerative diseases, (A) A-T, (B) retinal degeneration, and (C) Alzheimer's disease. Each panel depicts the key membrane-bound and cytoplasmic factors in the two primary innate immune response pathways and indicates through color-coding (see legend) which factors have been genetically implicated in neurodegeneration. Each panel also indicates through color-coding whether the innate immune response occurs in glial cells and whether nuclear events (innate immunity gene transcription) have been shown to occur.

A Petersen, et al. 2012

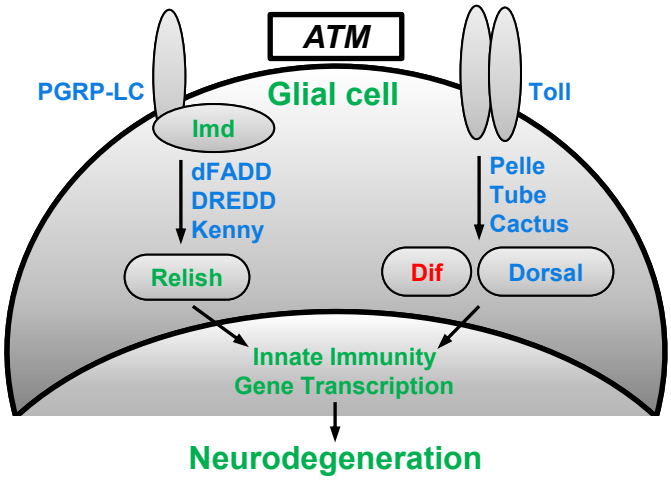

B Chinchore, et al. 2012

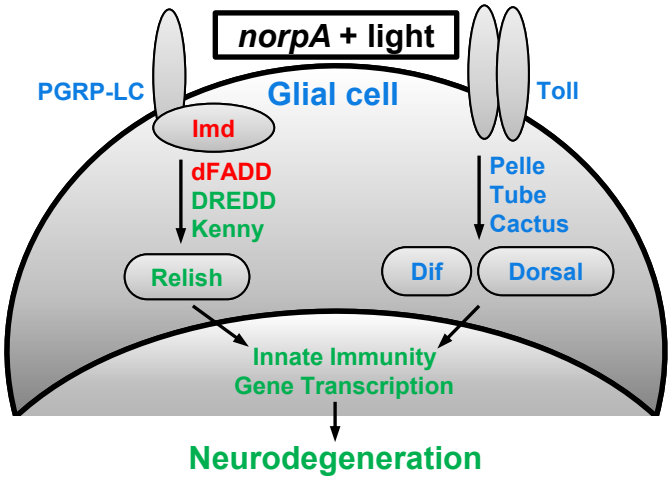

C Tan, et al. 2008

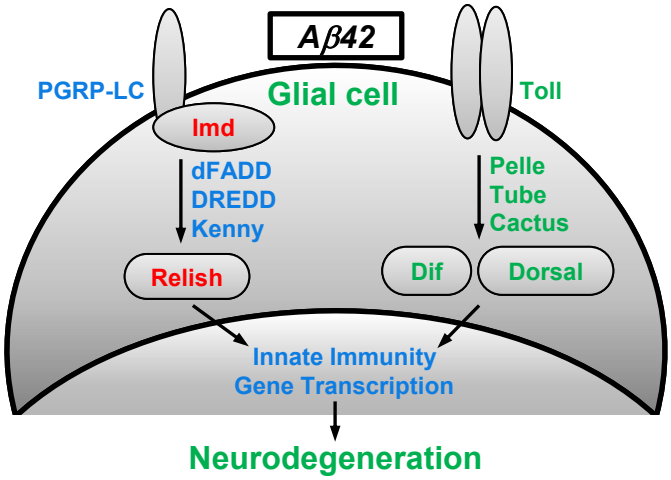

Legend:
Involved in neurodegeneration
Not involved in response
Not tested in response

Chapter Two

ATM kinase inhibition in glial cells activates the innate immune response and causes neurodegeneration in *Drosophila*

This chapter was published in:

Petersen AJ, Rimkus SA, and Wassarman DA. (2012) ATM kinase inhibition in glial cells activates the innate immune response and causes neurodegeneration in *Drosophila. Proc Natl Acad Sci U S A* 109: E656-E664.

A.J.P. performed the experiments for all figures and tables in the publication. S.A.R. provided a portion of the data in Table 2.1. A.J.P. wrote the text and revised it with D.A.W.

2.1 Abstract

To investigate the mechanistic basis for central nervous system (CNS) neurodegeneration in the disease Ataxia-telangiectasia (A-T), we analyzed flies mutant for the causative gene *A-T mutated* (*ATM*). *ATM* encodes a protein kinase that functions to monitor the genomic integrity of cells and control cell cycle, DNA repair, and apoptosis programs. Mutation of the C-terminal amino acid in *Drosophila* ATM inhibited the kinase activity and caused neuron and glial cell death in the adult brain and a reduction in mobility and longevity. These data indicate that reduced ATM kinase activity is sufficient to cause neurodegeneration in A-T. ATM kinase mutant flies also had elevated expression of innate immune response genes in glial cells. *ATM* knockdown in glial cells, but not neurons, was sufficient to cause neuron and glial cell death, a reduction in mobility and longevity, and elevated expression of innate immune response genes in glial cells, indicating that a non-cell autonomous mechanism contributes to neurodegeneration in A-T. Taken together, these data suggest that early onset CNS neurodegeneration in A-T is similar to late onset CNS neurodegeneration in diseases such as Alzheimer's wherein an uncontrolled inflammatory response mediated by glial cells drives neurodegeneration.

2.2 Introduction

Ataxia-telangiectasia (A-T) is a multisystem disease characterized by neurodegeneration in the central nervous system (CNS) (Sedgwick and Boder 1960; Bundey 1994; McKinnon 2012). Progressive neurodegeneration occurs during childhood and mainly affects Purkinje and granule cells in the cerebellum. A-T is caused by mutation of the *A-T mutated* (*ATM*) gene, which encodes a serine/threonine protein kinase of the phosphatidylinositol-3 kinase-related kinase (PIKK) family (Savitsky *et al*. 1995). ATM functions to ensure genome integrity by

controlling the cell cycle, DNA repair, and apoptosis programs in response to DNA damage (Derheimer and Kastan 2010; Bhatti *et al*. 2011). ATM is recruited to sites of DNA damage where autophosphorylation activates the kinase activity to allow phosphorylation of many downstream targets, including histone H2AX (Burma *et al*. 2001; Bakkenist and Kastan 2003; Matsuoka *et al*. 2007).

Insights into why ATM loss causes neurodegeneration have come from analyses of ATM-deficient animals. Analyses of post-mortem human A-T brains as well as mouse and fly models of A-T indicate that ATM protects post-mitotic neurons from degeneration by suppressing cell cycle reentry (Yang and Herrup 2005; Rimkus *et al*. 2008). ATM-deficient neurons reenter the cell cycle and may die rather than arrest or divide because of excessive DNA damage. Many aspects of neurodegeneration are not understood, including whether it is solely due to ATM loss in neurons (Biton *et al*. 2008). In neurodegenerative diseases such as Alzheimer's and Parkinson's, prolonged activation of microglia, the resident innate immune cells in the CNS, is thought to cause neurotoxicity (González-Scarano and Baltuch 1999; Amor *et al*. 2010; Halliday and Stevens 2011). In addition, in neurodegenerative diseases such as Amyotrophic lateral sclerosis (ALS), dysfunction of astrocytes, which serve to maintain neuronal metabolism and neurotransmitter release, drives neurodegeneration after onset (Ilieva *et al*. 2009). In the case of A-T, abnormal microglial cell morphology is observed in *ATM* knockout mice, and cultured astrocytes from *ATM* knockout mice show markers of oxidative and endoplasmic reticulum stress and exhibit a senescence-like growth defect (Kuljis *et al*. 1997; Liu *et al*. 2005). Furthermore, several lines of evidence suggest that systemic inflammation contributes to pathogenesis in A-T patients (McGrath-Morrow *et al*. 2010; Westbrook and Schiestl 2010). Thus, ATM loss in glial cells may contribute to neurodegeneration in A-T. To

investigate this possibility, we analyzed *Drosophila melanogaster* brains in which ATM kinase activity was reduced in all cells or *ATM* expression was specifically reduced in glial cells or neurons.

2.3 Results

ATM kinase activity is temperature-sensitive in ATM^{8} flies

Since *ATM* is essential for fly viability to the adult stage, a temperature-sensitive allele of *ATM* (ATM^{8}) was used to investigate the role of ATM in adult flies (Pedersen *et al*. 2010). ATM^{8}/ATM^{8} flies (hereafter referred to as ATM^{8}) developed to the adult stage when raised at 18°C but not at 25°C. Thus, to characterize adult phenotypes, ATM^{8} flies were raised at 18°C and shifted to 25°C shortly after eclosion.

ATM^{8} contains a leucine to phenylalanine mutation of the C-terminal amino acid, which is predicted to affect kinase activity but not protein stability (Lempiäinen and Halazonetis 2009; Joyce *et al*. 2011). Western blot analysis for histone H2Av phosphorylation (H2Av-pS137) revealed that ATM kinase activity in ATM^{8} adult fly heads was temperature-sensitive (Figure 2.1). H2Av is the *Drosophila* homolog of mammalian H2AX, an ATM substrate in response to ionizing radiation (IR)-induced DNA damage (Joyce *et al*. 2011). At 18°C, IR-induced H2Av phosphorylation was not affected in $ATM^{8}/+$ flies but was highly reduced in ATM^{8} flies relative to wildtype flies. Despite the reduction in activity, this level was sufficient for development of ATM^{8} flies to the adult stage. At 25°C, IR-induced H2Av phosphorylation was slightly reduced in $ATM^{8}/+$ flies and was below detection in ATM^{8} flies. This reduction in kinase ability is not due to absence of the protein itself, as immunohistochemistry studies in *Drosophila* testes revealed the presence of ATM^{8} protein. These data indicate that ATM^{8} kinase activity is

temperature-sensitive and that ATM kinase activity in adult heads is correlated with ATM^{8} allele dose. Since humans heterozygous for mutated *ATM* alleles show increased susceptibility to certain A-T phenotypes such as cancer, ATM^{8}/+ heterozygous flies may provide insight into the human disease as well (Chen *et al*. 1978; Ahmed and Rahman 2006).

Reduced ATM kinase activity reduces mobility and longevity

ATM^{8} flies had obvious mobility defects, including a lessened ability to walk, fly, or right themselves when turned onto their backs. A climbing assay was used to quantitate mobility. When tapped to the bottom of a vial, flies naturally respond by climbing to the top, referred to as negative geotaxis. Ten seconds after being tapped to the bottom of a vial, 65% of wildtype flies had climbed to the top quarter of the vial; however, only 19% of ATM^{8}/+ and 6% of ATM^{8} flies had climbed to the top quarter of the vial (Figure 2.2A). Similar effects were observed if climbing was assessed at different heights in the vial or if climbing was assessed after longer recovery times, 20 or 30 seconds, suggesting that the climbing defect was not due to incapacitation from the tapping action. The climbing defect was probably due to reduced ATM kinase activity, since the severity of the defect correlated with the level of ATM kinase activity - less severe defects were observed for ATM^{8}/+ flies than ATM^{8} flies. Furthermore, ATM^{8} flies kept at 18°C after eclosion, and therefore maintaining a slight level of ATM kinase function, exhibit a significantly better climbing ability than ATM^{8} flies maintained at 25°C (Figure 2.3). Thus, it appears that loss of ATM kinase function is sufficient to produce climbing defects. Many fly neurodegeneration mutants have decreased ability to climb, and *turtle* (*tutl*) mutants have decreased ability to right themselves when turned onto their backs (Bodily *et al*. 2001; Lessing and Bonini 2009). The *tutl* gene is specifically expressed in the CNS and regulates the

development of neuron dendrites (Bodily *et al*. 2001). These data suggest that reduced ATM kinase activity causes neurological problems.

Adult fly longevity was used to further assess the physiological requirements for ATM kinase activity. In the longevity assay, flies were raised at 18°C, shifted to 25°C shortly after eclosion, and the number of surviving flies was determined each day. This assay revealed that ATM^{8}/+ and ATM^{8} flies had significantly shorter lifespans than wildtype flies ($P<1X10^{-4}$) (Figure 2.2B). The 50% survival point for ATM^{8} flies was 18 days, compared to 27 and 50 days for ATM^{8}/+ and wildtype flies, respectively. Many fly neurodegeneration mutants have reduced longevity (Lessing and Bonini 2009). Thus, neurodegeneration may cause reduced mobility and longevity of flies with reduced ATM kinase activity, but other factors such as muscle degeneration are also plausible.

Reduced ATM kinase activity causes neuron and glial cell death

Light microscopic analysis of paraffin sections of adult heads was used to assess the extent to which abnormal brain morphology accompanied the mobility and longevity defects of ATM^{8} flies. Neurons in the adult *Drosophila* brain have cell bodies at the periphery and neurites that extend internally to form the synaptic neuropil (Cardona *et al*. 2010; Pereanu *et al*. 2010). After 7 days at 25°C, scattered, small holes were observed in the neuropil of ATM^{8}/+ and ATM^{8} flies but not wildtype flies (Figures 2.4A-C and Figures 2.5A-C). After 17 days at 25°C, the abundance and size of the holes was increased in ATM^{8}/+ and ATM^{8} flies, which typifies progressive neurodegeneration in flies (Figures 2.4D-F and Figures 2.5D-F) (Lessing and Bonini 2009).

To directly assess cell death, an antibody to activated Caspase 3 (α-$Casp^{Act}$) was used to detect cells undergoing apoptotic death (Fan and Bergmann 2010). In apoptotic cells,

cytoplasmic Caspase 3 is activated by cleavage and translocated to the nucleus, so nuclear α-Casp^{Act} staining was used to identify dying cells (Kamada *et al*. 2005). After 7 or 17 days at 25°C, *ATM*^{8} flies had significantly more Casp^{Act}-positive cells than wildtype or *ATM*^{8}/+ flies ($P<0.05$) (Figures 2.4H and K and Table 2.1). This finding suggests that continuous cell death underlies the progressive formation of holes in the brain and the reduced mobility and longevity of *ATM*^{8} flies.

To determine the identity of the dying cells, brains were co-stained with antibodies to Casp^{Act} and to the glial cell-specific protein Reversed polarity (Repo) or the neuron-specific protein Embryonic lethal abnormal vision (Elav) (Xiong *et al*. 1994; Soller and White 2004). This analysis revealed that neurons and glial cells were Casp^{Act}-positive in *ATM*^{8}/+ and *ATM*^{8} flies (Figures 2.4G-L). Quantitation of α-Repo-stained brains further revealed that 58-77% of the dying cells were glial cells (Table 2.1). Thus, reduced ATM kinase activity causes neuron and glial cell death in the adult fly brain.

Reduced ATM kinase activity causes increased expression of innate immune response genes

Gene expression microarray analysis was used to identify molecular and biological events caused by reduced ATM kinase activity. With the goal of identifying events that are causative for neurodegeneration, adult heads were examined after 3-4 days at 25°C, a time prior to the appearance of holes in the brain. Total RNA isolated from *ATM*^{8}/+ and *ATM*^{8} flies was converted to fluorescently labeled cDNA and used to probe Nimblegen oligonucleotide arrays representing ~15,000 *Drosophila* genes. The resulting data were quantile normalized via Robust Multichip Average (RMA) and *ATM*^{8} was compared to *ATM*^{8}/+ for fold change and statistical significance. Analysis of two independent biological replicates revealed that 163 genes met the

criteria of a >2-fold change with a moderated T-test value of $P<0.05$ and a False Discovery Rate (FDR) value of $P<0.10$; 117 genes were upregulated and 46 genes were downregulated in ATM^{8} flies relative to $ATM^{8}/+$ flies.

Gene Ontology analysis of the upregulated genes identified the innate immune response as the most significantly changed biological event (Ashburner *et al*. 2000). *Drosophila* lack an adaptive immune system that involves B and T cells and predominantly rely on an innate immune system for immune defense (Lemaitre and Hoffmann 2007). The fat body is the major immune-responsive tissue. In response to pathogens, the fat body expresses pathogen recognition proteins, such as peptidoglycan recognition proteins (PGRPs) and gram-negative binding proteins (GNBPs), that act upstream of the Toll and immune deficiency (Imd) signaling pathways to recognize pathogens (Lemaitre *et al*. 1995; Levashina *et al*. 1998; Werner *et al*. 2000; De Gregorio *et al*. 2002). These pathways function through NF-κB transcription factors to express antimicrobial peptides (AMPs) that combat pathogens (Dushay *et al*. 1996; Lemaitre *et al*. 1996).

Twenty innate immune response gene ontology categories were identified with a stringent P-value ($P<1X10^{-5}$) in the gene expression microarrays. Table 2.2 provides a complete list of genes that are included in these categories and is based on comparisons to published microarray analyses of the *Drosophila* innate immune response (De Gregorio *et al*. 2001; Irving *et al*. 2001; McDonald and Roshbash 2001). Table 2.3 provides a partial list that focuses on genes that encode pathogen recognition proteins and AMPs. The expression of PGRP genes, as well as members of six of seven classes of AMP genes, was upregulated. The exception was *Drosocin* (*Dro*), but validation studies indicated that it was also upregulated (Figure 2.6C).

Collectively, these data indicate that reduced ATM kinase activity activates the innate immune response in the adult head.

Quantitative PCR (qPCR) was used to independently examine innate immune response gene expression. Comparison of wildtype and ATM^{8} flies that had been shifted to 25°C for 0, 3, or 8 days confirmed the microarray finding that reduced ATM kinase activity caused upregulation of PGRP and AMP gene expression (Figure 2.7A). Furthermore, since wildtype flies rather than ATM^{8}/+ flies were used for the comparison, a higher level of innate immune response gene expression was observed relative to the microarray analysis. Finally, upregulation of PGRP and AMP gene expression was detected immediately after eclosion and, in some cases, persisted through the first eight days of adulthood. These data indicate that reduced ATM kinase activity throughout development induces a prolonged innate immune response in the head of young adult flies.

Reduced ATM kinase activity causes AMP gene expression in glial cells

To further characterize the innate immune response, transgenic reporter flies were used to determine the location of AMP gene expression in the head. Flies expressing Green Fluorescent Protein (GFP) under control of AMP gene transcriptional regulatory sequences were crossed to wildtype or ATM^{8}/+ flies at 25°C, the progeny were cultured for 3-5 days, and GFP expression was examined in dissected head fat body cells and brain whole mounts (Tzou *et al*. 2000). For the Attacin A (AttA)::GFP reporter, GFP expression was not detected in head fat body cells of either ATM^{8}/+ or wildtype flies. In contrast, GFP expression was detected in the brain of ATM^{8}/+ but not wildtype flies (Figures 2.7C and F). GFP expression was most prominent in the outer area of the optic lobe and the region where the optic lobe juxtaposes the central brain neuropil, regions that are highly populated by neuron cell bodies (Cardona *et al*. 2010; Pereanu

et al. 2010). Similar results were observed for other AMP transgenic reporter lines (Cecropin A1 (CecA1)::GFP, Defensin (Def)::GFP, Drosomycin (Drs)::GFP, Metchnikowin (Mtk)::GFP, and Dro::GFP) (Figure 2.6) (Tzou *et al*. 2000). These data indicate that reduced ATM kinase activity causes transcriptional upregulation of AMP genes in the brain.

To identify the AMP-expressing cell type in ATM^{8}/+ flies, brains were stained with antibodies to Repo or Elav (Xiong *et al*. 1994; Soller and White 2004). GFP was found to exclusively co-localize with Repo-positive cells, indicating that reduced ATM kinase activity causes transcriptional upregulation of AMP genes in glial cells (Figures 2.7B-G).

ATM knockdown in glial cells causes neurodegeneration

The studies of ATM^{8} flies indicated that reduced ATM kinase activity in glial cells is responsible for activation of the innate immune response and neuron and glial cell death. To test this hypothesis, RNA interference (RNAi) was used to knock down *ATM* only in glial cells. A *Repo-GAL4* transgene was used to drive expression of a $pWIZ\text{-}ATM^{T4}$ transgene that expresses an *ATM* short hairpin RNA under transcriptional control of *UAS* sequences (Lee *et al*. 2003; Sepp *et al*. 2001; Rimkus *et al*. 2008). Our prior studies demonstrated that GAL4-driven expression of $pWIZ\text{-}ATM^{T4}$ specifically knocks down *ATM* (Rimkus *et al*. 2008). Control *Repo-GAL4* flies and experimental *Repo-GAL4/*$pWIZ\text{-}ATM^{T4}$ (*Repo-ATMi*) flies were assayed as described for ATM^{8} flies.

Repo-ATMi flies had similar phenotypes to ATM^{8} flies. *Repo-ATMi* flies had impaired climbing ability; only 6-17% of *Repo-ATMi* flies compared to 82-84% of *Repo-GAL4* flies climbed to the top quarter of the vial within 10, 20, or 30 seconds after being tapped to the bottom (Figure 2.8A). *Repo-ATMi* flies also had significantly reduced longevity ($P<1X10^{-4}$) (Figure 2.8B). The 50% survival point for *Repo-ATMi* flies was 16 days, compared to 25 and 43

days for *Repo-GAL4* and wildtype flies, respectively. *Repo-ATMi* flies also had holes in the adult lamina and neuropil. At 1 day post-eclosion, large holes were present in the lamina and small holes in the neuropil, and at 7 days post-eclosion, numerous small and large holes were present in the neuropil (Figures 2.9A-C and Figure 2.5G-J). Lastly, at both 7 and 17 days post-eclosion, *Repo-ATMi* flies had significantly more $Casp^{Act}$-positive cells than *Repo-GAL4* flies ($P<0.05$) (Table 2.1). Co-staining for $Casp^{Act}$ and Elav or Repo revealed that cell death at 7 days was limited to neurons but at 17 days also included glial cells (Figures 2.9G-L and Table 2.1). Taken together, these data indicate that ATM is required in glial cells for the survival of neurons.

ATM knockdown in glial cells causes increased expression of innate immune response genes

Gene expression microarray analysis was used to identify molecular and biological events caused by *ATM* knockdown in glial cells. Using parameters described for the ATM^{8} microarray analysis, two independent biological replicates of 3-5 day old *Repo-GAL4* and *Repo-ATMi* flies were analyzed. This analysis revealed that 246 genes were upregulated and 106 genes were downregulated in *Repo-ATMi* flies relative to *Repo-GAL4* flies.

Gene Ontology analysis of the upregulated genes identified the innate immune response as the most significantly changed biological event (Ashburner *et al*. 2000). Twelve innate immune response categories were identified with the stringent P-value of $P<1X10^{-5}$. As expected from this result, comparison of the genes upregulated in ATM^{8} flies and *Repo-ATMi* flies showed a significant overlap ($P<0.01$), with 30 overlapping genes that were primarily innate immune response genes. A majority of these overlapping genes fall within 16 innate immune response categories (Figure 2.10). Table 2.2 provides a complete list of genes that were included in these categories, and Table 2.3 provides a partial list that focuses on pathogen recognition protein and AMP genes. qPCR analysis confirmed that PGRP and AMP genes were

upregulated in *Repo-ATMi* flies (Figure 2.11A). Analyses at 0, 3, and 8 days post-eclosion revealed prolonged AMP gene expression. Finally, the AMP::GFP transgenic reporter assay revealed AMP gene expression only in glial cells of *Repo-ATMi* flies (Figures 2.11B-G and Figure 2.6). Taken together, these data suggest that *ATM* knockdown in glial cells causes cell autonomous and prolonged activation of the innate immune response.

ATM knockdown in neurons does not cause neurodegeneration or increased expression of innate immune response genes

To determine the extent to which reduced ATM kinase activity in neurons plays a role in ATM^{8} phenotypes, *Elav-GAL4* and $pWIZ\text{-}ATM^{T4}$ transgenes were used to knock down *ATM* only in neurons. Two *Elav-GAL4* driver flies were utilized: *Elav-GAL4* flies, which have a transgene on the 2nd-chromosome that expresses GAL4 under control of the *Elav* promoter, and $Elav^{C155}$-*GAL4* flies, which have a GAL4-containing transgene insertion downstream of the endogenous *Elav* promoter on the X-chromosome (Luo *et al*. 1994; Yao and White 1994). Control *Elav-GAL4* and $Elav^{C155}$-*GAL4* flies and experimental *Elav-GAL4/pWIZ-*ATM^{T4} (*Elav-ATMi*) and $Elav^{C155}$-*GAL4/pWIZ-*ATM^{T4} ($Elav^{C155}$-*ATMi*) flies were assayed as described for ATM^{8} flies.

Mobility, longevity, brain morphology, and $Casp^{Act}$ expression were not adversely affected in *Elav-ATMi* flies (Figures 2.8C and D, 2.9D-F, Table 2.1, and Figure 2.5K-N). In fact, *Elav-ATMi* flies had significantly increased longevity relative to *Elav-GAL4* flies ($P<0.001$). Longevity and $Casp^{Act}$ expression were also not noticeably affected in $Elav^{C155}$-*ATMi* flies (Table 2.1 and Figure 2.12B). However, mobility and brain morphology were affected in $Elav^{C155}$-*ATMi* flies. $Elav^{C155}$-*ATMi* flies had slightly reduced climbing ability immediately (10 seconds) after being tapped to the bottom of the vial, but climbing ability was not affected at the 20 and 30 second timepoints (Figure 2.12A). This contrasts the sustained and more severe

reduction in climbing ability observed for *ATM*^{8} and *Repo-ATMi* flies (Figures 2.2A and 2.8A). *Elav*^{C155}*-ATMi* brains contained several 2-4 μm round structures that were distinct in location and morphology from holes that are characteristic of neurodegeneration (Figure 2.5O-R and 2.12C-E) (Lessing and Bonini 2009). The round structures occurred within the optic lobes, but not the neuropil, and had a clear zone around the periphery and a darkly stained interior core. This contrasts the holes in *ATM*^{8} and *Repo-ATMi* flies that occurred in both the optic lobes and the neuropil and had an empty core (Figures 2.4C and 2.9C). Take together, these data indicate that *ATM* knockdown in neurons is not sufficient to cause neurodegeneration in the brain.

Gene expression microarray analysis was used to identify molecular and biological events caused by *ATM* knockdown in neurons. Using parameters described for the *ATM*^{8} microarray analysis, ≥2 independent biological replicates of 3-5 day old flies were analyzed. This analysis revealed that 124 genes were upregulated and 36 genes were downregulated in *Elav-ATMi* flies relative to *Elav-GAL4* flies and that 81 genes were upregulated and 39 genes were downregulated in *Elav*^{C155}*-ATMi* flies relative to *Elav*^{C155}*-GAL4* flies. Gene Ontology analysis revealed that the innate immune response was not significantly affected in *Elav-ATMi* or *Elav*^{C155}*-ATMi* flies, and qPCR analysis confirmed that the expression of PGRP and AMP genes was not affected in *Elav-ATMi* or *Elav*^{C155}*-ATMi* flies (Figure 2.13) (Ashburner *et al*. 2000). The genes that were affected will be reported elsewhere. These data indicate that *ATM* knockdown in neurons is not sufficient to activate the innate immune response in the brain.

2.4 Discussion

ATM kinase activity is required for neuron survival

This study indicates that the kinase activity of *ATM*^{8} is temperature-sensitive. *ATM*^{8} was identified in a screen for *ATM* alleles and was found to contain a leucine to phenylalanine mutation of the final amino acid (Pedersen *et al*. 2010). This amino acid falls within the FATC (FRAP, ATM, TRRAP C-terminal) domain, which is located directly downstream of the kinase domain in PIKK family members (Jiang *et al*. 2006). Functional and structural analyses indicate that the FATC domain regulates PIKK kinase activity (Lempiäinen *et al*. 2009). Mutation of one or two amino acids in the FATC domain of several PIKKs reduces kinase activity. Structural studies demonstrate that the FATC domain is physically close to the activation loop of the kinase domain, suggesting that temperature-sensitivity of ATM^{8} kinase activity is due to disruption of FATC domain contacts with the kinase domain at high temperature (25°C) that are weak but functionally sufficient at low temperature (18°C) (Rivera-Calzada *et al*. 2005). Taken together with the finding that a single amino acid mutation in the FATC domain was found to naturally occur in an A-T patient, evidence of neurodegeneration in *ATM*^{8} flies suggests that ATM kinase activity is required for neuron survival in humans (Cavalieri *et al*. 2006).

Reduced ATM kinase activity in glial cells causes neurodegeneration

This study indicates that neuron survival requires ATM kinase activity in glial cells. Phenotypes caused by *ATM* knockdown only in glial cells (*Repo-ATMi* flies) were similar to those caused by reduced ATM kinase activity in both neurons and glial cells (*ATM*^{8} flies). These phenotypes include reduced mobility, reduced longevity, holes in the brain, and neuron and glial cell death. Collectively, these data indicate that reduced ATM kinase activity in glial cells causes neurodegeneration and imply that interactions between glial cells and neurons are

important for neuron survival. Reduced ATM kinase activity in glial cells may inhibit the production of protective signals or allow the production of toxic signals that result in neurodegeneration.

ATM knockdown only in neurons (*Elav-ATMi* and *Elav^{C155}-ATMi* flies) did not cause neurodegeneration in the adult brain. This does not mean that ATM loss in neurons does not contribute to neurodegeneration; rather it means that ATM loss in neurons is not sufficient to cause neurodegeneration in particular cellular contexts. In fact, we previously found that *ATM* knockdown in neurons (*Elav^{C155}-ATMi* flies) causes neurodegeneration in another cellular context, the eye (Rimkus *et al*. 2008). The different results observed in the brain and the eye may be due to different levels of *ATM* knockdown. Alternatively, the different results may be due to unique properties of neurons, glial cells, or other cells in the brain or eye. This alternative explanation is attractive because, in A-T and other neurodegenerative diseases, neuron types differ in their susceptibility to degeneration, with Purkinje and granule neurons being particularly susceptible in A-T (Sedgwick and Boder 1960; Bundey 1994).

Reduced ATM kinase activity triggers an innate immune response in glial cells

This study indicates that glial cells in the *Drosophila* CNS produce an innate immune response. This adds glial cells in the CNS to the existing list of innate immune response-competent cells that includes surface epithelia and the fat body in adult labellar glands, midgut, malpighian tubules, trachea, and male and female reproductive tracts (Ferrandon *et al*. 1998; Tzou *et al*. 2000). However, among the identified types of glial cells, the relevant type remains to be determined (Doherty *et al*. 2009; Hartenstein 2011). Additionally, the involvement of the Toll and Imd pathways in the glial cell innate immune response remains to be determined. None of the components of these pathways, including the NF-κB genes that are transcriptionally

upregulated in response to microbial infection, was found to have altered expression in the *ATM*^{8} or *Repo-ATMi* microarrays (De Gregorio *et al*. 2001, Irving *et al*. 2001). Activation of AMP gene expression independently of the Toll and Imd pathways is not unprecedented. FOXO and GATA transcription factors have been shown to mediate the innate immune response independently of the pathogen-responsive innate immunity pathways (Senger *et al*. 2006; Becker *et al*. 2010). Future studies will assess the details of the glial cell innate immune response.

Increased expression of innate immune response genes may directly result from reduced ATM kinase activity or indirectly result from increased susceptibility to infection or altered physiology. Data presented here are consistent with a model in which ATM directly represses the innate immune response through protein phosphorylation. However, there are no obvious candidates for substrates. ATM-dependent phosphorylation is essential for activation of NF-κB in response to DNA damage (Miyamoto 2011). Although NF-κB proteins are also activated in the innate immune response, results presented here suggest that ATM-dependent phosphorylation inhibits NF-κB proteins, since reduced ATM kinase activity activated the innate immune response. In regard to an indirect mechanism, AMP gene expression in glial cells has not been observed in response to infection or to physiological perturbations such as starvation, altered circadian rhythm, and altered sleep pattern that upregulate AMP gene expression in the fat body (McDonald and Roshbash 2001; Bauer *et al*. 2006; Zimmerman *et al*. 2006). However, AMP gene expression in glial cells may not have been adequately examined under these conditions. Lastly, prolonged expression of AMP genes in *ATM*^{8} flies argues against a burst of pathogen growth that is fought back but it does not rule out persistent infection. Future studies will establish the role of ATM in regulating the glial cell innate immune response.

Activation of the innate immune response may be a common feature of neurodegeneration

This study revealed a correlation between neurodegeneration and the innate immune response in a fly model of the human neurodegenerative disease A-T. Activation of the innate immune response may be a common phenomenon during neurodegeneration in flies. Innate immune response genes are upregulated in a fly model of Parkinson's disease, and the Toll pathway mediates neurodegeneration in a fly model of Alzheimer's disease (Greene *et al*. 2005; Tan *et al*. 2008). Moreover, studies in mammalian systems have uncovered considerable evidence linking the innate immune response and neurodegeneration in a variety of human neurological disorders, including Alzheimer's disease, Parkinson's disease, Huntington's disease, multiple sclerosis, and ALS (González-Scarano and Baltuch 1999; Amor *et al*. 2010; Arroyo *et al*. 2011). In mammals, microglial cells are primarily responsible for the innate immune response. They recognize pathogens through their Toll-like receptors leading to release of pro-inflammatory cytokines including tumor necrosis factor-α (TNF-α) (Parkhurst and Gan 2010). Current thinking is that prolonged activation of microglial cells is a causative factor for neurodegeneration. For example, in Alzheimer's, Amyloid-β activates microglia to release neurotoxic factors such as TNF-α and reactive oxygen species (ROS), and in Parkinson's overactivated microglia produce ROS in response to damaged ascending dopaminergic neurons (Miller *et al*. 2009; Morales *et al*. 2010). The discovery of a glial cell immune response in *Drosophila* makes this model organism well suited for studying the effects of neuroinflammation on neuron survival.

2.5 Materials and Methods

Drosophila genetics

Flies were maintained on standard molasses medium at 25°C unless otherwise stated. For all of the experiments, wildtype flies were w^{1118}. *pWIZ-ATM*^{T4} is described in Rimkus *et al*. (2008). *ATM*^{8}, *Repo-GAL4*, and *Elav-GAL4* flies were obtained from the Bloomington Stock Center, *Elav*^{C155}*-GAL4* flies were obtained from Barry Ganetzky (University of Wisconsin-Madison) and AMP::GFP flies were obtained from Ylva Engström (Stockholm University) (Luo *et al*. 1994; Yao and White 1994; Tzou *et al*. 2000; Sepp *et al*. 2001; Pedersen *et al*. 2010). *Repo-ATMi* flies were generated by recombining the *Repo-GAL4* and the *pWIZ-ATM*^{T4} transgenes onto the same chromosome. To generate *ATM*^{8} flies, *ATM*^{8}*/TM3* flies were raised at 18°C and their progeny were screened for the absence of *TM3*. For *ATM*^{8} experiments, flies were cultured at 18°C until 0-3 days post-eclosion and then transferred to 25°C for the indicated time.

Western blot analysis

For analysis of ATM kinase activity, vials containing 10 flies (4-5 days old) were either untreated or irradiated with 50 gy using a Mark 1 irradiator. Flies were allowed to recover for 30 min and heads were isolated by manual dissection and homogenized in Laemmli sample buffer (Bio-Rad). Head lysates were fractionated on 12% polyacrylamide gels and probed with H2Av-pS137 (1:500, Rockland) and α-tubulin (1:10,000, Sigma) antibodies. The 2° antibody was α-rabbit IgG horseradish peroxidase (1:5,000, GE Healthcare/Amersham).

Mobility assay

A climbing assay was used to quantitate mobility. Groups of 20 adult flies of the indicated genotype were aged for 3 days and were placed in 2.5 cm by 9.5 cm (diameter by

height) plastic vials with graduation marks at 25, 50, and 75% of the vial height. Vials were sealed with parafilm. Flies were tapped to the bottom of the vial and videotaped for 30 s. The tape was paused at 10, 20, and 30 s and the number of flies in each quadrant was counted. For each genotype, four independent replicates were averaged and plotted as a percentage of flies in each quadrant at the indicated time points.

Longevity assay

Longevity assays were performed in triplicate with control and experimental genotypes at the same time. For each of the triplicate experiments, 100 flies were examined (5 vials of 20 flies/vial). ATM^{8}, $ATM^{8}/+$, and w^{1118} flies were raised at 18°C and transferred to 25°C 0-1 day post-eclosion. All other flies were collected 0-3 days post-eclosion at 25°C. The day of collection was designated day 1, and the number of surviving flies was counted daily until all flies had died. Flies were transferred to new vials approximately every 3 days. The number of surviving flies for each genotype was averaged, with errors representing the SEM between replicates. Statistical significance was determined using log rank analysis and the chi-square statistic.

Paraffin sectioning

Fly heads were hand dissected and incubated in ethanol:chloroform:acetic acid (6:3:1) at room temperature over night. Heads were washed in 70% ethanol, processed into paraffin, sectioned at 5 μm, and stained with hematoxylin (Harris modified with acetic acid, Fisher) and eosin (Eosin Y powder, Polysciences) using standard procedures (Kretzschmar *et al*. 1997).

Microarray analysis

For each genotype, ~150 flies (approximately equal numbers of males and females) were collected and aged for 3 days at 25°C. To collect head, flies were transferred to 1.5 ml tubes and

frozen in liquid N_2, tubes were shaken vigorously to shear heads from bodies, and heads were isolated from other body parts by sequential use of US Standard #25 (710 μm) and #40 (425 μm) sieves. Total RNA was isolated from heads using TRI reagent (Sigma). The resulting RNA was resuspended in 40 μl DEPC-treated water and subjected to DNase treatment using the TURBO DNA-free kit (Ambion). The resulting RNA was ammonium acetate precipitated and resuspended in 20 μl of DEPC-treated water. Typically, 40 μg of RNA was recovered per sample. RNA (1 mg/ml) was shipped at -80°C to NimbleGen in Reykjavik, Iceland for probe generation and analysis on *D. melanogaster* 4x72 plex arrays, containing a minimum of 4 probes per gene for 15,473 genes. The data were analyzed using the ArrayStar program (DNAStar). Pair files were used as input, and normalization was conducted using RMA processing and quantile normalization. Two replicates were performed for all genotypes except *Elav-GAL4* and *Elav-ATMi* flies, which had four replicates. All replicates were used to generate fold changes and statistical confidence limits. Prior to statistical analysis, genes with a low coefficient of variation (CV<0.05) were filtered. Initial statistical analysis identified genes with P<0.05 using a moderated T-test analysis with no additional corrections. Further statistical analysis using the FDR test was used to generate the final list of genes, with the final criteria being a >2-fold change in expression, P<0.05 significance via moderated T-test, and P<0.10 significance via FDR. Raw and normalized microarray data have been deposited in the Gene Expression Omnibus (GEO) database (accession number GSE34315).

qPCR

Flies were collected as indicated for the microarrays and aged for the stated times. The 0-day timepoint indicates that RNA was processed on the day of collection. Heads were isolated from ~25 flies per genotype and RNA was isolated using the RNeasy Plus Mini Kit (Qiagen).

cDNA was generated with an iScript cDNA Synthesis Kit (Bio-Rad). Real-time qPCR was carried out as in Katzenberger *et al.* (2006). Primer sequences are provided in Table 2.4.

Immunofluorescence microscopy

For the AMP::GFP experiments, brains were dissected from flies aged 4-6 days at 25°C. For the $Casp^{Act}$ experiments, brains were dissected, fixed for 15 minutes in fresh 4% formaldehyde, washed in 1xPBS with 0.3% Triton-X, and incubated in primary antibody overnight at 4°C. Primary antibodies used were α-Repo (1:200, Developmental Studies Hybridoma Bank), α-Elav (1:200, Developmental Studies Hybridoma Bank), and α-$Casp^{Act}$ (1:50, Millipore). Fluorescently-labeled secondary antibodies used were α-mouse rhodamine (1:300, Invitrogen), α-rat rhodamine (1:200, Invitrogen), and α-rabbit AlexaFluor 594 (1:300, Invitrogen). Brains were mounted in Vectashield (Vector Laboratories) and imaged on a Zeiss Axiovert 200M inverted microscope or a Bio-Rad MRC-1024 confocal microscope (W. M. Keck Laboratory for Biological Imaging, UW-Madison).

2.6 Acknowledgments

We thank Grace Boekhoff-Falk, Barry Ganetzky, and Randy Tibbetts for providing advice throughout the course of this research, Ylva Engström for providing AMP reporter flies, Satoshi Kinoshita for paraffin sectioning, Matt Wagoner and Jean-Yves Sgro for assistance analyzing the microarray data, Becky Katzenberger for technical support, and the two anonymous reviewers for thoughtful comments on the manuscript. This work was supported by a grant from the NIH (R01 NS059001 to D. A. W.) and a pre-doctoral fellowship from NIH training grant T32 GM08688 (to A. J. P.).

Table 2.1: Cell death in adult brains				
Genotype	**Casp^{Act} cells per brain (brains)**		**Percent Casp^{Act} glial cells (Casp^{Act} cells)**	
	7 d	**17 d**	**7 d**	**17 d**
WT	4.9 ± 1.5 (n=14)*	2.5 ± 0.5 (n=17)	0% (n=81)†	5% (n=43)
ATM^{8}/+	12.4 ± 4.1 (n=14)	7.3 ± 1.9 (n=9)	77% (n=77)	73% (n=56)
ATM^{8}	45.9 ± 8.1 (n=14)*	21.4 ± 5.8 (n=14)†	69% (n=191)	58% (n=218)
Repo-GAL4	1.8 ± 0.4 (n=18)	2.2 ± 0.4 (n=18)	0% (n=32)	8% (n=40)
Repo-ATMi	14.5 ± 3.7 (n=16)‡	5.1 ± 1.3 (n=18)‡	1% (n=199)	29% (n=131)
Elav-GAL4	2.3 ± 0.8 (n=9)	2.1 ± 0.4 (n=12)	10% (n=21)	4% (n=25)
Elav-ATMi	3.7 ± 0.7 (n=9)	2.7 ± 0.4 (n=12)	9% (n=33)	3% (n=32)
Elav^{C155}-GAL4	2.0 ± 0.4 (n=12)	1.3 ± 0.3 (n=12)	0% (n=24)	0% (n=16)
Elav^{C155}-ATMi	2.3 ± 0.6 (n=12)	1.4 ± 0.3 (n=13)	0% (n=29)	0% (n=18)

**P<0.01 vs. WT and ATM^{8}/+, †P<0.05 vs. WT and ATM^{8}/+, ‡P<0.05 vs. Repo-GAL4*

Table 2.2: Innate immunity genes upregulated in *ATM*^{s} or *Repo-ATMi* fly heads

CG #	Gene	*ATM*^{s}	*Repo-ATMi*
Pathogen Recognition			
CG13422	*Gram negative binding protein-like (GNBP-like)*	2.05	2.06
CG11709	*Peptidoglycan recognition protein-SA (PGRP-SA)*	2.24	
CG9681	*Peptidoglycan recognition protein-SB1 (PGRP-SB1)*	2.65	3.47
CG14745	*Peptidoglycan recognition protein-SC2 (PGRP-SC2)*	6.45	5.22
CG7496	*Peptidoglycan recognition protein-SD (PGRP-SD)*	2.25	2.81
Antimicrobial Peptides (AMPs)			
CG10146	*Attacin-A (AttA)*	4.16	3.11
CG18372	*Attacin-B (AttB)*	4.56	2.47
CG4740	*Attacin-C (AttC)*	3.37	2.94
CG7629	*Attacin-D (AttD)*	7.91	
CG1365	*Cecropin A1 (CecA1)*	5.07	3.85
CG1367	*Cecropin A2 (CecA2)*	2.35	
CG1878	*Cecropin B (CecB)*	8.55	
CG1373	*Cecropin C (CecC)*	7.04	2.30
CG1385	*Defensin (Def)*	3.33	
CG12763	*Diptericin (Dpt)*	2.29*	
CG10794	*Diptericin B (DptB)*	2.99*	
CG10810	*Drosomycin (Drs)*	5.11	
CG32282	*drosomycin-4 (dro4)*	2.13	
CG8175	*Metchnikowin (Mtk)*	3.01	2.26
Proteases/Protease Inhibitors			
CG11459	cysteine-type endopeptidase	2.05	
CG5896	*gram positive specific serine protease (grass)*		2.27
CG9733	serine-type endopeptidase	3.76	4.07
CG18563	serine-type endopeptidase	3.04	
CG6639	serine-type endopeptidase	2.97	
CG11836	serine-type endopeptidase	2.75	
CG4914	serine-type endopeptidase	2.35	
CG30371	serine-type endopeptidase	2.24	
CG30098	serine-type endopeptidase	2.21*	
CG11836	serine-type endopeptidase	2.14*	
CG10232	serine-type endopeptidase	2.11	
CG8870	serine-type endopeptidase	2.09	
CG17404	serine-type endopeptidase		2.67
CG4998	serine-type endopeptidase		2.64
CG7542	serine-type endopeptidase		2.37
CG10663	serine-type endopeptidase		2.29
CG14227	serine-type endopeptidase		2.13
CG30090	serine-type endopeptidase		2.08
CG6687	*Serpin 88Eb (Spn88Eb)*	2.53	2.28
Stress Response			
CG9438	*Cytochrome P450-6a2 (Cyp6a2)*		5.48
CG9964	*Cytochrome P450-309a1 (Cyp309a1)*		4.75
CG4105	*Cytochrome P450-4e3 (Cyp4e3)*		3.41
CG8687	*Cytochrome P450-6a14 (Cyp6a14)*		3.36
CG30489	*Cytochrome P450-12d1-p (Cyp12d1-p)*		3.06
CG8540	*Cytochrome P450-316a1 (Cyp316a1)*		3.04
CG33503	*Cytochrome P450-12d1-d (Cyp12d1-d)*		2.99
CG8453	*Cytochrome P450-6g1 (Cyp6g1)*		2.77
CG14728	*Cytochrome P450-315a1 (Cyp315a1)*		2.35
CG18559	*Cytochrome P450-309a2 (Cyp309a2)*		2.30
CG10242	*Cytochrome P450-6a23 (Cyp6a23)*		2.08
CG12242	*Glutathione S transferase D5 (GstD5)*	7.39	
CG4423	*Glutathione S transferase D6 (GstD6)*	2.35	
CG17531	*Glutathione S transferase D7 (GstD7)*	2.03	
CG2830	*Heat shock protein 60 (Hsp60B)*		13.05
CG7756	*Heat shock protein cognate 2 (Hsc70-2)*		8.74
CG2559	*Larval serum protein 1 (Lsp1alpha)*		2.35
CG4178	*Larval serum protein 1 (Lsp1beta)*	2.01	3.04
CG6806	*Larval serum protein 2 (Lsp2)*	2.11	6.78
CG31509	*Turandot A (TotA)*	4.15	
CG31508	*Turandot C (TotC)*	6.33	
CG14027	*Turandot M (TotM)*	3.57	2.72
CG31193	*Turandot X (TotX)*	2.84	
Miscellaneous Innate Immune Response			
CG9538	*Antigen 5-related (Ag5r)*	16.96	
CG1180	*Lysozyme E (LysE)*	14.96	
CG33109		6.87	
CG18096	*Thiolester containing protein I (TepI)*	5.38	2.90
CG11086	*GADD45*	3.94	
CG18816	*Tetraspanin 42Eb (Tsp42Eb)*	3.28	
CG13335		2.91	3.06
CG3397		2.89	3.49
CG7738	immune induced peptide	2.82	3.27
CG15678	*poor IMD response upon knock-in (PIRK)*	2.77	2.20
CG4269	immune induced peptide	2.68	2.27
CG9116	*Lysozyme P (LysP)*	2.50*	
CG18550	*yellow-f*	2.44	
CG17107	immune induded peptide	2.25	2.76
CG17795	*methuselah-like 2 (mthl2)*	2.23	
CG33460		2.22	
CG16978	immune induced peptide	2.17	
CG3666	*Transferrin 3 (Tsf3)*	2.13	
CG11994	*Adenosine deaminase (Ada)*	2.09	
CG18466	*Nmdmc*	2.08	2.56
CG2914	*Ets at 21C (Ets21C)*	2.04	2.15
CG3212	*Scavenger receptor class C, type IV (Sr-CIV)*		8.87
CG3699			5.42
CG5971	*Cdc6*		3.76
CG4306			3.16
CG9616	immune induced peptide		2.97*
CG5999			2.94
CG17760			2.92
CG15155			2.88
CG7702			2.87
CG18279	*Immune induced molecule 10 (IM10)*		2.36
CG6788			2.35
CG6124	*eater*		2.29
CG15066	*Immune induced molecule 23 (IM23)*		2.22
CG12990			2.11
Additional Overlapping Genes			
CG34414	*sprint (spri)*	3.35	2.04
CG13704		2.85	4.04
CG7512		2.24	10.41
CG13965		2.12	2.37
CG11538		2.10	5.68
CG5379		2.05	4.73

* *FDR P<0.14*

Table 2.3: Upregulated pathogen recognition and AMP genes			
CG #	**Gene**	***ATM[8]***	***Repo-ATMi***
Pathogen recognition genes			
CG13422	*GNBP-like*	2.05	2.06
CG11709	*PGRP-SA*	2.24	
CG9681	*PGRP-SB1*	2.65	3.47
CG14745	*PGRP-SC2*	6.45	5.22
CG7496	*PGRP-SD*	2.25	2.81
Antimicrobial peptide genes			
CG10146	*Attacin-A (AttA)*	4.16	3.11
CG18372	*Attacin-B (AttB)*	4.56	2.47
CG4740	*Attacin-C (AttC)*	3.37	2.94
CG7629	*Attacin-D (AttD)*	7.91	
CG1365	*Cecropin A1 (CecA1)*	5.07	3.85
CG1367	*Cecropin A2 (CecA2)*	2.35	
CG1878	*Cecropin B (CecB)*	8.55	
CG1373	*Cecropin C (CecC)*	7.04	2.30
CG1385	*Defensin (Def)*	3.33	
CG12763	*Diptericin (Dpt)*	2.29*	
CG10794	*Diptericin B (DptB)*	2.99*	
CG10810	*Drosomycin (Drs)*	5.11	
CG32282	*drosomycin-4 (dro4)*	2.13	
CG8175	*Metchnikowin (Mtk)*	3.01	2.26

** FDR P<0.14*

Table 2.4: Primer sequences for qPCR		
Gene	**Forward Primer (5'-3')**	**Reverse Primer (5'-3')**
Actin	CGAAGAAGTTGCTGCTCTGGTTGT	GGACGTCCCACAATCGATGGGAAG
Attacin C	CTGCACTGGACTACTCCCACATCA	CGATCCTGCGACTGCCAAAGATTG
Cecropin A1	CATTGGACAATCGGAAGCTGGGTG	TAATCATCGTGGTCAACCTCGGGC
Defensin	CCAGAGGATCATGTCCTGGTGCAT	ACTTGGAGAGTAGGTCGCATGTGG
Diptericin B	AGGATTCGATCTGAGCCTCAACGG	TGAAGGTATACACTCCACCGGCTC
Drosomycin	AGTACTTGTTCGCCCTCTTCGCTG	CCTTGTATCTTCCGGACAGGCAGT
Metchnikowin	CATCAATCAATTCCCGCCACCGAG	AAATGGGTCCCTGGTGACGATGAG
PGRP-SC2	ATCCTTCTGGCCGTACTCTTCTGC	GATCACGGCGTAGCTCAGGTAGTT

Figure 2.1. ATM^{8} kinase activity is temperature-sensitive. Shown is Western blot analysis of H2Av-pS137 in adult head extracts from flies of the indicated genotypes exposed (+) or not exposed (-) to ionizing radiation (IR). Analyses of WT, *ATM*^{8}/+, and *ATM*^{8} flies at 18°C (lanes 1-6) and 25°C (lanes 7-12) are shown. The upper panel is a short exposure of the middle panel. The bottom panel, probed for α-tubulin, served as a loading control.

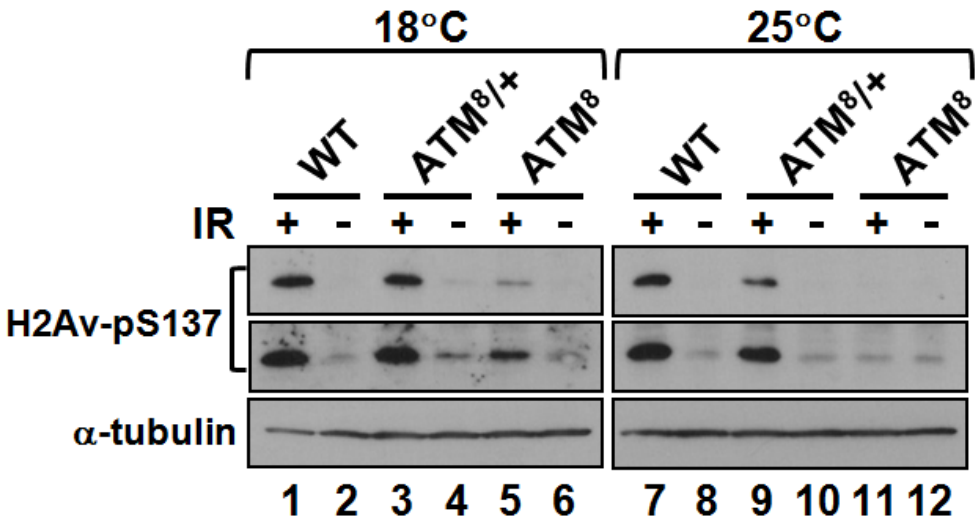
18°C
25°C
WT
ATM8/+
ATM8
WT
ATM8/+
ATM8
IR
+ - + - + - + - + - + -
H2Av-pS137
α-tubulin
1 2 3 4 5 6 7 8 9 10 11 12

Figure 2.2. Reduced ATM kinase activity causes reduced mobility and longevity. (A) Graphed is the average percent of WT, ATM^{8}/+, and ATM^{8} flies that climbed >75% (green), 50-75% (blue), 25-50% (gray), or <25% (red) of the vial height in the indicated time. Unlabeled bars had values of less than 5%. Statistical analysis by one-way ANOVA indicated a significant difference at all timepoints between ATM^{8} and WT flies ($P<0.01$). (B) Graphed is the average percent survival at the indicated number of days post-eclosion with error bars (SEM) for three independent trials of WT, ATM^{8}/+, and ATM^{8} flies. Dotted lines indicate the 50% survival point for each genotype.

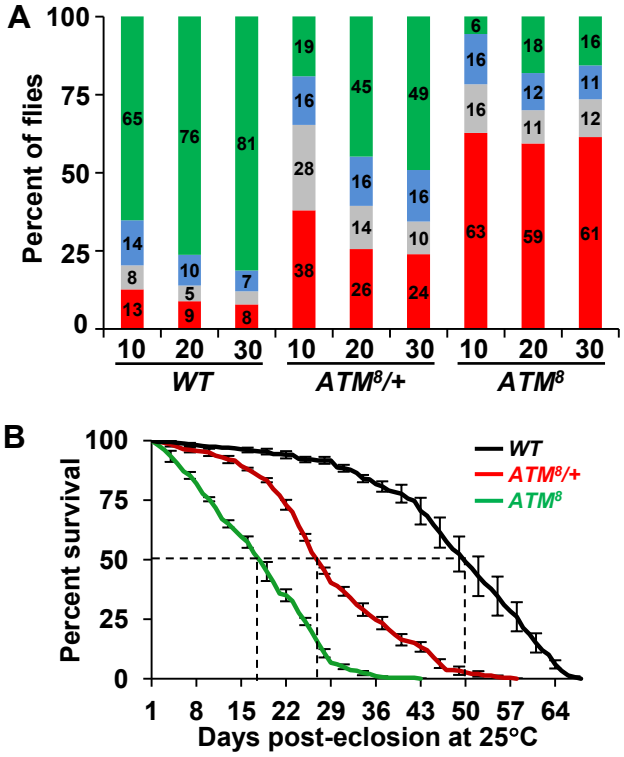
A
Percent of flies
100
75
50
25
0
65
14
8
13
76
10
5
9
81
7
8
19
16
28
38
45
16
14
26
49
16
10
24
6
16
16
63
18
12
11
59
16
11
12
61
10
20
30
10
20
30
10
20
30
WT
ATM8/+
ATM8
B
Percent survival
100
75
50
25
0
1
8
15
22
29
36
43
50
57
64
Days post-eclosion at 25°C
WT
ATM8/+
ATM8

Figure 2.3. *ATM*^{8} flies exhibit better climbing ability at 18°C than at 25°C. Graphed is the average percent of *ATM*^{8} flies raised at 18°C that climbed >75% (green), 50-75% (blue), 25-50% (gray), or <25% (red) of the vial height in the indicated time. See Figure 2.2A for climbing data from *ATM*^{8} flies at 25°C. Unlabeled bars had values of less than 5%. Statistical analysis by one-way ANOVA indicated a significant difference between *ATM*^{8} flies at 18°C and 25°C ($P<0.05$).

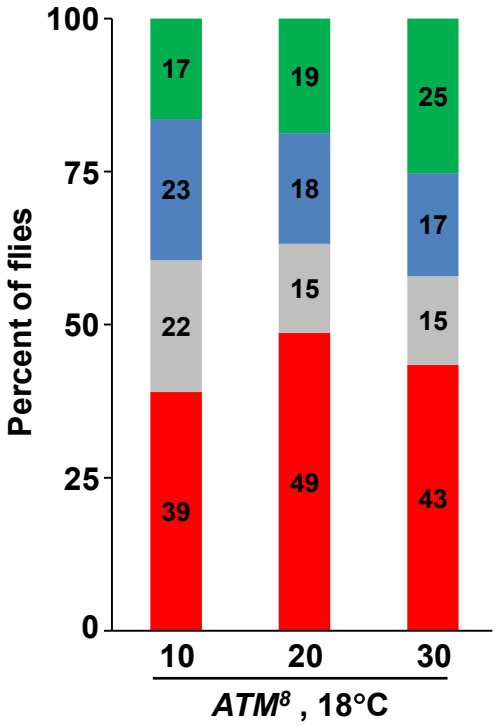
100
75
50
25
0
Percent of flies
17
23
22
39
19
18
15
49
25
17
15
43
10
20
30
ATM8 , 18°C

Figure 2.4. Reduced ATM kinase activity causes neuron and glial cell death in the adult brain. Shown are representative paraffin sections of WT, ATM^{8}/+, and ATM^{8} brains after 7 days (A-C) or 17 days (D-F) at 25°C. Holes are indicated by arrows. Images are shown of the same region of the brain and at the same magnification, with anterior at the top. Full brain sections are shown in Figure 2.5. Shown are representative immunofluorescence images of ATM^{8} brains stained for Repo and $Casp^{Act}$ (G-I) or Elav and $Casp^{Act}$ (J-L).

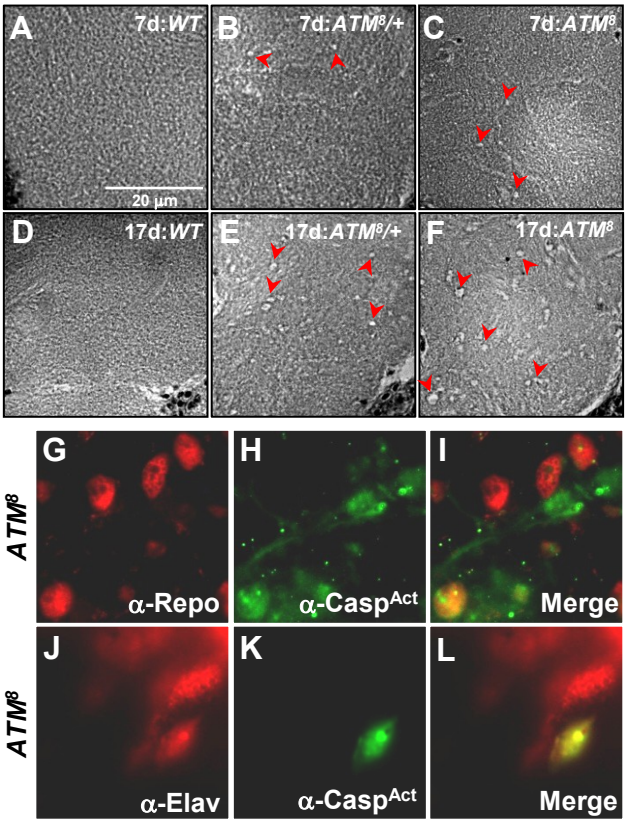
A
7d:WT
20 µm
B
7d:ATM8/+
C
7d:ATM8
D
17d:WT
E
17d:ATM8/+
F
17d:ATM8
G
α-Repo
H
α-CaspAct
I
Merge
ATM8
J
α-Elav
K
α-CaspAct
L
Merge
ATM8

Figure 2.5. Shown are representative paraffin sections of fly heads of the indicated genotypes and ages. *Elav^{C155}-GAL4* flies are denoted as *C155-GAL4*, and *Elav^{C155}-ATMi* flies are denoted as *C155-ATMi*.

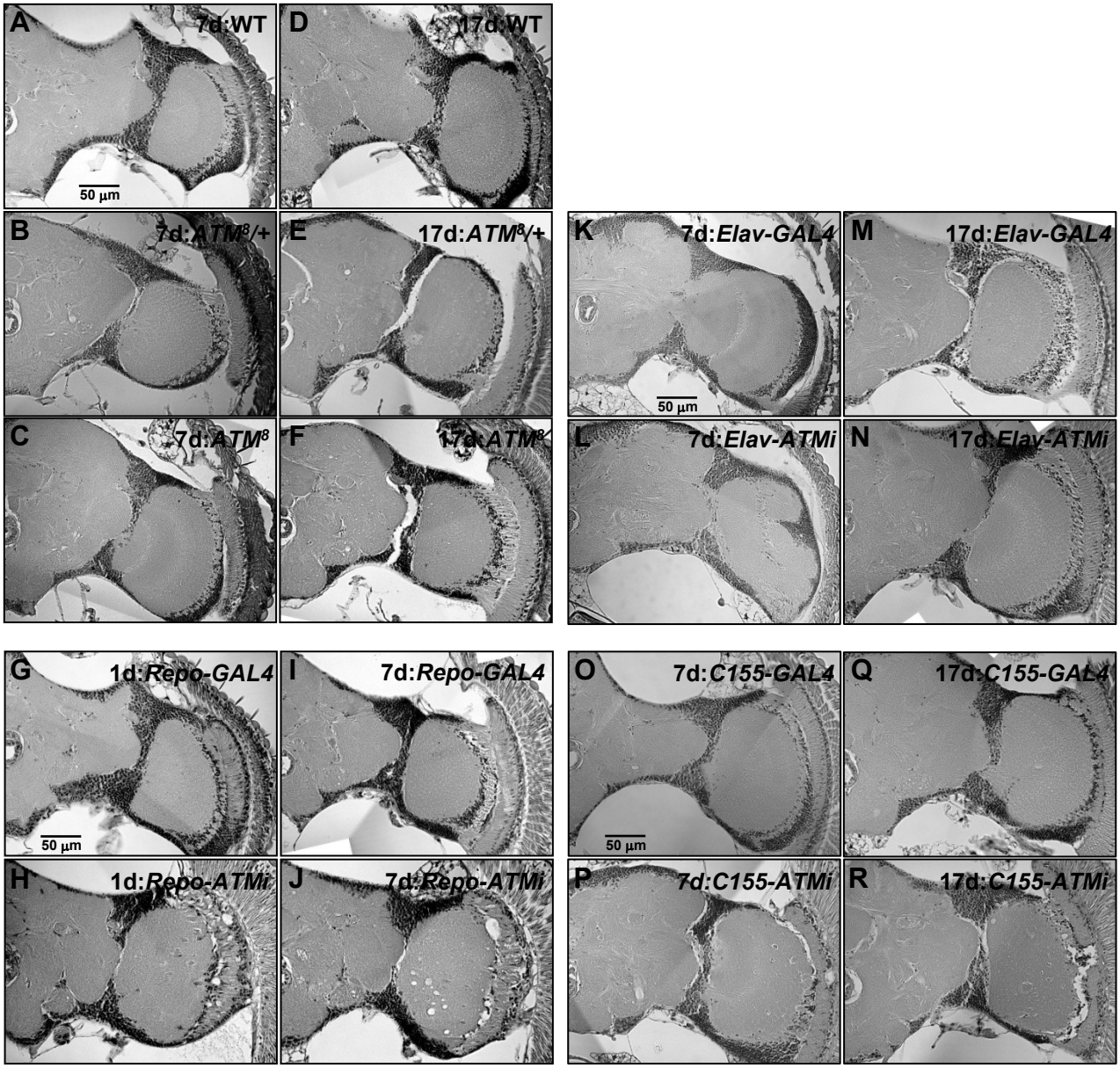
A
7d:WT
50 µm
D
17d:WT
B
7d:ATM8/+
E
17d:ATM8/+
C
7d:ATM8
F
17d:ATM8
K
7d:Elav-GAL4
50 µm
M
17d:Elav-GAL4
L
7d:Elav-ATMi
N
17d:Elav-ATMi
G
1d:Repo-GAL4
50 µm
I
7d:Repo-GAL4
H
1d:Repo-ATMi
J
7d:Repo-ATMi
O
7d:C155-GAL4
50 µm
Q
17d:C155-GAL4
P
7d:C155-ATMi
R
17d:C155-ATMi

Figure 2.6. Shown are representative immunofluorescence images of flies of the indicated genotypes stained for Repo and detecting the Cec::GFP (A), Def::GFP (B), Dro::GFP (C), Drs::GFP (D), or Mtk::GFP (E) reporter gene.

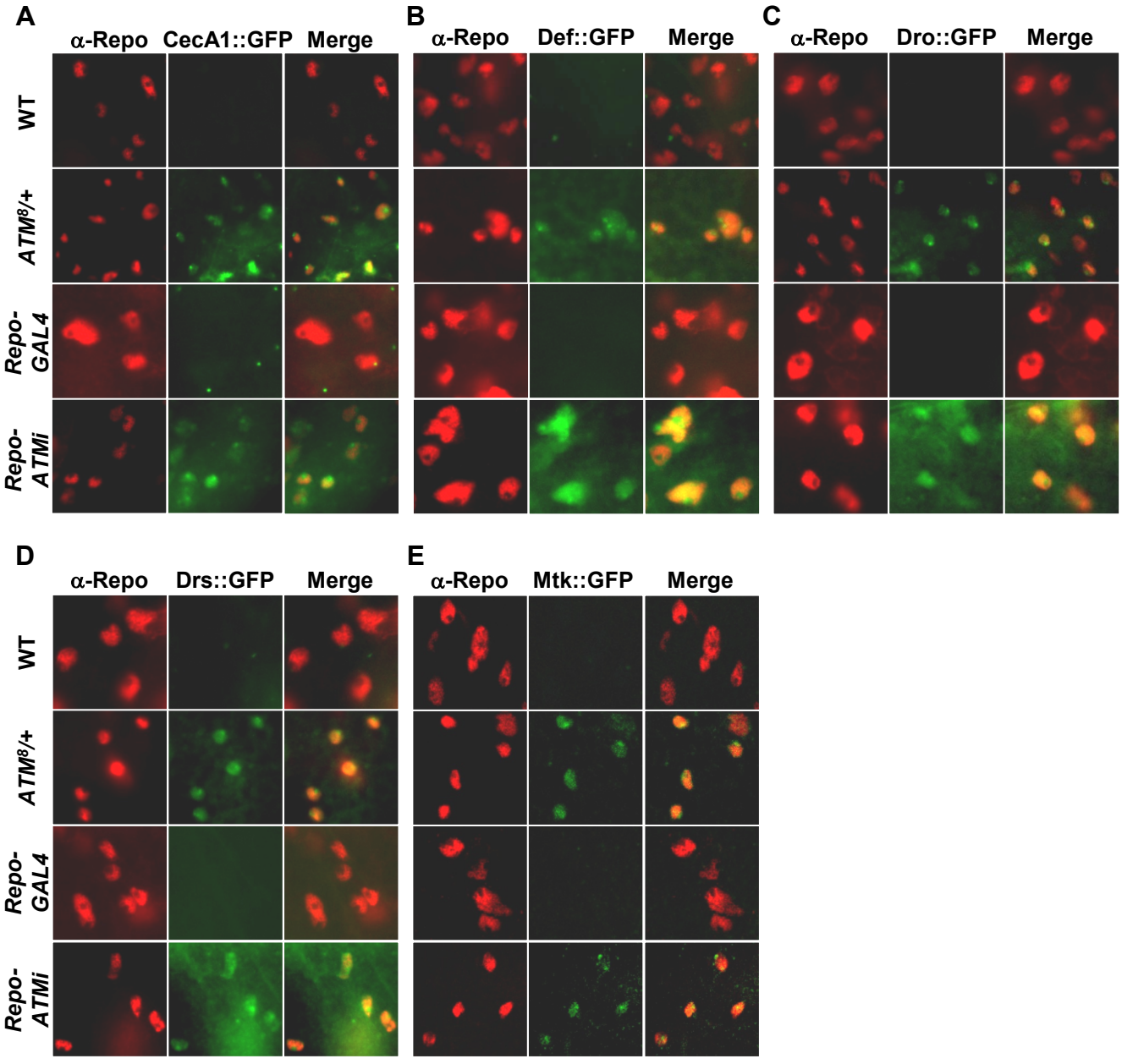
A
α-Repo
CecA1::GFP
Merge
WT
ATM^8/+
Repo-GAL4
Repo-ATMi
B
α-Repo
Def::GFP
Merge
C
α-Repo
Dro::GFP
Merge
D
α-Repo
Drs::GFP
Merge
E
α-Repo
Mtk::GFP
Merge

Figure 2.7. Reduced ATM kinase activity causes upregulation of AMP gene expression in glial cells. (A) Shown is qPCR analysis of mRNA expression in ATM^{8} heads after 0, 3, or 8 days at 25°C that was normalized to age-matched WT heads. Asterisks represent $P<0.05$, based on student's T-test analysis. Shown are representative immunofluorescence images of WT (B-D) or $ATM^{8}/+$ (E-G) brains stained for Repo and detecting the AttA::GFP reporter gene. Other AMP::GFP reporter genes are shown in Figure 2.6.

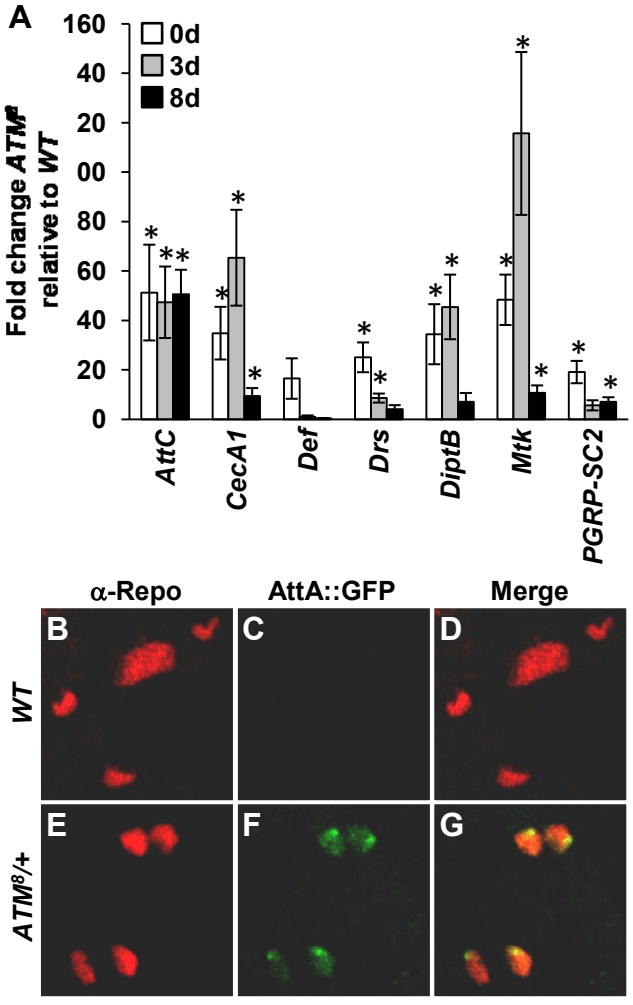
A
160
40
20
00
80
60
40
20
0
0d
3d
8d
Fold change ATM8 relative to WT
AttC
CecA1
Def
Drs
DiptB
Mtk
PGRP-SC2
α-Repo
AttA::GFP
Merge
B
C
D
E
F
G
WT
ATM8/+

Figure 2.8. *ATM* knockdown in glial cells, but not neurons, causes reduced mobility and longevity. Graphed is the average percent of *Repo-GAL4* and *Repo-ATMi* flies (A) or *Elav-GAL4* and *Elav-ATMi* flies (C) that climbed >75% (green), 50-75% (blue), 25-50% (gray), or <25% (red) of the vial height in the indicated time. See Figure 2.2A for wildtype fly climbing data. Unlabeled bars had values of less than 5%. Statistical analysis by one-way ANOVA indicated a significant difference at all timepoints between *Repo-ATMi* and *Repo-GAL4* flies ($P<0.01$) but not between *Elav-ATMi* and *Elav-GAL4* flies ($P>0.05$). Graphed is the average percent survival at the indicated number of days post-eclosion with error bars (SEM) for three independent trials of WT, *Repo-GAL4*, and *Repo-ATMi* flies (B) or WT, *Elav-GAL4*, and *Elav-ATMi* flies (D). Dotted lines indicate the 50% survival point for each genotype.

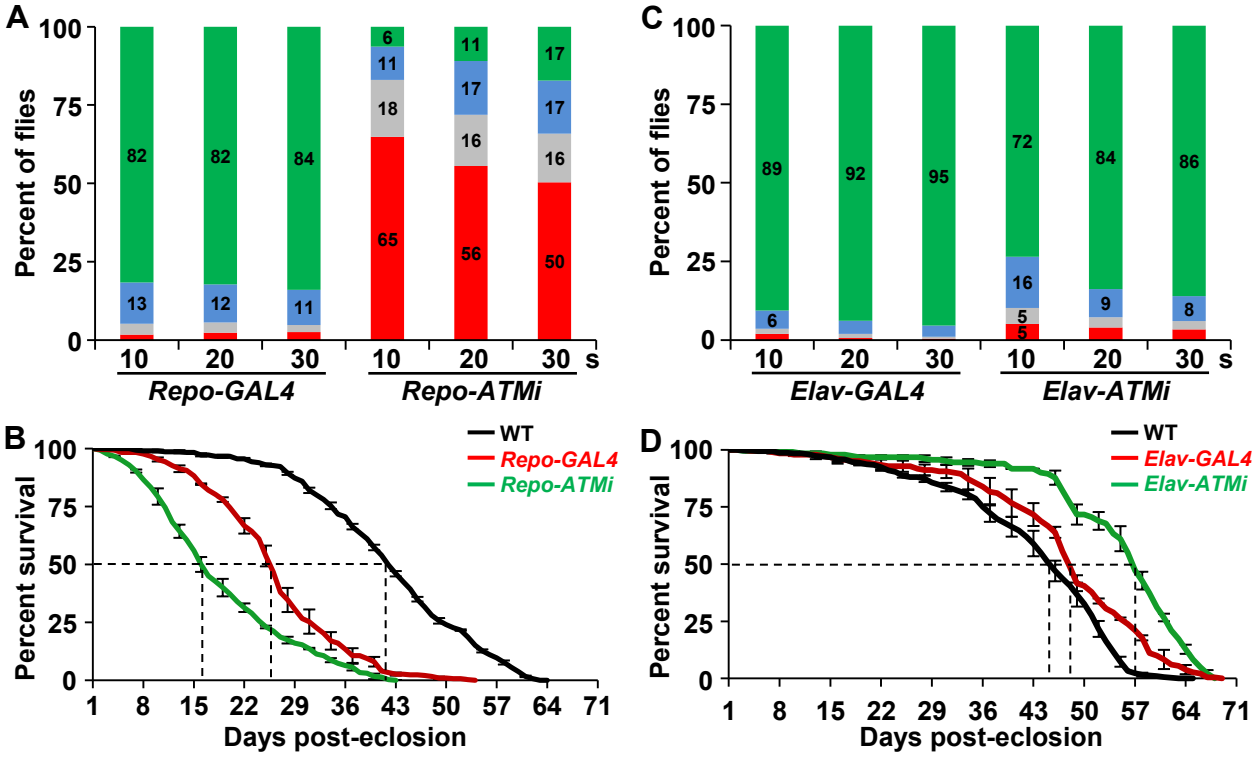
A
Percent of flies
100
75
50
25
0
82
13
82
12
84
11
6
11
18
65
11
17
16
56
17
17
16
50
10
20
30
10
20
30
s
Repo-GAL4
Repo-ATMi
C
Percent of flies
89
6
92
95
72
16
5
5
84
9
86
8
Elav-GAL4
Elav-ATMi
B
Percent survival
WT
Repo-GAL4
Repo-ATMi
1
8
15
22
29
36
43
50
57
64
71
Days post-eclosion
D
Percent survival
WT
Elav-GAL4
Elav-ATMi
Days post-eclosion

Figure 2.9. *ATM* knockdown in glial cells, but not neurons, causes neuron and glial cell death in the adult brain. Shown are representative paraffin sections of *Repo-GAL4* and *Repo-ATMi* brains (A-C) or *Elav-GAL4* and *Elav-ATMi* brains (D-F) at the indicated age in days. Holes are indicated by arrows. Images are shown of the same region of the brain and at the same magnification, with anterior at the top. Full brain sections are shown in Figure 2.5. Shown are representative immunofluorescence images of *Repo-ATMi* brains stained for Repo and $Casp^{Act}$ (G-I) or Elav and $Casp^{Act}$ (J-L).

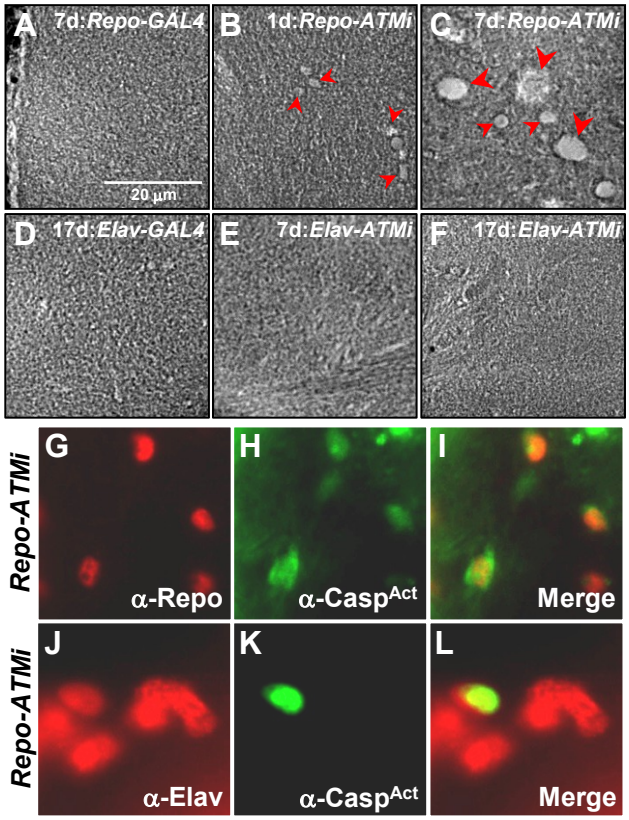
A
7d:Repo-GAL4
20 µm
B
1d:Repo-ATMi
C
7d:Repo-ATMi
D
17d:Elav-GAL4
E
7d:Elav-ATMi
F
17d:Elav-ATMi
Repo-ATMi
G
α-Repo
H
α-CaspAct
I
Merge
Repo-ATMi
J
α-Elav
K
α-CaspAct
L
Merge

Figure 2.10. Comparison of upregulated genes in *ATM*^{8} and *Repo-ATMi* flies via Gene Ontology identifies categories involving the innate immune response. P-values for *Repo-ATMi* (P1) and *ATM*^{8} (P2) are depicted for each category. Yellow categories represent significant upregulation in both microarrays while green categories represent significant upregulation only in *ATM*^{8} ($P<0.05$). Red represents not significantly altered in either array ($P>0.05$).

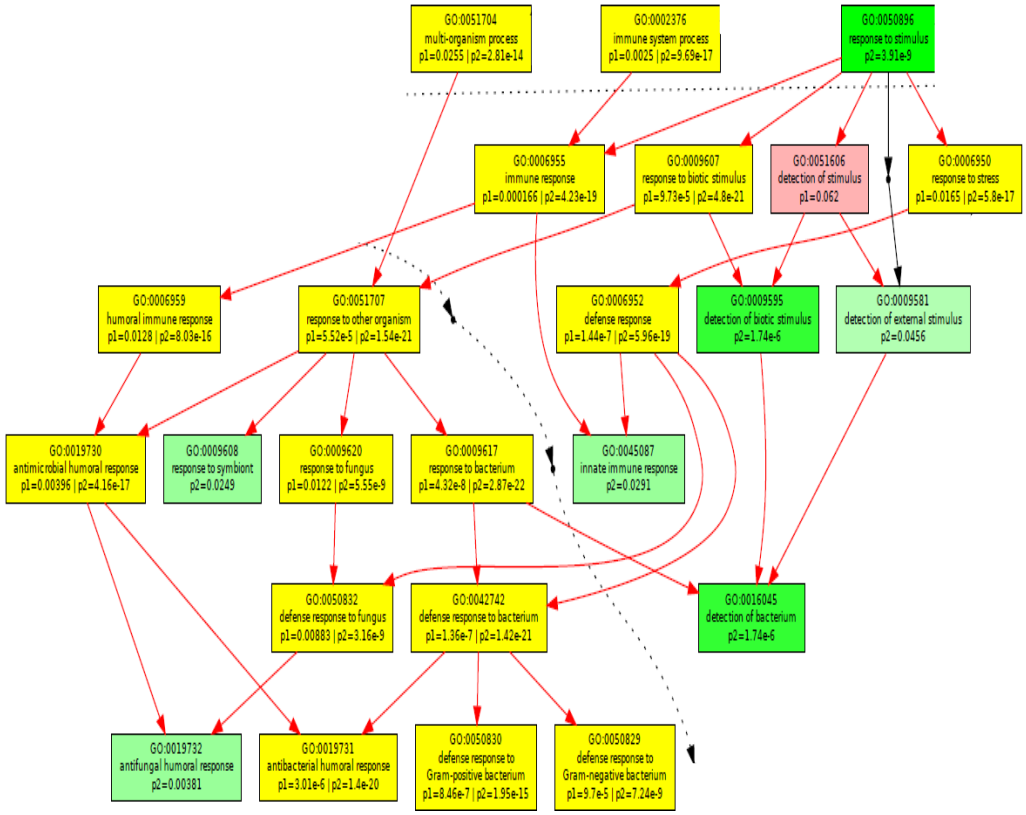
GO:0051704
multi-organism process
p1=0.0255 | p2=2.81e-14
GO:0002376
immune system process
p1=0.0025 | p2=9.69e-17
GO:0050896
response to stimulus
p2=3.91e-9
GO:0006955
immune response
p1=0.000166 | p2=4.23e-19
GO:0009607
response to biotic stimulus
p1=9.73e-5 | p2=4.8e-21
GO:0051606
detection of stimulus
p1=0.062
GO:0006950
response to stress
p1=0.0165 | p2=5.8e-17
GO:0006959
humoral immune response
p1=0.0128 | p2=8.03e-16
GO:0051707
response to other organism
p1=5.52e-5 | p2=1.54e-21
GO:0006952
defense response
p1=1.44e-7 | p2=5.96e-19
GO:0009595
detection of biotic stimulus
p2=1.74e-6
GO:0009581
detection of external stimulus
p2=0.0456
GO:0019730
antimicrobial humoral response
p1=0.00396 | p2=4.16e-17
GO:0009608
response to symbiont
p2=0.0249
GO:0009620
response to fungus
p1=0.0122 | p2=5.55e-9
GO:0009617
response to bacterium
p1=4.32e-8 | p2=2.87e-22
GO:0045087
innate immune response
p2=0.0291
GO:0050832
defense response to fungus
p1=0.00883 | p2=3.16e-9
GO:0042742
defense response to bacterium
p1=1.36e-7 | p2=1.42e-21
GO:0016045
detection of bacterium
p2=1.74e-6
GO:0019732
antifungal humoral response
p2=0.00381
GO:0019731
antibacterial humoral response
p1=3.01e-6 | p2=1.4e-20
GO:0050830
defense response to
Gram-positive bacterium
p1=8.46e-7 | p2=1.95e-15
GO:0050829
defense response to
Gram-negative bacterium
p1=9.7e-5 | p2=7.24e-9

Figure 2.11. *ATM* knockdown in glial cells causes upregulation of AMP gene expression in glial cells. (A) Shown is qPCR analysis of mRNA expression in *Repo-ATMi* heads after 0, 3, or 8 days that was normalized to age-matched *Repo-GAL4* heads. Asterisks represent $P<0.05$ based on student's T-test analysis. Shown are representative immunofluorescence images of *Repo-GAL4* (B-D) or *Repo-ATMi* (E-G) brains stained for Repo and detecting the AttA::GFP reporter gene. Other AMP::GFP reporter genes are shown in Figure 2.6.

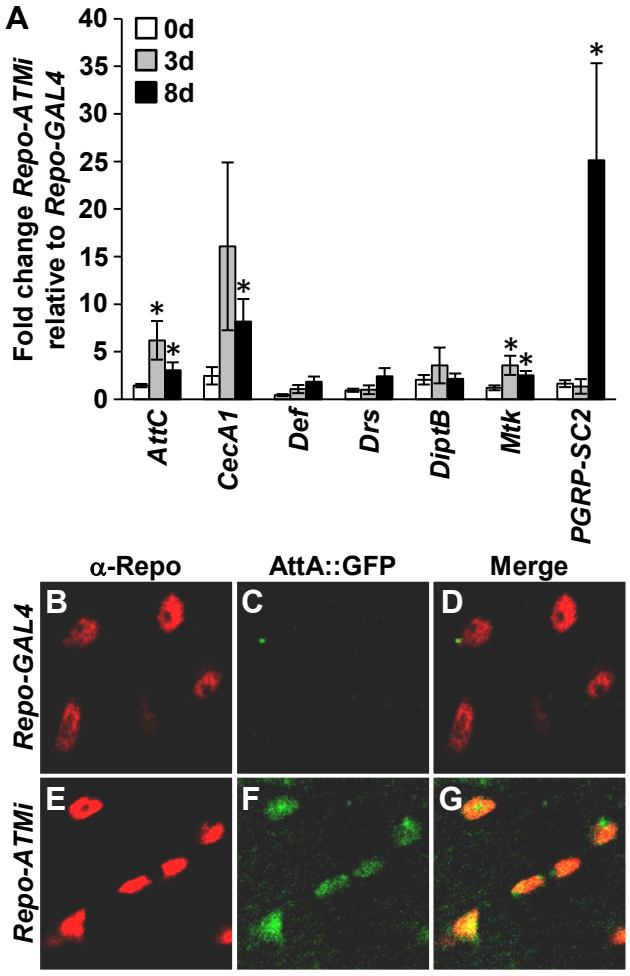
A
Fold change Repo-ATMi relative to Repo-GAL4
0d
3d
8d
40
35
30
25
20
15
10
5
0
AttC
CecA1
Def
Drs
DiptB
Mtk
PGRP-SC2
α-Repo
AttA::GFP
Merge
Repo-GAL4
Repo-ATMi
B
C
D
E
F
G

Figure 2.12. *Elav^{C155}-ATMi* flies do not exhibit characteristics of neurodegeneration. (A) Graphed is the average percent of *Elav^{C155}-GAL4* (denoted *C155-GAL4*), and *Elav^{C155}-ATMi* (denoted *C155-ATMi*) flies that climbed >75% (green), 50-75% (blue), 25-50% (gray), or <25% (red) of the vial height in the indicated time. Unlabeled bars had values of less than 5%. Statistical analysis by one-way ANOVA indicated a significant difference at 10 s between *Elav^{C155}-ATMi* and *Elav^{C155}-GAL4* flies ($P<0.01$) but no significant difference at 20 or 30 s ($P>0.05$). See Figure 2.2A for wildtype fly climbing data. (B) Graphed is the average percent survival at intervals post-eclosion with error bars (SEM) for three independent trials of WT, *Elav^{C155}-GAL4*, and *Elav^{C155}-ATMi* flies. Dotted lines indicate the 50% survival point for each genotype. *Elav^{C155}-ATMi* and *Elav^{C155}-GAL4* flies had similar longevity ($P=0.47$). Shown are representative *Elav^{C155}-GAL4* and *Elav^{C155}-ATMi* brains after 7 days (D) or 17 days (C and E) of age. Abnormalities are indicated by arrows. Images are shown of the same region of the brain at the same magnification with anterior at the top.

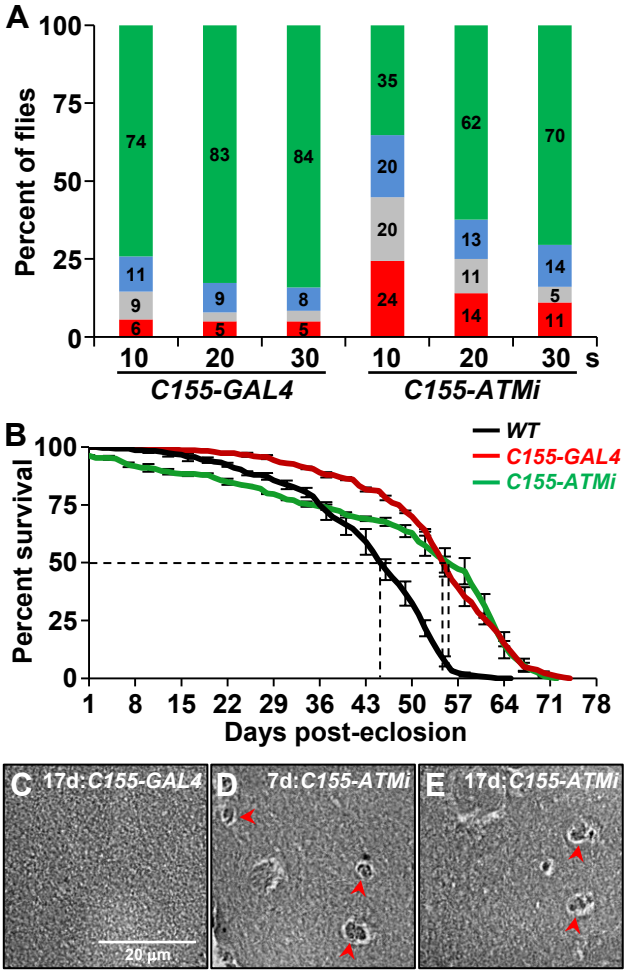
A
Percent of flies
100
75
50
25
0
74
11
9
6
83
9
5
84
8
5
35
20
20
24
62
13
11
14
70
14
5
11
10
20
30
10
20
30
s
C155-GAL4
C155-ATMi
B
Percent survival
WT
C155-GAL4
C155-ATMi
1
8
15
22
29
36
43
50
57
64
71
78
Days post-eclosion
C 17d:C155-GAL4
20 μm
D 7d:C155-ATMi
E 17d:C155-ATMi

Figure 2.13. *Elav-ATMi* and *Elav^{C155}-ATMi* do not upregulate innate immune response genes. (A) Shown is qPCR analysis of mRNA expression in *Elav-ATMi* heads after 0, 3, or 8 days at 25°C that was normalized to age-matched *Elav-GAL4* heads. (B) Shown is qPCR analysis of mRNA expression in *Elav^{C155}-ATMi* heads after 0, 3, or 8 days at 25°C that was normalized to age-matched *Elav^{C155}-GAL4* heads. Based on student's T-test analysis, no significant changes in gene expression occurred between experimental and control flies.

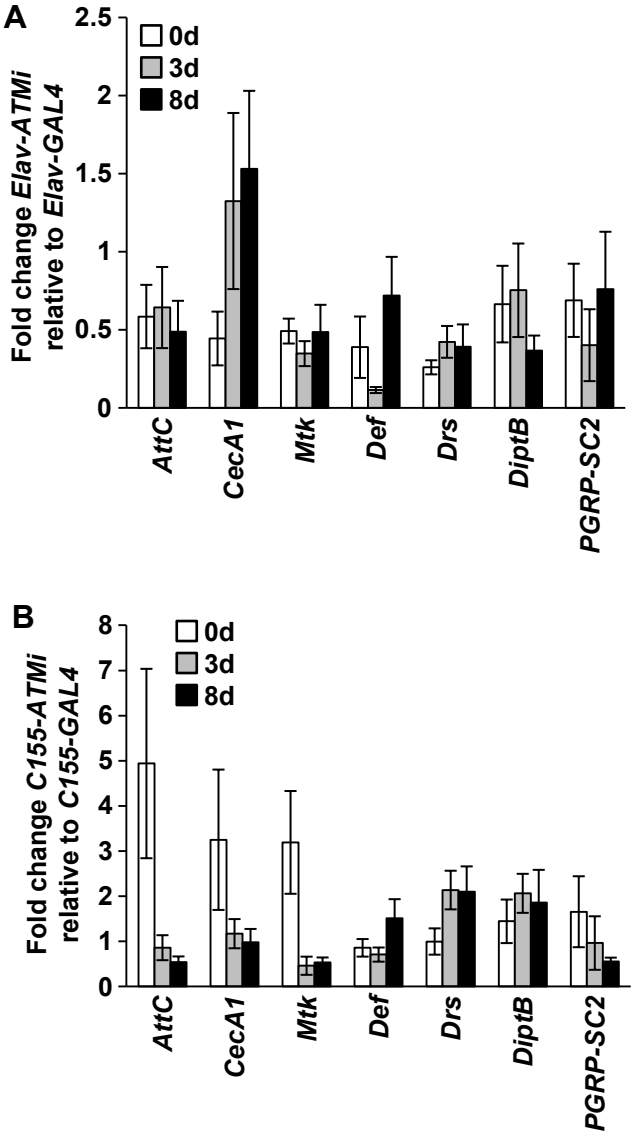
A
Fold change Elav-ATMi relative to Elav-GAL4
0d
3d
8d
2.5
2
1.5
1
0.5
0
AttC
CecA1
Mtk
Def
Drs
DiptB
PGRP-SC2
B
Fold change C155-ATMi relative to C155-GAL4
0d
3d
8d
8
7
6
5
4
3
2
1
0
AttC
CecA1
Mtk
Def
Drs
DiptB
PGRP-SC2

Chapter Three

The innate immune response transcription factor Relish is necessary for neurodegeneration in a *Drosophila* model of Ataxia-telangiectasia

This chapter was submitted in:

Petersen AJ, Katzenberger RJ, and Wassarman DA. (2012) The innate immune response transcription factor Relish is necessary for neurodegeneration in a *Drosophila* model of Ataxia-telangiectasia*. Genetics*. *Under review.*

R.J.K. performed the experiments for Figures 3.1B, 3.2A, 3.2B, and 3.3. A.J.P. performed the statistics for and compiled Figures 3.2A, 3.2B, and 3.3 and performed the experiments for all other figures and tables. A.J.P. wrote the text and revised it with D.A.W.

3.1 Abstract

Neurodegeneration is a hallmark of the human disease Ataxia-telangiectasia (A-T), which is caused by mutation of the *A-T mutated* (*ATM*) gene. To determine the molecular mechanisms underlying neurodegeneration in A-T, we have characterized fruit flies, *Drosophila melanogaster*, that contain conditional *ATM* alleles. We previously found that ATM inactivation in glial cells results in cell autonomous activation of the innate immune response and cell non-autonomous neurodegeneration in the adult fly brain. Here, we present three types of data indicating that activation of the innate immune response in glial cells causes neurodegeneration in ATM-deficient flies. First, the level of neurodegeneration in ATM-deficient flies was directly correlated with the level of expression of innate immunity genes. Second, mutation of the NF-κB transcription factor Relish, an essential effector of the Imd innate immune response pathway, reduced innate immunity gene expression and neurodegeneration in ATM-deficient flies. Third, overexpression of a constitutively active form of Relish in glial cells was sufficient to activate expression of innate immunity genes and cause vacuolar-like holes in the brain, a common feature of neurodegeneration in flies. Other data bring into question the role of Imd in Relish activation and which transcriptional targets of Relish are involved in triggering neurodegeneration. Taken together, these data add A-T to a growing list of human diseases in which an NF-κB-mediated innate immune response has been implicated in promoting neurodegeneration.

3.2 Introduction

Ataxia-telangiectasia (A-T) is a rare human disease characterized by progressive degeneration of Purkinje and granule neurons in the cerebellum (Sedgwick and Boder 1960; Bundey 1994; McKinnon 2004). A-T is caused by recessive mutation of the *A-T mutated* (*ATM*)

gene, which encodes a protein kinase (Savitsky *et al.* 1995). The molecular mechanisms underlying neurodegeneration in A-T are not well understood but probably involve events that go awry in neurons and glial cells due to inadequate phosphorylation of ATM substrate proteins. ATM phosphorylates hundreds of proteins in response to DNA damage, most notably proteins that initiate cell cycle checkpoints, DNA damage repair mechanisms, and apoptotic pathways (Bakkenist and Kastan 2003; Matsuoka *et al.* 2007; Derheimer and Kastan 2010; Bhatti *et al.* 2011).

In an effort to understand the molecular mechanisms underlying neurodegeneration in A-T, we have used *Drosophila melanogaster* as a model experimental system. We have analyzed the brains of ATM^{8} and *Repo-ATMi* flies that have reduced ATM kinase activity. ATM^{8} is a temperature-sensitive allele (Pedersen *et al*. 2010). When ATM^{8} flies are cultured at 25°C they are pupal lethal, but when cultured at 18°C they are viable. ATM^{8} homozygous flies that are cultured at 18°C and shifted to 25°C post-eclosion have dramatically reduced ATM kinase activity, as assayed by phosphorylation of serine 137 (pS137) in histone H2Av in response to ionizing radiation (IR)-induced DNA damage (Joyce *et al.* 2011; Petersen *et al*. 2012). $ATM^{8}/+$ heterozygous flies that are cultured at 18°C and shifted to 25°C post-eclosion have an intermediate level of ATM kinase activity (Petersen *et al.* 2012). *Repo-ATMi* flies have reduced ATM kinase activity in glial cells due to *ATM* knockdown by RNA interference (RNAi). *Repo-ATMi* flies contain two transgenes, a transgene that expresses an *ATM*-targeted short hairpin RNA (shRNA) under transcriptional control of GAL4 UAS sequences and a *Repo-GAL4* transgene that expresses the GAL4 transcription factor only in glial cells and drives expression of the first transgene (Xiong *et al.* 1994; Sepp *et al*. 2001; Rimkus *et al.* 2008).

Our analyses of *ATM*^{8} and *Repo-ATMi* flies indicate that ATM inactivation in glial cells causes neurodegeneration. Both *ATM*^{8} and *Repo-ATMi* flies have phenotypes that typify neurodegeneration in flies: reduced lifespan, reduced climbing ability, increased death of neurons and glial cells in the brain, and abnormal brain morphology characterized by vacuolar-like holes (Lessing and Bonini 2009; Petersen *et al*. 2012). Furthermore, gene expression analysis of adult fly heads revealed that both *ATM*^{8} and *Repo-ATMi* flies activate the innate immune response in glial cells (Petersen *et al.* 2012). The innate immune response regulates photoreceptor neuron degeneration in fly models of human retinal degeneration and Alzheimer's disease, suggesting a causative link between the innate immune response and neurodegeneration in A-T (Tan *et al*. 2008; Chinchore *et al*. 2012; Petersen and Wassarman 2012).

The innate immune response is primarily known to combat pathogens. In *Drosophila*, there are two major innate immune response pathways, the Toll pathway and the Imd (Immune deficiency) pathway (Lemaitre and Hoffmann 2007). These pathways activate different Nuclear Factor-κB (NF-κB) transcription factors to stimulate innate immunity gene expression. The Toll pathway responds to eukaryotic pathogens and gram-positive bacteria. Extracellular pathogens are recognized by peptidoglycan recognition proteins (PGRPs) and facilitate cleavage of the cytokine Spätzle, which binds to and activates the Toll receptor. Toll activation stimulates degradation of the Inhibitor of κB (IκB) protein Cactus in the cell cytoplasm, releasing the NF-κB transcription factor Dif and allowing it to enter the nucleus. In the nucleus, Dif promotes the transcription of innate immunity genes, including the antimicrobial peptide (AMP) genes that encode secreted immune response effector proteins. The Imd pathway, which is homologous to the mammalian tumor necrosis factor α (TNFα) pathway, recognizes gram-negative bacteria through membrane-bound PGRP proteins. PGRP activation signals through the Imd protein to

promote activation of the NF-κB protein Relish. Relish contains a N-terminal NF-κB motif and a C-terminal IκB motif. Activation of the Imd pathway promotes Relish cleavage, releasing the NF-κB motif from its inhibitory IκB motif. Activated Relish translocates to the nucleus and promotes the transcription of innate immunity genes, including AMP genes. In support of this mechanism, overexpression of the Relish NF-κB motif is sufficient to stimulate Relish target gene expression (DiAngelo *et al*. 2009; Wiklund *et al.* 2009). Lastly, NF-κB-independent pathways activate portions of the innate immune response, but these pathways are primarily involved in tissue-specific, constitutive expression of innate immunity genes rather than inducible pathogen-mediated expression (Tzou *et al.* 2000; Han *et al.* 2004; Ryu *et al.* 2004; Peng *et al.* 2005; Senger *et al.* 2006).

Here, we present studies that tested whether the innate immune response is required for neurodegeneration in the brain of ATM^{8} and *Repo-ATMi* flies. Specifically, we tested whether innate immunity gene expression correlates with neurodegeneration in ATM^{8} and *Repo-ATMi* flies, whether components of canonical innate immune response pathways are required for innate immunity gene expression and neurodegeneration in ATM^{8} flies, and whether activation of the innate immune response in glial cells is sufficient to promote innate immunity gene expression and neurodegeneration in flies.

3.3 Results

Differences in climbing ability are not due to variable inactivation of ATM kinase activity in ATM^{8} flies

Previously, we found that ATM^{8} and *Repo-ATMi* flies are heterogeneous in their ability to climb (Petersen *et al.* 2012). When tapped to the bottom of a vial flies naturally respond by

climbing to the top. About 50% of *ATM*^{8} or *Repo-ATMi* flies have impaired climbing ability and are unable to climb beyond the bottom quarter of a vial within 30 seconds of being tapped to the bottom, but about 15% of *ATM*^{8} or *Repo-ATMi* have normal climbing ability and are able to climb to the top quarter of a vial within 30 seconds of being tapped to the bottom. This finding suggested that ATM inactivation does not always cause neurodegeneration. To test this hypothesis, we sorted flies based on climbing ability and assayed them for other features of neurodegeneration.

A countercurrent assay, based on an assay developed by Benzer (1967), was used to separate flies into three groups: poor climbers were unable to climb to the top of a vial in any of four 1-minute trials (vial 1 in Figure 3.1A), moderate climbers were able to climb to the top of a vial between one and three times in four to seven 1-minute trials (vials 2-4), and good climbers were able to climb to the top of a vial four times in seven 1-minute trials (vials 5-8). For *ATM*^{8} and *Repo-ATMi* flies, 55% and 70% were poor climbers, 30% and 16% were moderate climbers, and 15% and 14% were good climbers, respectively. In contrast, for control w^{1118} flies, which have a wildtype *ATM* gene, 13% were either poor or moderate climbers and 87% were good climbers. Since the percentage of flies in the poor, moderate, and good climber groups was similar to the percentage of flies in the bottom, middle, and top of the vial in the 30-second climbing assay, respectively, we concluded that the countercurrent method accurately separates flies based on climbing ability.

The difference in climbing ability could be due to variable inactivation of ATM. To test this possibility, we analyzed the ability of flies to carry out ATM-mediated phosphorylation of H2Av in response to IR (Joyce *et al.* 2011; Petersen *et al.* 2012). *ATM*^{8} flies that were separated by climbing ability and w^{1118} flies that were not separated were exposed to 50 Gy of IR, and

Western blot analysis was used to detect H2Av-pS137 in head extracts. As expected, no H2Av-pS137 was detected in flies not exposed to IR, and a high level of H2Av-pS137 was detected in w^{1118} flies exposed to IR (Figure 3.1B). In contrast, irrespective of climbing ability, H2Av-pS137 was not detected in ATM^{8} flies exposed to IR, indicating that differences in climbing ability are not due to variable inactivation of ATM kinase activity.

Climbing ability correlates with other neurodegenerative phenotypes in *ATM^{8}* and *Repo-ATMi* flies

Differences in climbing ability among ATM^{8} and *Repo-ATMi* flies could be due to variable levels of neurodegeneration. To determine if climbing ability reflects the severity of neurodegeneration, we subjected countercurrent-separated flies to three assays for neurodegeneration. First, fly heads were embedded in paraffin and thin sections of the brain were analyzed for vacuolar-like holes, a common feature of neurodegeneration (Lessing and Bonini 2009). Analysis of ATM^{8} and *Repo-ATMi* flies failed to show obvious differences in the number, size, or distribution of holes between poor and good climbers. Second, flies were assayed for lifespan. Commonly, neurodegeneration shortens the lifespan of flies. For both ATM^{8} and *Repo-ATMi* flies, poor climbers had significantly shorter lifespans than good climbers ($P<0.01$) and moderate climbers had intermediate lifespans (Figures 3.2A and B). Thus, climbing ability directly correlated with lifespan. Third, ATM^{8} flies were assayed for cell death in the brain. To identify cells undergoing apoptosis, brains were stained with an antibody to the activated form of Caspase-3 ($Casp^{Act}$) and analyzed by immunofluorescence microscopy (Kamada *et al.* 2005; Fan and Bergmann 2010). When flies were assayed immediately after countercurrent separation, poor climbers exhibited a higher average number of $Casp^{Act}$-positive cells than good climbers (33.5±8.4 and 16.3±4.2 cells/brain, respectively) (Figure 3.2C). If all

brains were considered, this difference was not significant (P=0.058). However, many brains in both samples showed no staining possibly because of excessive fixation. If these brains were omitted from the analysis then the difference between poor and good climbers was significant (P=0.001), with poor and good climbers averaging 60.9±8.9 and 25.4±5.3 $Casp^{Act}$-positive cells/brain, respectively. When flies were assayed four days after countercurrent separation the number of $Casp^{Act}$-positive cells was not significantly different between poor and good climbers (P=0.67). Thus, immediately after separation, climbing ability directly correlated with cell death, but this difference was lost over time. In summary, the lifespan and cell death data indicate that the climbing ability of ATM^{8} and *Repo-ATMi* flies reflects the severity of neurodegeneration: good climbing flies have less neurodegeneration than poor climbing flies. Furthermore, these data indicate that good climbing flies undergo neurodegeneration but it is delayed relative to poor climbing flies.

Climbing ability correlates with innate immunity gene expression in ATM^{8} and *Repo-ATMi* flies

Differences in climbing ability and severity of neurodegeneration among ATM^{8} and *Repo-ATMi* flies could be due to variable activation of the innate immune response. To test this possibility, we used quantitative real-time PCR (qPCR) to determine the level of innate immunity gene expression in the head of countercurrent-separated flies. Genes that were examined included AMPs (*Attacin C* (*AttC*), *Cecropin A1* (*CecA1*), *Diptericin B* (*DiptB*), and *Metchnikowin* (*Mtk*)) and *PGRP-SC2* that are targets of both the Imd and Toll pathways, *Relish* that is specific to the Imd pathway, and *Cactus* and *Dif* that are specific to the Toll pathway (Ten *et al*. 1992; Sun *et al.* 1993; Lemaitre and Hoffmann 2007). For ATM^{8} flies, *AttC*, *CecA1*, *DiptB*, *Mtk*, *PGRP-SC2*, and *Relish* were upregulated in all of the separated groups, except for *PGRP-*

SC2 in the case of poor climbing flies, but *Cactus* and *Dif* were not upregulated in any of the separated groups (Figures 3.3A and B). These data suggest that ATM inactivation turns on the Imd pathway but not the Toll pathway. Furthermore, poor climbers had significantly higher AMP gene expression than good climbers and moderate climbers had an intermediate level of expression (Figure 3.3A). Thus, the level of AMP gene expression directly correlates with the severity of neurodegeneration in ATM^{8} flies. Similar trends were observed for *Repo-ATMi* flies, but only *CecA1*, *DiptB*, and *Relish* had significantly higher expression in poor climbers relative to good climbers (Figures 3.3C and D). Taken together, these data indicate that the level of activation of the Imd pathway in glial cells determines the severity of neurodegeneration in ATM^{8} and *Repo-ATMi* flies.

Relish mutations block innate immunity gene expression in ATM^{8} and ATM^{8}/+ flies

To determine whether the Imd pathway is necessary for activation of the innate immune response in ATM-deficient flies, we examined innate immunity gene expression in ATM^{8} and ATM^{8}/+ flies that carried mutations in *Relish* (*Rel*) or *Imd*. The Rel^{E20} and Rel^{E38} alleles result from imprecise excision of a P-element (Hedengren *et al.* 1999). Both alleles eliminate the *Relish* translation start codon suggesting that they are null alleles. Since both *Relish* and ATM^{8} are on the same chromosome, recombination was performed to generated ATM^{8},Rel^{E20} and ATM^{8},Rel^{E38} double-mutant chromosomes. Western blot analysis was utilized to confirm the generation of recombinant chromosomes. To test presence of the ATM^{8} allele, H2Av-pS137 levels were tested in response to IR. H2Av-pS137 levels are normal in all WT lanes (lanes 1, 4, and 7), reduced in all ATM^{8}/+ lanes (lanes 2, 5, and 8), and absent in all ATM^{8} lanes (lanes 3, 6, and 9), indicating that the proper genotype for *ATM* is present for each (Figure 3.4A) (Petersen *et al*. 2012). To detect the presence of the Rel^{E20} or Rel^{E38} mutations, an antibody to Relish was

used. Relish protein is detected in WT lanes (lanes 1-3) but is absent in Rel^{E20} and Rel^{E38} lanes (lanes 4-6 and 7-9, respectively), indicating that the proper *Relish* genotype is present in each stock (Figure 3.4B) (Stöven *et al*. 2000).

For study of *Imd*, the $Imd^{EY08573}$ allele contains a P-element insertion within the 5' UTR, and the Imd^{10191} and Imd^{SDK} alleles have unknown lesions. However, all three alleles inhibit activation of the innate immune response by gram-negative bacteria (Taylor and Kimbrell 2007; Costa *et al.* 2009). To determine whether effects on innate immunity gene expression are specific to the Imd pathway, we examined ATM^{8} and ATM^{8}/+ flies that carried a mutation in the Toll pathway gene *Dif*. The Dif^{1} allele contains a missense mutation that is thought to inhibit the ability of Dif to interact with DNA (Rutschmann *et al.* 2000a).

qPCR analysis of RNA isolated from fly heads revealed that *Relish* mutations significantly reduced the expression of innate immunity genes in ATM^{8} and ATM^{8}/+ flies (Table 3.1). For almost all of the innate immunity genes tested, the Rel^{E20} and Rel^{E38} mutations reduced expression to near normal levels indicating that Relish is essential for transcriptional activation of innate immunity genes in ATM-deficient flies. The Dif^{1} mutation had the opposite effect, causing an increase in innate immunity gene expression in ATM^{8} and ATM^{8}/+ flies, although the increase was significant only in ATM^{8}/+ flies. These data suggest that Dif represses the ability of Relish to activate innate immunity gene expression, possibly by competing with Relish for binding to DNA. Lastly, the $Imd^{EY08573}$, Imd^{SDK}, and Imd^{10191} mutations had dramatically different effects on innate immunity gene expression in ATM^{8} and ATM^{8}/+ flies; the $Imd^{EY08573}$ and Imd^{SDK} mutations significantly reduced gene expression to near normal levels in ATM^{8}/+ flies but not in ATM^{8} flies, and the Imd^{10191} mutation did not affect gene expression in either ATM^{8}/+ or ATM^{8} flies. Thus, for Relish activation, Imd is required to a greater extent when

ATM kinase activity is reduced than when it is eliminated. This suggests that an Imd-independent mechanism activates Relish when ATM kinase activity is eliminated. Taken together, the gene expression data indicate that in response to ATM inactivation Relish is essential for transcriptional activation of innate immunity genes and that under some circumstances Dif and Imd modulate Relish activity.

Relish mutations suppress neurodegeneration in *ATM*^{8} flies

The data presented thus far indicate that expression of innate immunity genes in ATM-deficient flies correlates with neurodegeneration and that Relish is required for the expression of innate immunity genes. To determine if Relish is required for neurodegeneration in ATM-deficient flies, we examined the effect of *Relish* mutations on the neurodegeneration phenotypes of *ATM*^{8} flies. We also examined the effect of *Dif* and *Imd* mutations because these mutations had some effect on innate immunity gene expression.

In the lifespan assay, the number of days it took for 50% of the flies to die (i.e. median survival) was used as a measure of lifespan. The lifespan of *ATM*^{8} flies was not affected by *Dif* or *Imd* mutations, but it was significantly increased from 16.1 to 24.3 or 24.9 days by *Rel*^{E20} and *Rel*^{E38} mutations, respectively (Figure 3.5B). *Relish* mutations likely have an even greater suppressive effect on lifespan than observed because on their own they significantly reduced fly lifespan (Figure 3.5A). The complete lifespan graphs revealed that *Relish* mutations delayed the onset of death in *ATM*^{8} flies, suggesting that Relish functions to initiate neurodegeneration (Figure 3.6). These data indicate that Relish activation is a cause of the shorter lifespan of *ATM*^{8} flies.

In the climbing assay, flies were tapped to the bottom of an empty vial and the percentage of flies that climbed into the top three-quarters of a vial in 30 seconds was used as a measure of

climbing ability. The climbing ability of ATM^{8} flies was not affected by Rel^{E38}, Dif^{1}, $Imd^{EY08573}$, or Imd^{10191} mutations, but it was significantly increased by Rel^{E20} and Imd^{SDK} mutations (Figure 3.5D). The complete climbing graphs are presented in Figure 3.7. The lack of an effect with the Rel^{E38} mutation may be due to the fact that it had a climbing defect on its own (Figure 3.5C). These data suggest that Relish activation and possibly Imd signaling are causes of impaired climbing of ATM^{8} flies.

In the cell death assay, the number of $Casp^{Act}$-positive cells per adult brain was used as a measure of cell death. Cell death was not significantly affected by *Rel*, *Dif*, or *Imd* mutations on their own, and cell death in ATM^{8} flies was not affected by Dif^{1} or Imd^{SDK} mutations (Figures 3.8A and C). In contrast, cell death in ATM^{8} flies was significantly reduced by Rel^{E20}, Rel^{E38}, $Imd^{EY08573}$, and Imd^{10191} mutations (Figure 3.8C). Rel^{E20} and Rel^{E38} mutations also appeared to reduce cell death in ATM^{8}/+ flies, but individual significance could not be determined because one-way ANOVA analysis on the whole dataset failed to identify a significant difference (Figure 3.8B). These data indicate that Relish is required to cause cell death in the brain of ATM^{8}/+ flies and that Relish activation and probably Imd signaling cause cell death in the brain of ATM^{8} flies.

In the brain morphology assay, the number, size, and distribution of holes in the central brain was used as a measure of brain morphology. Heads from five flies for each of 14 genotypes were chosen at random, embedded in paraffin, sectioned, and imaged by light microscopy. Sections from approximately the same region of the brain were photographed, the photographs were assigned coded numbers to hide the genotype, and the photographs were independently analyzed by four members of the laboratory. Each photograph was ranked from 1 to 10, with a ranking of 1 representing normal brain morphology with no holes and a ranking of 10 representing the most aberrant brain morphology based on holes. Typical examples of

paraffin sections are shown in Figures 3.9C-H. The results were highly consistent among the members of the laboratory, with an average standard error of 0.41. Furthermore, the results were consistent with our prior findings. w^{1118} flies had an average ranking of 2.0 (control flies in Figure 3.9A and C), which reflects normal brain morphology, and ATM^{8} flies had an average ranking of 6.4 (control flies in Figure 3.9B and F), which reflects an abnormal brain morphology with numerous small holes scattered throughout the central brain. The brain morphology of ATM^{8} flies was not affected by Dif^{1}, Rel^{E38}, Imd^{SDK}, or Imd^{10191} mutations but was suppressed by the Rel^{E20} mutation and enhanced by the $Imd^{EY08573}$ mutation (Figure 3.9B). The lack of an effect with the Rel^{E38} mutation may be due to the fact that it had a worse brain morphology on its own than the Rel^{E20} mutation (Figure 3.9A). These data indicate that Relish activation causes holes in the brain of ATM^{8} flies.

Overexpression of constitutively activity Relish in glial cells is sufficient to activate the innate immune response and cause neurodegeneration

The data presented thus far indicate that Relish activity in glial cells is required to activate the innate immune response and cause neurodegeneration in ATM-deficient flies. To determine whether Relish activation in glial cells is sufficient to produce these outcomes, we characterized *Repo-GAL4*,*UAS-RelD* flies that overexpressed the constitutively active Relish NF-κB motif only in glial cells (Sepp *et al*. 2001; DiAngelo *et al.* 2009). To control for effects due to overexpression, we characterized *Repo-GAL4,UAS-Relish* and *Repo-GAL4,UAS-Rel-49* flies that overexpressed full-length Relish and the Relish IκB motif, respectively, which in other contexts is not sufficient to activate the transcription of Relish target genes (Hedengren *et al.* 1999; Wiklund *et al.* 2009). To control for the cell type-specificity of the effects, we used *Elav-*

GAL4 to drive overexpression of the *UAS-RelD* transgene only in neurons (Luo *et al*. 1994; Yao *et al.* 1994).

qPCR was used to determine the level of innate immunity gene expression in the head of flies that overexpressed Relish proteins. This analysis revealed that only overexpression of constitutively active Relish, RelD, in glial cells was sufficient to activate innate immunity gene expression (Table 3.2). RelD was expressed in *Elav-GAL4,UAS-RelD* flies arguing against the possibility that the lack of an effect was due to the lack of transgene expression in neurons. These data suggest that signal-mediated cleavage of Relish in glial cells activates innate immunity gene expression in ATM^{8} and *Repo-ATMi* flies.

Analysis of paraffin sections revealed that RelD overexpression in glial cells but not in neurons caused holes in the central brain. The holes were infrequent, <5 per section, and were larger than those that typically occurred in ATM^{8} flies (Figures 3.10A-D). In addition, RelD overexpression in glial cells caused numerous very large holes in the lamina and the retina (Figure 3.10F). This is similar to the phenotype of *Repo-ATMi* flies (Figure 3.10G). Lastly, RelD overexpression in glial cells caused mislocalization of cell bodies from the periphery to the central region of the optic lobe (Figure 3.10F). Cell body mislocalization also occurred in *Repo-ATMi* flies but to a lesser extent. At this point, it is unclear why cell bodies are mislocalized and whether cell body mislocalization is relevant to neurodegeneration. Taken together, these data suggest that signal-mediated cleavage of Relish in glial cells causes neurodegeneration in ATM^{8} and *Repo-ATMi* flies.

3.4 Discussion

Insights into why neurodegeneration occurs in A-T

Our data indicate that in ATM-deficient flies a glial cell innate immune response promotes neurodegeneration. Furthermore, our data indicate that the level of activation of the innate immune response affects the severity of neurodegeneration. Flies with the same *ATM* mutation activated the innate immune response to different extents and had correspondingly different onsets and severities of neurodegeneration (Figures 3.1-3.3). This suggests that there are environmental or genetic factors that modulate the innate immune response in ATM-deficient flies. Analogous factors may underlie variability in the onset and severity of neurodegeneration in A-T patients. For example, suppressing factors may explain why some individuals with undetectable levels of ATM have mild clinical phenotypes (Lavin *et al.* 2006). Our findings also suggest that the type of interacting glial cell may dictate which neurons are susceptible to degeneration in response to ATM inactivation. Neurons that are proximal to glial cells that produce an innate immune response may be more susceptible to degeneration. In humans, microglia are the major innate immune response cells of the brain, suggesting that microglial cells in the cerebellum are a cause of increased susceptibility of Purkinje and granule cells to degeneration (González-Scarano and Baltuch 1999).

Activators of NF-κB in the process of neurodegeneration

Our data indicate that the NF-κB transcription factor Relish is required for activation of the innate immune response and neurodegeneration in ATM-deficient flies. Likewise, Chinchore *et al.* (2012) have also shown that Relish is required for activation of the innate immune response and neurodegeneration in a fly model of human retinal degeneration. However, in neither case is it known what factor substitutes for the pathogen to initiate the innate immune response or what

pathway of events is required to trigger Relish activation. We found that mutation of *Imd*, a canonical activator of Relish in response to pathogens, had variable effects on innate immunity gene expression and neurodegeneration, and Chinchore *et al.* (2012) found that mutation of *Imd* had no effect on neurodegeneration. This suggests that a non-canonical pathway activates Relish to cause neurodegeneration. This unknown pathway is likely to be specific to Relish since mutation of another NF-κB protein Dif did not reduce innate immunity gene expression in ATM-deficient flies (Table 3.1). This does not mean that Dif is not involved in neurodegeneration. In fact, Tan *et al.* (2008) have shown that Dif is required for photoreceptor neuron degeneration in a fly model of Alzheimer's disease. Additionally, we found that a *Dif* mutation significantly increased innate immunity gene expression in $ATM^{8}/+$ flies suggesting that Dif represses the ability of Relish to activate transcription in glial cells (Table 3.1). Therefore, future efforts will focus on determining the mechanisms that regulate Relish activation in ATM-deficient cells.

Relish transcriptional targets that cause neurodegeneration

Our data indicate that proteins encoded by transcriptional targets of Relish cause neurodegeneration in ATM-deficient flies. Indeed, constitutive activation of Relish in glial cells was sufficient to promote innate immunity gene expression and cause neurodegeneration (Table 3.2 and Figure 3.10). Proteins encoded by AMP genes are obvious candidates because their expression was highly increased in ATM-deficient flies and correlated with the severity of neurodegeneration (Figure 3.3 and Table 3.1). AMPs are small secreted peptides that contribute to the elimination of pathogens through mechanisms that remain largely unknown. However, it is generally believed that positively charged AMPs bind negatively charged membranes of pathogens, leading to increased membrane permeability and death (Zaiou 2007). Thus, neurodegeneration may be caused by AMP-mediated disruption of neuron membranes. Arguing

against a role for AMPs in neurodegeneration is our finding that cell death is not increased in ATM^{8}/+ flies that have a Dif^{1} mutation, despite the fact that AMP gene expression is equivalent to that of ATM^{8} flies (Figure 3.8B and Table 3.1). Furthermore, the $Imd^{EY08573}$ mutation significantly enhanced the abnormal brain morphology of ATM^{8} flies but did not affect AMP gene expression (Figure 3.9B and Table 3.1). Therefore, knowledge of the genomewide transcriptional changes caused by *Relish* mutation in ATM-deficient flies may help identify gene targets that are relevant to neurodegeneration.

3.5 Materials and Methods

Drosophila stocks and crosses

Flies were maintained on standard molasses medium at 25°C unless otherwise stated. All experiments involving ATM^{8} flies were performed on flies raised at 18°C throughout development and transferred to 25°C at 0-3 days post-eclosion. The *pWiz-ATM* construct is described by Rimkus *et al.* (2008). *Repo-ATMi* flies contained a recombined chromosome with both the *Repo-GAL4* and the $pWiz\text{-}ATM^{T4}$ transgenes. For ATM^{8} experiments with the Rel^{E20} and Rel^{E38} mutations, recombination was used to combine the mutations on a single chromosome. ATM^{8}, Rel^{E20}, Rel^{E38}, $Imd^{EY08573}$, *Repo-GAL4*, and *UAS-Relish* flies were obtained from the Bloomington Stock Center. Dif^{1} and *UAS-Rel-49* flies were provided by Barry Ganetzky (University of Wisconsin-Madison), Imd^{SDK} and Imd^{10191} flies were provided by Mimi Shirasu-Hiza (Columbia University), *UAS-RelD* flies were provided by Sara Cherry (University of Pennsylvania), and *UAS-GFP* flies were provided by Morris Birnbaum (University of Pennsylvania).

Countercurrent climbing assay

The countercurrent apparatus is diagrammed in Figure 3.1A, and is based on an apparatus developed by Benzer (1967). The apparatus consists of two sets of four fly vials that were taped together. 100 flies were loaded into the first vial of the bottom set, with the other set inverted and staggered on top of this vial. Flies were tapped to the bottom of the vial and allowed to climb for 1 minute, after which time the top set of vials was shifted over 1 vial. Flies that were able to climb into the top vial were tapped to the bottom, resulting in flies in the first and second bottom vials. This process was repeated seven times. Vials that were not engaged with another vial were plugged with cotton to prevent the flies from escaping. Flies in vials 1, 2-4, and 5-8 were designated poor, moderate, and good climbers, respectively.

Western blot analysis

For Figure 3.1B, ATM^{8} and w^{1118} flies were collected at 18°C and shifted to 25°C for 3 days. After three days, ATM^{8} flies were subjected to countercurrent-separation, but w^{1118} flies were not separated because very few were poor or moderate climbers. For Figure 3.4, flies were collected at 18°C and shifted to 25°C for 3 days. IR exposure and Western blot analysis were performed as described in Petersen *et al.* (2012). Relish antibody was obtained from the Developmental Studies Hybridoma Bank (The University of Iowa) and was used at 1:1000 concentration (Stöven *et al*. 2000).

Neurodegeneration assays

The lifespan, climbing, cell death, and brain morphology assays were performed as described in Petersen *et al.* (2012). Ranking of brain morphology was performed as described in the Results section. Statistical analysis for the lifespan assay was either log-rank analysis via the chi-square statistic (Figures 3.2A and B) or one-way ANOVA with Bonferroni post-test (Figure

3.4). Statistical analysis of the climbing, cell death, and brain morphology data was performed using one-way ANOVA with Bonferroni post-test, except for Figure 3.2C, which was analyzed using Student's t-test. Statistical analyses were performed using Prism software (Graphpad).

RNA isolation and qPCR

RNA isolation and qPCR was performed according to Petersen *et al.* (2012). Sequences of primer sets for *Cactus*, *Relish*, and *Dif* are provided in Table 3.3. Statistical analysis of the qPCR data was performed using one-way ANOVA with Bonferroni post-test.

3.6 Acknowledgements

We thank Nicole Bertram, Grace Boekhoff-Falk, Barry Ganetzky and members of his laboratory, and Randy Tibbetts, for their insights throughout the course of the research. We also thank Satoshi Kinoshita for paraffin sectioning. Flies were kindly provided by Mimi Shirasu-Hiza, Sara Cherry, Morris Birnbaum, and Barry Ganetzky. This work was supported by a grant from the NIH (R01 NS059001 to D. A. W.) and a pre-doctoral fellowship from NIH training grant T32 GM08688 (to A. J. P.).

Table 3.1: Effect of innate immunity pathway mutations on gene expression							
WT							
	w*^{1118}	***Rel*^{E20}**	***Rel*^{E38}**	***Dif*^{1}**	***Imd*^{EY08573}**	***Imd*^{SDK}**	***Imd*^{10191}**
AttC	1.0 ± 0.2	0.7 ± 0.1	40.0 ± 12.0	4.5 ± 1.2	0.3 ± 0.4	2.8 ± 0.4	0.7 ± 0.2
CecA1	1.0 ± 0.2	0.5 ± 0.2	0.4 ± 0.4	1.3 ± 0.6	0.5 ± 0.2	1.1 ± 0.2	0.2 ± 0.01
DiptB	1.0 ± 0.4	0.4 ± 0.1	1.1 ± 0.3	2.0 ± 0.3	0.6 ± 0.1	1.4 ± 0.1	0.1 ± 0.02
Mtk	1.0 ± 0.2	0.9 ± 0.4	12.8 ± 2.8	1.4 ± 0.4	1.1 ± 0.2	2.8 ± 0.5	0.8 ± 0.1
PGRP-SC2	1.0 ± 0.3	0.8 ± 0.2	0.5 ± 0.1	0.5 ± 0.1	0.7 ± 0.1	0.4 ± 0.1	0.2 ± 0.1
***ATM*^{8}/+**							
	Control	***Rel*^{E20}**	***Rel*^{E38}**	***Dif*^{1}**	***Imd*^{EY08573}**	***Imd*^{SDK}**	***Imd*^{10191}**
AttC	39.4 ± 13.1	1.7 ± 0.6	3.6 ± 0.9	223.1 ± 43.6	3.0 ± 0.9	7.3 ± 2.1	31.0 ± 10.1
CecA1	36.0 ± 13.5	0.8 ± 0.3	0.1 ± 0.1	158.3 ± 38.0	1.46 ± 0.4	4.3 ± 3.0	13.5 ± 4.0
DiptB	11.5 ± 2.7	1.0 ± 0.2	1.5 ± 0.5	54.7 ± 10.3	1.2 ± 0.3	2.5 ± 0.9	6.8 ± 1.8
Mtk	50.9 ± 10.1	4.8 ± 3.7	9.7 ± 1.7	88.0 ± 26.1	10.1 ± 2.1	4.1 ± 1.3	31.0 ± 7.1
PGRP-SC2	1.3 ± 0.4	1.0 ± 0.2	0.4 ± 0.1	8.6 ± 4.3	0.7 ± 0.3	0.4 ± 0.04	0.6 ± 0.2
***ATM*^{8}**							
	Control	***Rel*^{E20}**	***Rel*^{E38}**	***Dif*^{1}**	***Imd*^{EY08573}**	***Imd*^{SDK}**	***Imd*^{10191}**
AttC	156.5 ± 48.0	0.6 ± 0.2	4.8 ± 1.7	211.5 ± 80.1	149.7 ± 11.0	132.6 ± 35.7	189.5 ± 37.9
CecA1	65.4 ± 19.4	0.2 ± 0.1	0.1 ± 0.01	133.0 ± 38.7	141.3 ± 30.1	166.5 ± 76.3	45.0 ± 5.6
DiptB	45.5 ± 13.1	0.7 ± 0.3	0.5 ± 0.1	67.7 ± 27.3	41.8 ± 8.9	42.2 ± 8.5	51.8 ± 11.3
Mtk	134.9 ± 31.7	0.8 ± 0.4	11.1 ± 3.2	111.3 ± 34.6	132.3 ± 27.0	59.5 ± 4.9	134.2 ± 20.4
PGRP-SC2	5.7 ± 2.1	0.5 ± 0.1	0.4 ± 0.04	39.0 ± 28.1	20.0 ± 4.6	9.7 ± 4.6	4.1 ± 1.6

Green text indicates a significant increase in expression relative to the control ($P<0.05$)
Red text indicates a significant reduction in expression relative to the control ($P<0.05$)
*All values were normalized to the expression level in *w*^{1118} flies

Table 3.2: Effects on gene expression of Relish overexpression in glial cells or neurons						
	Repo-GAL4				***Elav-GAL4***	
	UAS-GFP	***UAS-Relish***	***UAS-Rel-49***	***UAS-RelD***	***UAS-GFP***	***UAS-RelD***
AttC	1.0 ± 0.4	1.1 ± 0.5	0.5 ± 0.2	84.1 ± 32.3	1.0 ± 0.3	1.1 ± 0.5
CecA1	1.0 ± 0.3	0.6 ± 0.1	1.0 ± 0.3	442.4 ± 70.7	1.0 ± 0.5	0.6 ± 0.3
DiptB	1.0 ± 0.3	0.2 ± 0.1	0.2 ± 0.1	31.5 ± 7.9	1.0 ± 0.3	0.4 ± 0.1
Mtk	1.0 ± 0.3	0.7 ± 0.3	0.7 ± 0.1	70.1 ± 19.1	1.0 ± 0.2	1.9 ± 0.6
Rel	1.0 ± 0.1	8.2 ± 1.7*	0.9 ± 0.2	20.8 ± 4.8*	1.0 ± 0.1	4.5 ± 1.8*

Values were normalized to *UAS-GFP* expression for each *GAL4* construct
Green values indicate a significant increase compared to *Repo-GAL4,UAS-GFP* and *Elav-GAL4,UAS-RelD* ($P<0.01$)
* Represents a significant increase compared to the corresponding *UAS-GFP* control ($P<0.05$)

Table 3.3: Primer sequences for qPCR		
Gene	**Forward Primer (5'-3')**	**Reverse Primer (5'-3')**
Cactus	CCGTCGAAAGCCATTTGGTCAGTC	GCTGTGGAGGATTGAACCTTGCTG
Relish	GGCATCATACACACCGCCAAGAAG	GTAGCTGTTTGTGGGACAACTCGC
Dif	CAGTTTGCTACGACCGGAGAGCTA	GAATATCCGCCAGTTGCAGAGTGC

Figure 3.1. A countercurrent method was used to separate *ATM*^{8} and *Repo-ATMi* flies based on climbing ability. (A) Shown is a schematic diagram of the countercurrent climbing apparatus. A description of the countercurrent assay is provided in the Materials and Methods. Gray dots indicate flies that began in vial 1. Indicated are the numbered vials that contained poor, moderate, and good climbers after the seven steps of the assay. (B) Shown is Western blot analysis for H2Av-pS137 in adult head extracts from control w^{1118} (lanes 1 and 2) and *ATM*^{8} (lanes 3-8) flies exposed (+) or not exposed (-) to IR. w^{1118} flies were not separated by the countercurrent assay, and *ATM*^{8} flies were separated by the countercurrent assay into poor, moderate, and good climbers. As a loading control, the same membrane was probed for α-tubulin (lower panel).

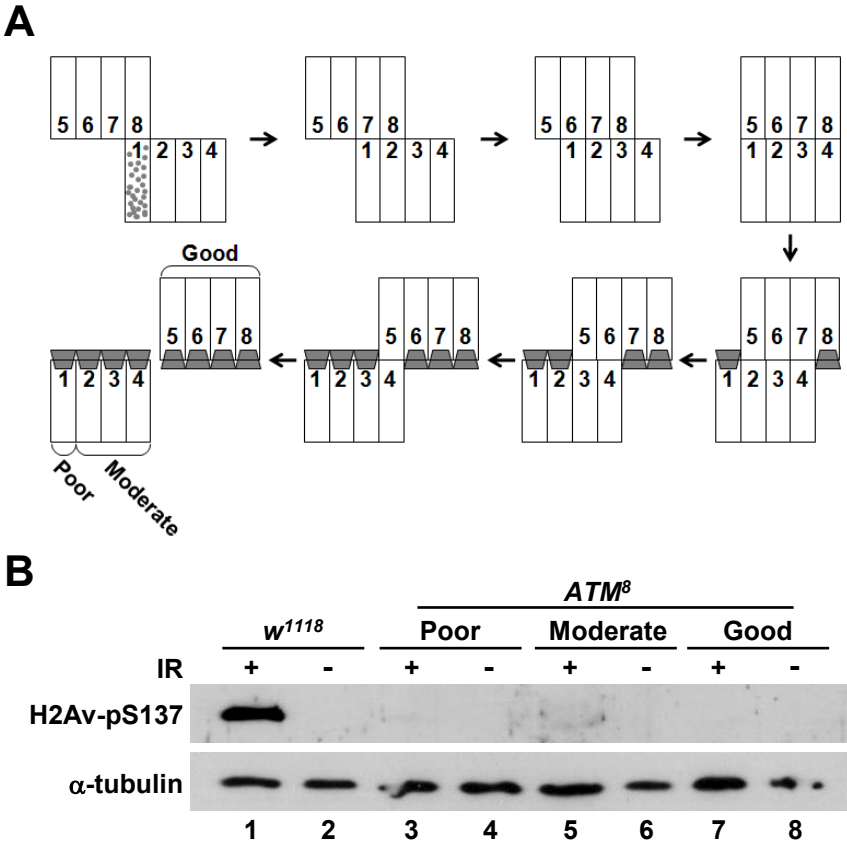
A
5 6 7 8
1 2 3 4
Good
Poor
Moderate
B
ATM8
w1118
Poor
Moderate
Good
IR
+ - + - + - + -
H2Av-pS137
α-tubulin
1 2 3 4 5 6 7 8

Figure 3.2. Lifespan correlated with climbing ability in ATM^{8} and *Repo-ATMi* flies and cell death in the brain correlated with climbing ability in ATM^{8} flies. Graphed is the lifespan of (A) ATM^{8} and (B) *Repo-ATMi* flies that were countercurrent-separated into poor, moderate, and good climber groups. For ATM^{8} flies, the analysis was performed on 409 poor climber, 178 moderate climbers, and 122 good climbers. For *Repo-ATMi* flies, the analysis was performed on 625 poor climber, 231 moderate climbers, and 197 good climbers. Error bars indicate standard errors of the mean. Dotted lines indicate the median survival for each group. The difference between ATM^{8} poor and good climbers is significant ($P<0.01$), and the difference between *Repo-ATMi* poor, moderate, and good climbers is significant for all comparisons ($P<0.01$). (C) Graphed is the number of $Casp^{Act}$-positive cells counted in the brains of ATM^{8} flies that were countercurrent-separated into poor or good climbers. Flies were assayed either 0 or 4 days after countercurrent-separation. Each dot represents a single brain. Horizontal lines indicate the average.

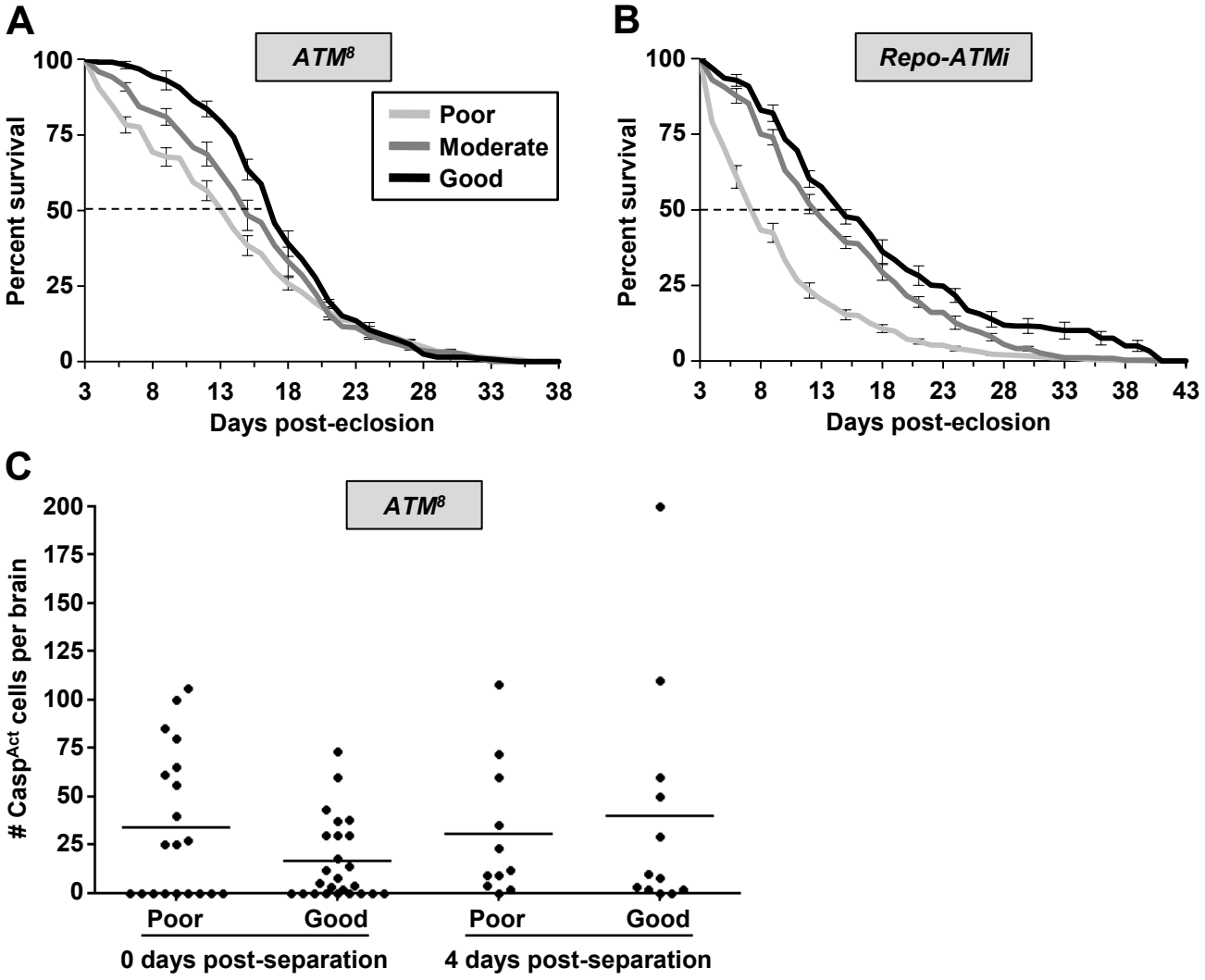
A
ATM8
Poor
Moderate
Good
Percent survival
100
75
50
25
0
3
8
13
18
23
28
33
38
Days post-eclosion
B
Repo-ATMi
Percent survival
100
75
50
25
0
3
8
13
18
23
28
33
38
43
Days post-eclosion
C
ATM8
CaspAct cells per brain
200
175
150
125
100
75
50
25
0
Poor
Good
Poor
Good
0 days post-separation
4 days post-separation

Figure 3.3. The expression of innate immunity genes correlated with climbing ability in *ATM*^{8} and *Repo-ATMi* flies. Graphed is qPCR analysis depicting the fold change in expression of the indicated genes in (A and B) *ATM*^{8} flies relative to unseparated control w^{1118} flies or in (C and D) *Repo-ATMi* flies relative to unseparated control *Repo-GAL4* flies. Note that the scale is different for each panel. Error bars indicate standard errors of the mean. Asterisks above a bar indicates a significant difference relative to the control and asterisks above a line that spans poor and good climber bars indicate a significant difference between poor and good climber groups. Single asterisks indicate $P<0.05$ and double asterisks indicate $P<0.01$ based on one-way ANOVA analysis.

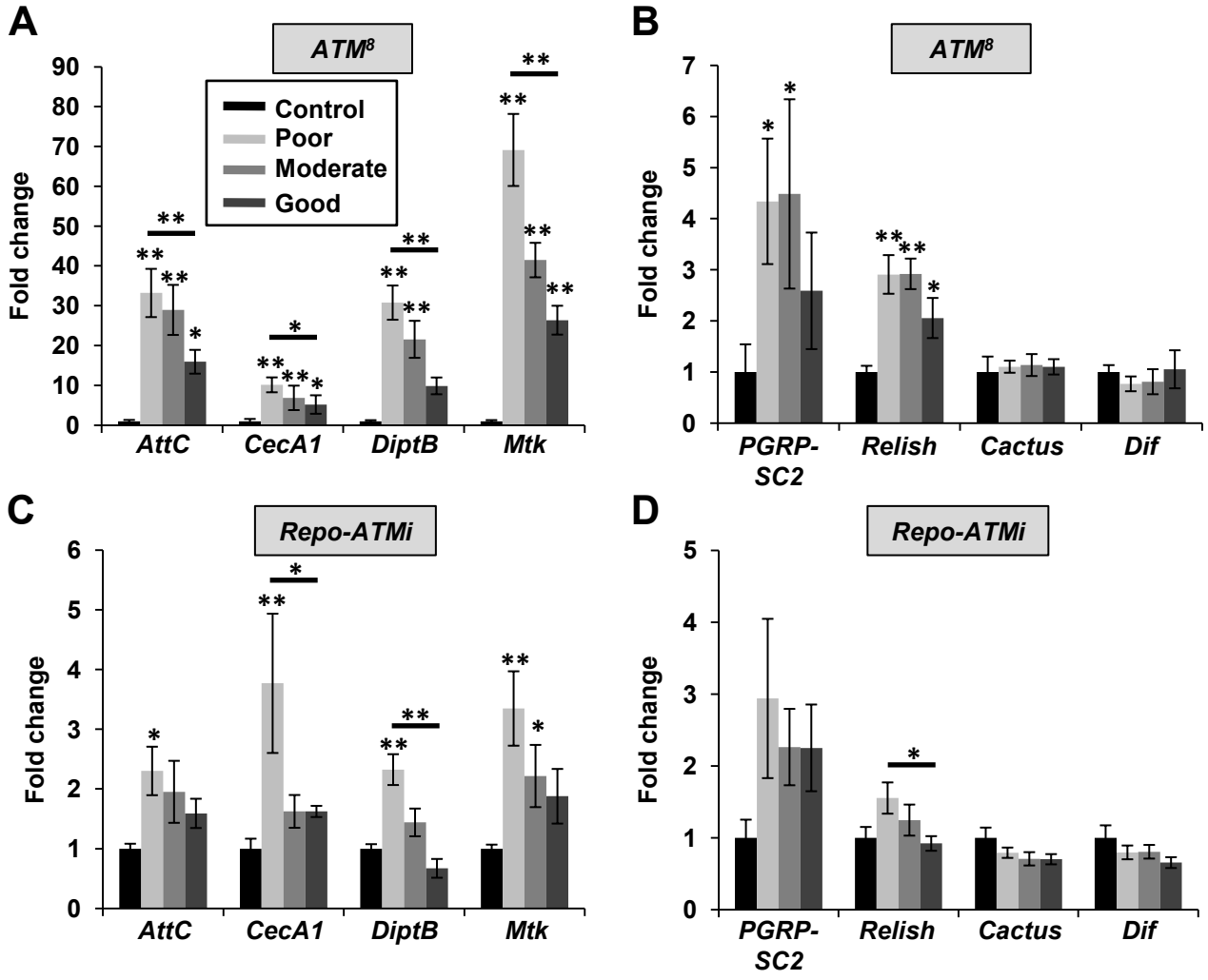
A
ATM8
Control
Poor
Moderate
Good
Fold change
AttC
CecA1
DiptB
Mtk
B
ATM8
Fold change
PGRP-SC2
Relish
Cactus
Dif
C
Repo-ATMi
Fold change
AttC
CecA1
DiptB
Mtk
D
Repo-ATMi
Fold change
PGRP-SC2
Relish
Cactus
Dif

Figure 3.4. Confirmation that the ATM^{8} allele was recombined with the Rel^{E20} and Rel^{E38} alleles. Shown is Western blot analysis for (A) H2Av-pS137 or (B) Relish in adult head extracts from control w^{1118}, ATM^{8}/+, and ATM^{8} flies exposed to IR following recombination with nothing (WT), Rel^{E20}, or Rel^{E38}. As a loading control, the same membrane was probed for α-tubulin (lower panels).

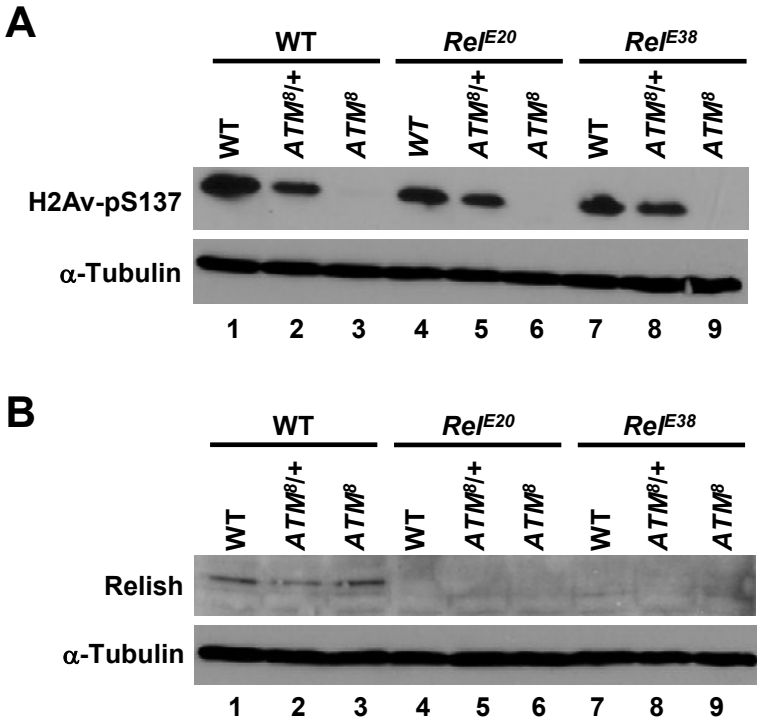
A
WT
RelE20
RelE38
WT
ATM8/+
ATM8
WT
ATM8/+
ATM8
WT
ATM8/+
ATM8
H2Av-pS137
α-Tubulin
1 2 3 4 5 6 7 8 9
B
WT
RelE20
RelE38
WT
ATM8/+
ATM8
WT
ATM8/+
ATM8
WT
ATM8/+
ATM8
Relish
α-Tubulin
1 2 3 4 5 6 7 8 9

Figure 3.5. *Relish* mutations suppressed the lifespan and climbing defects of ATM^{8} flies. (A and B) Graphed is the median survival in days of 200 flies of the indicated genotype in (A) a wildtype or (B) an ATM^{8} background. Note that the scale is different for panels A and B. Complete lifespan graphs are presented in Figure 3.6. (C and D) Graphed is the percentage of 120 flies that were able to climb higher than the bottom quarter of a vial within 30 seconds of being tapped to the bottom. Shown are flies of the indicated genotypes in (C) a wildtype or (D) an ATM^{8} background. Error bars indicate standard error of the mean. Complete climbing results are presented in Figure 3.7. For statistical analysis of panels A and C, mutant flies were compared to control w^{1118} flies. For statistical analysis of panels B and D, mutant flies were compared to control ATM^{8} flies. Single asterisks indicate $P<0.05$ and double asterisks indicate $P<0.01$, based on one-way ANOVA analysis.

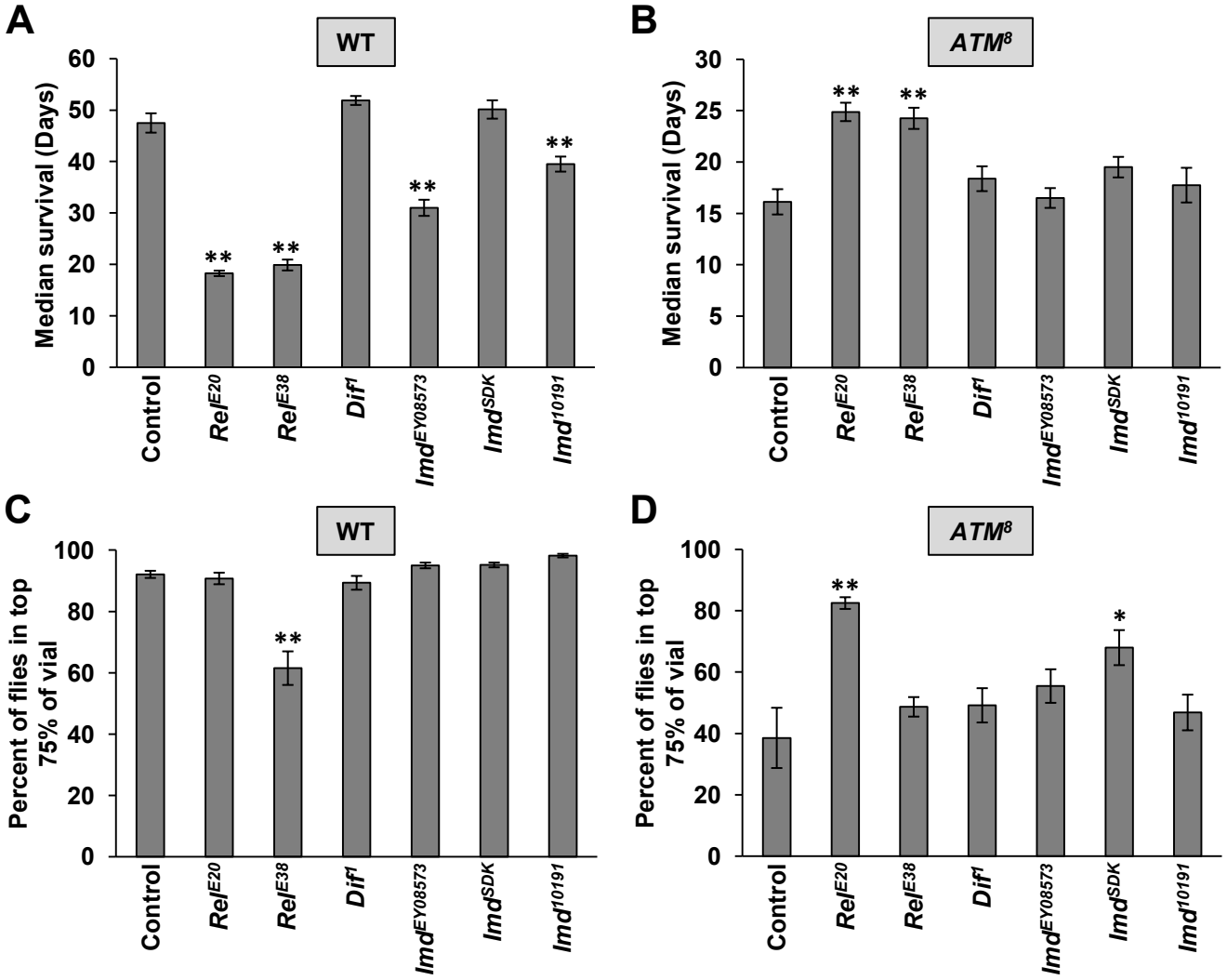
A
WT
Median survival (Days)
60
50
40
30
20
10
0
**
**
**
**
Control
Rel^E20
Rel^E38
Dif^1
Imd^EY08573
Imd^SDK
Imd^10191
B
ATM^8
Median survival (Days)
30
25
20
15
10
5
0
**
**
Control
Rel^E20
Rel^E38
Dif^1
Imd^EY08573
Imd^SDK
Imd^10191
C
WT
Percent of flies in top 75% of vial
100
80
60
40
20
0
**
Control
Rel^E20
Rel^E38
Dif^1
Imd^EY08573
Imd^SDK
Imd^10191
D
ATM^8
Percent of flies in top 75% of vial
100
80
60
40
20
0
**
*
Control
Rel^E20
Rel^E38
Dif^1
Imd^EY08573
Imd^SDK
Imd^10191

Figure 3.6. Full longevity graphs for ATM^{8} flies carrying innate immunity mutations. Graphed is the percent survival at days post-eclosion for the indicated mutants in (A and C) a wildtype or (B and D) an ATM^{8} background. 200 flies were analyzed for each genotype. Dotted lines indicate the median survival for each group.

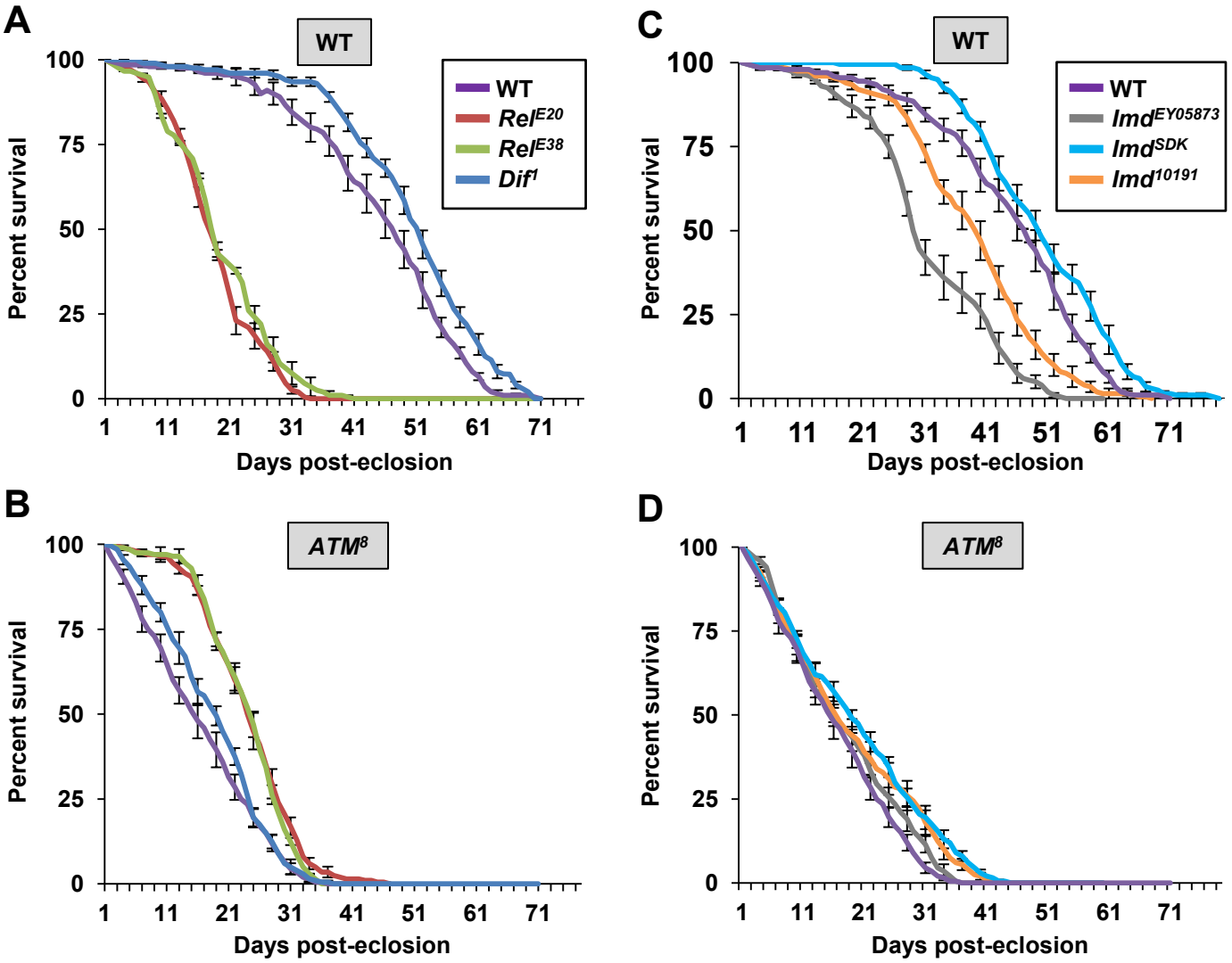
A
WT
WT
Rel^E20
Rel^E38
Dif^1
Percent survival
Days post-eclosion
B
ATM^8
C
WT
WT
Imd^EY05873
Imd^SDK
Imd^10191
D
ATM^8

Figure 3.7. Full climbing graphs of *ATM*^{8} flies carrying innate immunity mutations. Graphed is the average percent of flies of the indicated genotypes in (A) a wildtype or (B) an *ATM*^{8} background that climbed more than 75% (green), 50%-75% (blue), 25%-50% (gray), or less than 25% (red) of the height of the vial in 30 seconds. Unlabeled bars had values of less than 5%.

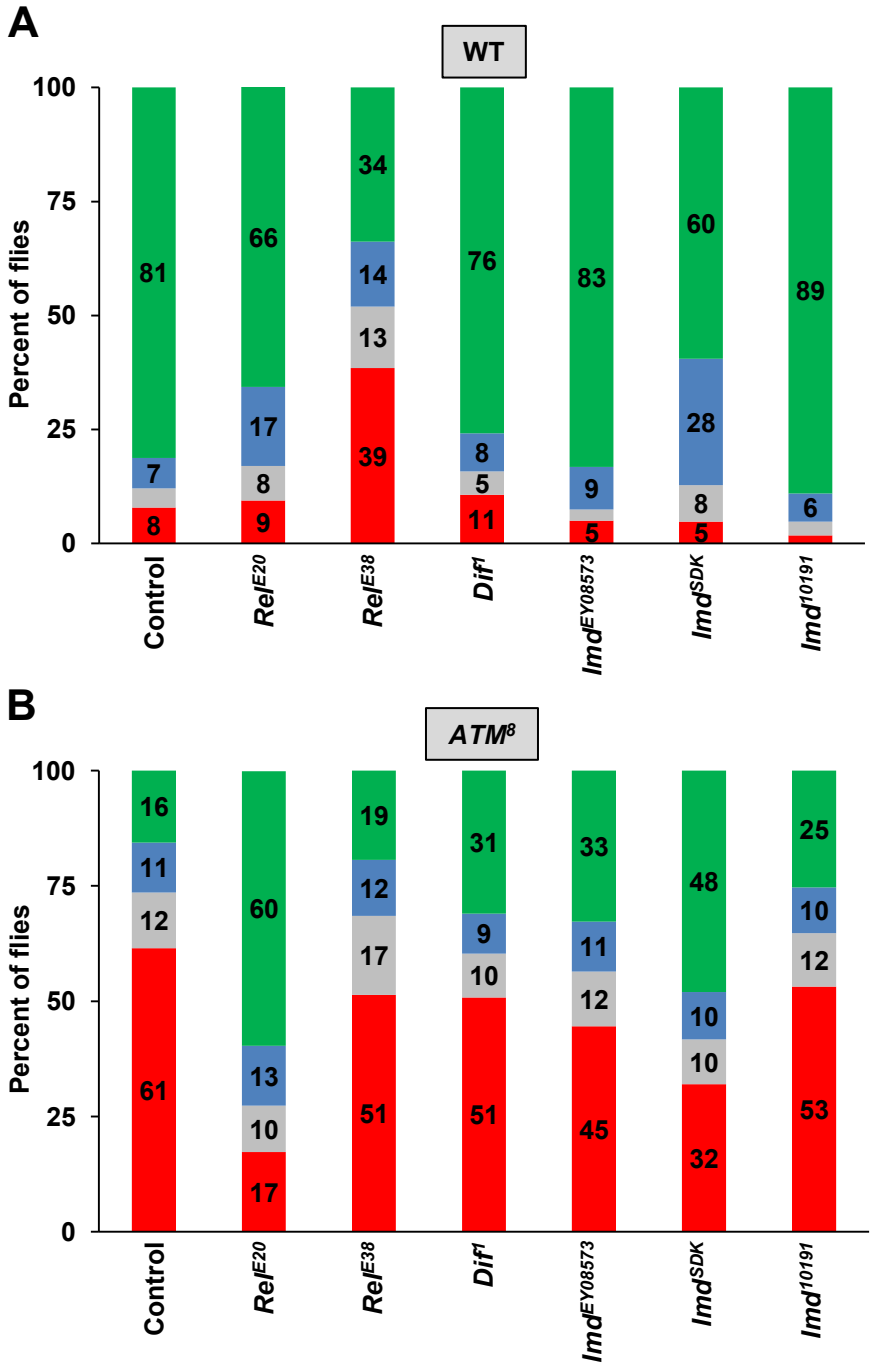
A
WT
Percent of flies
100
75
50
25
0
81
7
8
66
17
8
9
34
14
13
39
76
8
5
11
83
9
5
60
28
8
5
89
6
Control
RelE20
RelE38
Dif1
ImdEY08573
ImdSDK
Imd10191
B
ATM8
Percent of flies
100
75
50
25
0
16
11
12
61
60
13
10
17
19
12
17
51
31
9
10
51
33
11
12
45
48
10
10
32
25
10
12
53
Control
RelE20
RelE38
Dif1
ImdEY08573
ImdSDK
Imd10191

Figure 3.8. A *Relish* mutation reduced cell death in the brain of ATM^{8} flies. Graphed is the number of $Casp^{Act}$-positive cells in the brains of flies of the indicated genotype in a (A) wildtype, (B) ATM^{8}/+, or (C) ATM^{8} background. Note that the scale is different for each panel. Each dot represents a single brain. Horizontal lines indicate the average. For statistical analysis of panel A, mutant flies were compared to control w^{1118} flies. For statistical analysis of panel B, mutant flies were compared to control ATM^{8}/+ flies. For statistical analysis of panel C, mutant flies were compared to control ATM^{8} flies. Single asterisks in a gray box indicate $P<0.05$ and double asterisks in a gray box indicate $P<0.01$, based on one-way ANOVA analysis.

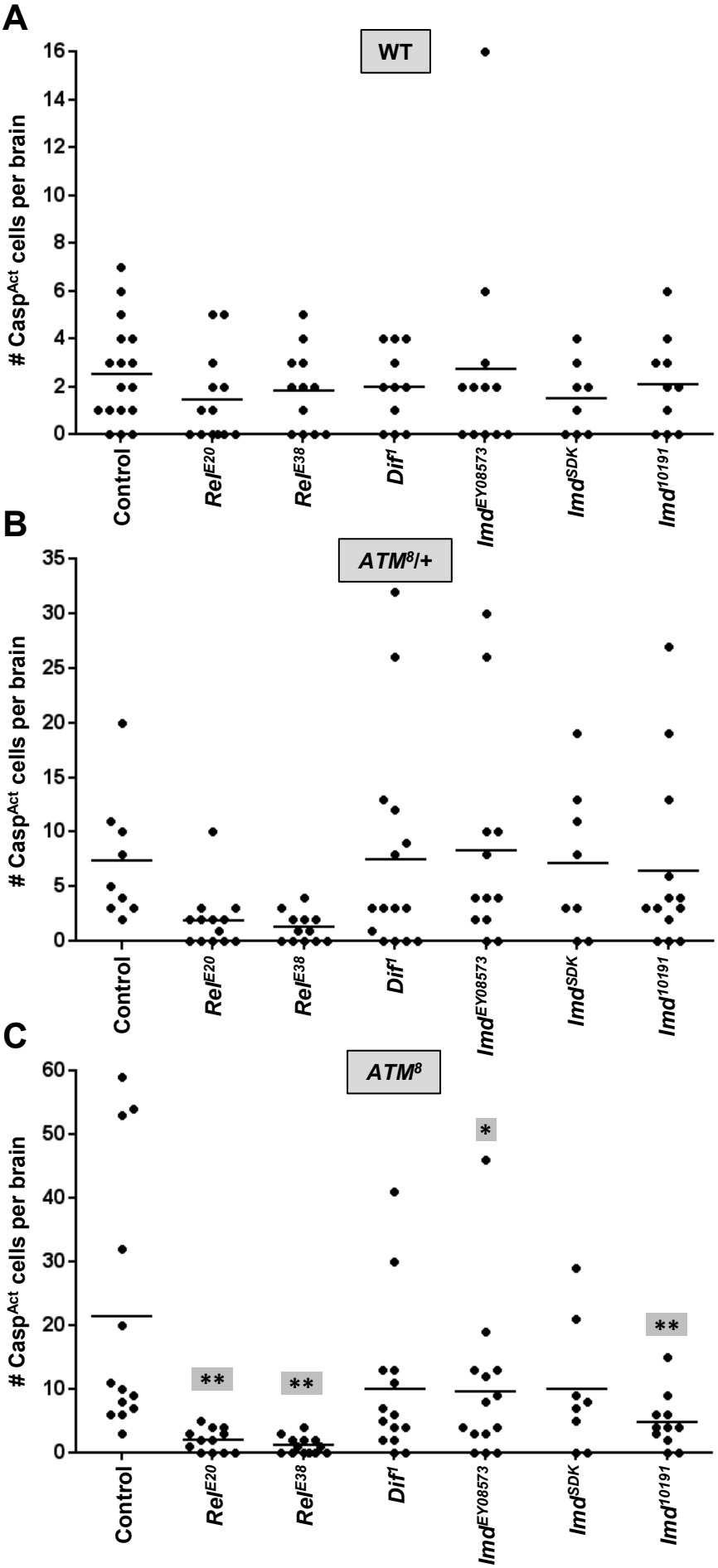
A
WT
Casp^Act cells per brain
0
2
4
6
8
10
12
14
16
Control
RelE20
RelE38
Dif1
ImdEY08573
ImdSDK
Imd10191
B
ATM8/+
Casp^Act cells per brain
0
5
10
15
20
25
30
35
Control
RelE20
RelE38
Dif1
ImdEY08573
ImdSDK
Imd10191
C
ATM8
Casp^Act cells per brain
0
10
20
30
40
50
60
**
**
*
**
Control
RelE20
RelE38
Dif1
ImdEY08573
ImdSDK
Imd10191

Figure 3.9. A *Relish* mutation suppressed the brain morphology defects of ATM^{8} flies. Graphed is the ranking of brain morphology of flies of the indicated genotype in a (A) wildtype or (B) ATM^{8} background. Rankings were based on the number, size, and distribution of holes in the central brain. A ranking of 1 indicates no holes and a ranking of 10 was the most aberrant phenotype observed. Error bars indicate standard errors of the mean. (C-H) Examples of paraffin sections, with rankings indicated in the lower right of each panel. Insets in the bottom left of panels C and H show high magnification images of the regions indicated by dotted boxes. The inset image for panel C shows tissue with no holes, and the inset image for panel H shows tissue with many small holes (i.e. white regions). For statistical analysis of panel A, mutant flies were compared to control w^{1118} flies. For statistical analysis of panel B, mutant flies were compared to control ATM^{8} flies. Single asterisks indicate $P<0.05$ and double asterisks indicate $P<0.01$, based on one-way ANOVA analysis.

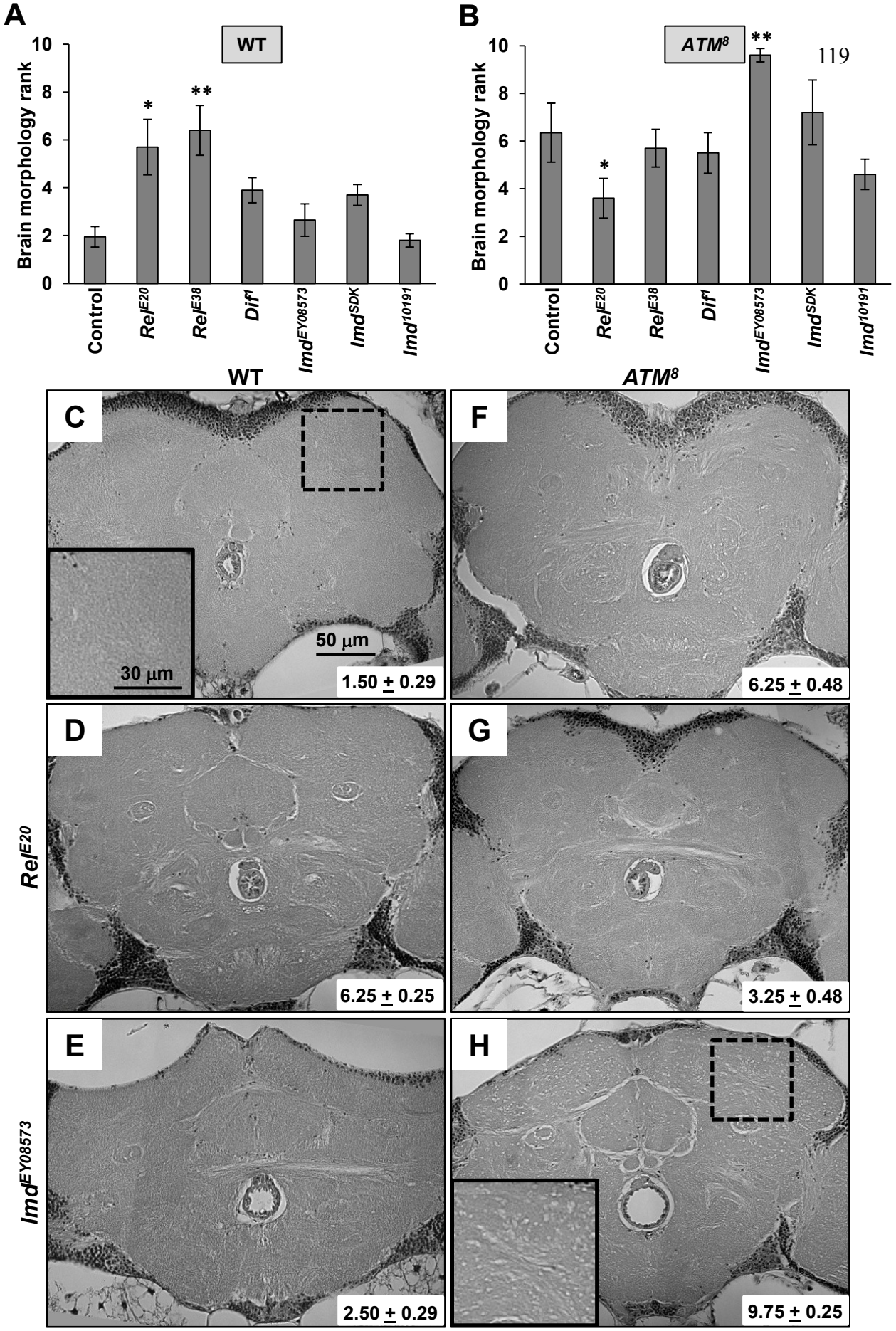
A
WT
Brain morphology rank
10
8
6
4
2
0
*
**
Control
RelE20
RelE38
Dif1
ImdEY08573
ImdSDK
Imd10191
B
ATM8
Brain morphology rank
10
8
6
4
2
0
**
*
Control
RelE20
RelE38
Dif1
ImdEY08573
ImdSDK
Imd10191
WT
ATM8
C
30 μm
50 μm
1.50 ± 0.29
F
6.25 ± 0.48
RelE20
D
6.25 ± 0.25
G
3.25 ± 0.48
ImdEY08573
E
2.50 ± 0.29
H
9.75 ± 0.25

Figure 3.10. Overexpression of a constitutively active form of Relish, RelD, in glial cells but not in neurons caused a neurodegeneration phenotype that is similar to the one caused by *ATM* knockdown in glial cells. (A-D) Examples of paraffin sections of the central brain of flies of the indicated genotypes. In panel B, holes are indicated by white arrows. (E-G) Examples of paraffin sections of the optic lobe and retina of flies of the indicated genotypes. In panel E, the optic lobe (OL), lamina (LA), and retina (RE) are labeled. In panels F and G, black arrows indicate mislocalized cell bodies and white arrows indicate large holes in the lamina.

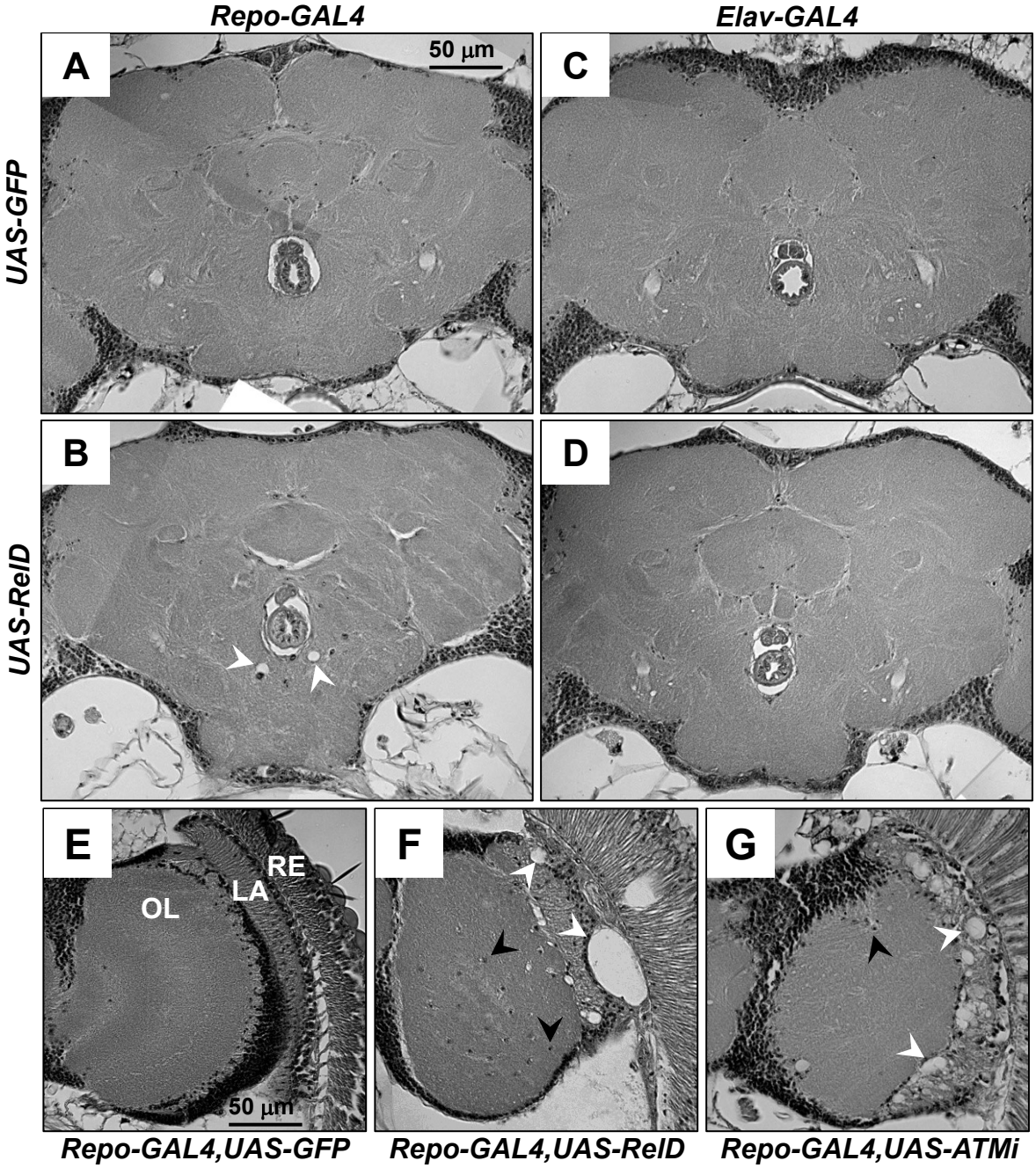
Repo-GAL4
Elav-GAL4
UAS-GFP
UAS-RelD
A
B
C
D
50 μm
E
F
G
RE
LA
OL
50 μm
Repo-GAL4,UAS-GFP
Repo-GAL4,UAS-RelD
Repo-GAL4,UAS-ATMi

Chapter 4

Germline gene expression in glial cells is regulated by ATM and prevents neurodegeneration in *Drosophila*

The majority of this work was submitted in:

Petersen AJ, Katzenberger RJ, and Wassarman DA. (2012) Germline gene expression in glial cells is regulated by ATM and prevents neurodegeneration in *Drosophila*. *Hum Mol Genet*. *In revision*.

A.J.P. performed the experiments for all tables and figures. A.J.P. and D.A.W. compiled the figures and tables and wrote the text.

4.1 Abstract

Mutations in the *Ataxia-telangiectasia mutated* (*ATM*) gene cause neurodegeneration in the human disease Ataxia-telangiectasia (A-T). Previously, we showed that *ATM* is required in glial cells to prevent neurodegeneration in the adult *Drosophila* brain. Here, we show that *ATM* regulates the expression of germline genes such as *piwi* in glial cells. Defects in ATM-mediated regulation of germline gene expression may cause neurodegeneration since germline gene knockdown in glial cells was sufficient to cause neurodegeneration. In other animal contexts, germline gene misexpression in somatic cells promotes cell proliferation, suggesting that glial cell proliferation protects neurons from degeneration in A-T.

4.2 Introduction

Ataxia-telangiectasia (A-T) is a multisystem disease caused by mutations in the *A-T mutated* (*ATM*) gene (Sedgwick and Boder 1960; Bundey 1994; Savitsky *et al*. 1995; McKinnon 2004). The hallmark clinical feature of A-T is progressive ataxia due to degeneration of cerebellar Purkinje and granule neurons. Another clinical feature of A-T is predisposition to cancer, particularly leukemia and lymphoma. An open question in A-T is why *ATM* mutations cause opposing cellular abnormalities: death of neurons and resistance to death of blood cells. This question is also relevant to other human neurodegenerative diseases, such as Parkinson's disease, which are associated with increased risk of some cancers (Plun-Favreau *et al*. 2010).

We have used *Drosophila* to model A-T and investigate the role that ATM plays in protecting neurons from degeneration. Most recently, we determined the consequences in adult flies of *ATM* knockdown in neurons or glial cells (Petersen *et al*. 2012). A primary finding from this study is that *ATM* is required in glial cells to protect neurons from degeneration. *ATM*

knockdown in glial cells, but not in neurons, causes neurodegeneration in the adult fly brain. Also, *ATM* knockdown in glial cells, but not in neurons, results in increased expression of innate immune response genes, which has been shown in other *Drosophila* systems to cause neurodegeneration (Tan *et al*. 2008; Chinchore *et al*. 2012; Petersen and Wassarman 2012). Thus, glial cells play a leading role in controlling the viability of neurons in *Drosophila* models of A-T.

Here, we show that ATM functions in both neurons and glial cells to control the expression of germline genes in glial cells. Furthermore, we show that germline gene expression in glial cells is required to protect neurons from degeneration. These findings are discussed in the context of other studies that have implicated somatic cell misexpression of germline genes in cell proliferation and cancer, thus providing a molecular link between neurodegeneration and cancer in A-T.

4.3 Results and Discussion

ATM knockdown causes gene expression changes in the adult *Drosophila* head

To investigate the role of ATM in neuron survival, microarray analysis was used to determine the effect of neuron-specific *ATM* knockdown on steady state mRNA expression in the adult *Drosophila* head. *ATM* knockdown was specifically induced in neurons using the GAL4-UAS system (Brand and Perrimon 1993). An *Elav-GAL4* transgene that expresses the GAL4 transcription factor in all post-mitotic neurons was used to drive expression of *pWIZ-ATM*^{T4}, a UAS-controlled transgene that expresses a short hairpin RNA (shRNA) that targets *ATM* mRNA for degradation by RNA interference (RNAi) (Lee and Carthew 2003; Soller and White 2004; Rimkus *et al*. 2008). Hereafter, *Elav-GAL4* refers to control flies that only

contained the driver (*Elav-GAL4*) transgene and *Elav-ATMi* refers to *ATM* knockdown flies that contained both the driver (*Elav-GAL4*) and target (*pWIZ-ATM^{T4}*) transgenes.

RNA extracted from the heads of 3-5 day old *Elav-GAL4* and *Elav-ATMi* flies was used to probe NimbleGen *Drosophila* gene expression microarrays containing probes for 15,473 genes. The resulting data were quantile normalized via RMA (Robust Multichip Average) and *Elav-GAL4* was compared to *Elav-ATMi* for fold change and statistical significance. Analysis of four independent biological replicates revealed that 160 genes met the criteria of a >2-fold change with a moderated T-test value of $p<0.05$ and a False Discovery Rate (FDR) value of $p<0.10$; 124 genes were upregulated and 36 genes were downregulated in *Elav-ATMi* flies relative to *Elav-GAL4* flies (Figure 4.1A).

A parallel study was performed to investigate the role of ATM in glial cells of the adult head. A *Repo-GAL4* transgene, which expresses GAL4 in all glial cells, was used to drive expression of *pWIZ-ATM^{T4}* (Xiong *et al*. 1994; Rimkus *et al.* 2008). RNA extracted from the heads of 3-5 day old flies, an age at which neurodegeneration was detected in *Repo-ATMi* flies (Petersen *et al*. 2012). Microarray analysis of two independent biological replicates revealed that 377 genes had altered expression in the adult head; 254 genes had higher expression and 123 genes had lower expression in *Repo-ATMi* flies relative to *Repo-GAL4* flies (Figure 4.1A). Comparison of the datasets by Gene Ontology analysis and literature analysis of individual genes identified cellular processes affected by *ATM* knockdown in neurons and/or glial cells (Ashburner *et al*. 2000). Some of these findings have already been published and are summarized in the Introduction (Petersen *et al.* 2012).

Upregulation of cell cycle genes in *Elav-ATMi* flies supports the finding that *ATM* regulates cell cycle reentry in neurons

Many genes involved in promoting the mitotic cell cycle increased in expression in *Elav-ATMi* heads (Table 4.1). Genes involved in cell cycle progression include *polo*, *stg*, *cdc2*, *cyclin A*, *cyclin B*, and *cyclin B3* (Goshima *et al*. 2007; Somma *et al*. 2008). Entry into mitosis is governed by mitotic Cyclin A, Cyclin B, and Cyclin B3 levels and the phosphorylation status of the Cdc2 kinase, also known as cyclin dependent kinase 1 (Cdk1). At the G2-M transition, the Polo kinase phosphorylates and activates the Stg/Cdc25 phosphatase, which removes inhibitory phosphate modifications from Cdc2 and in doing so promotes mitotic entry. Genes involved in DNA replication include the Minichromosome maintenance (Mcm) genes *Mcm7* and *Mcm10*. Numerous genes have functions related to mitotic spindles, including *Kinesin-like protein at 61F*, *Borealin-related*, *Inner centromere protein*, and *RacGAP50C*, which when knocked down in S2 cells disrupt spindle shape (Goshima *et al*. 2007). Finally, genes involved in cytokinesis include *sticky*.

Increased expression of genes involved in spindle assembly checkpoint (SAC) activation suggests that SAC activation is a signal that induces neuron death. As in all higher eukaryotes, SAC activation in *Drosophila* serves to prevent mitotic anaphase until all chromosomes are properly attached to kinetochores; however, prolonged SAC activation causes cell death through an unknown mechanism (Musacchio and Salmon 2007). Genes aberrantly expressed in *Elav-ATMi* flies that are relevant to SAC activation are *CENP-meta* and *zwilch*, which encode components of complexes that are recruited to unattached kinetochores during metaphase, *Cdc20* (also known as *fizzy*), which encodes the regulatory factor that controls sister chromatid separation, and *Anaphase promoting complex 7* (*APC7*) which encodes a component of the APC

complex that is regulated by Cdc20 (Table 4.1). Consistent with SAC activation serving as a signal that induces neuron death, we previously found that ATM knockdown in larval eye imaginal discs causes post-mitotic photoreceptor neurons to reenter the cell cycle and die after S-phase but prior to cytokinesis (Rimkus *et al*. 2008).

These data are consistent with the observed increase in expression of cell cycle regulatory proteins in the brain of A-T humans and mice (Yang and Herrup 2005). Furthermore, this data indicates that cell cycle reentry is not confined to photoreceptor neurons in the fly, but may occur in other neuronal types as well. The lack of equivalent upregulation of cell cycle genes in *Repo-ATMi* flies suggests that ATM regulation of cell cycle maintenance may represent a neuronal-specific function of ATM.

A major consequence of *ATM* knockdown is altered expression of germline genes

Analysis of the microarray data reveals 27 genes that were upregulated in *Elav-ATMi* flies and downregulated in *Repo-ATMi* flies (Figure 4.1A, Table 4.2). For simplicity, these genes will be referred to as Elav-up/Repo-down (EURD) genes. Three features of EURD genes suggest that they are interrelated, both in regard to their transcription regulation and their function. First, there were more EURD genes than expected. EURD genes represented a significant overlap between *Elav-ATMi* upregulated and *Repo-ATMi* downregulated genes ($p<0.001$), and the percentage of EURD genes was high (22% of the upregulated genes in Elav-ATMi flies and 22% of the downregulated genes in *Repo-ATMi* flies) (Figure 4.1A). For comparison, the complementary set of genes (Elav-down/Repo-up (EDRU) genes) did not represent a significant overlap between *Elav-ATMi* downregulated and *Repo-ATMi* upregulated genes ($p=0.59$), and the percentage of EDRU genes was low (3% of the downregulated genes in *Elav-ATMi* flies and <1% of the upregulated genes in *Repo-ATMi* flies).

Second, EURD genes showed a linear correlation between the level of upregulation in *Elav-ATMi* flies and downregulation in *Repo-ATMi* flies (R^2=0.82) (Figure 4.1B). For example, the *deadhead* (*dhd*) gene was upregulated in *Elav-ATMi* flies to a similar extent as it was downregulated in *Repo-ATMi* flies (21-fold and 25-fold, respectively) (Table 4.2). In support of the linear correlation, inactivation of ATM kinase activity in all cells does not significantly affect the expression of any EURD gene in the adult head (Petersen *et al*. 2012). These data suggest that *ATM* knockdown in neurons and glial cells oppositely affects the same mechanism that regulates EURD gene transcription.

Third, almost all of the EURD genes are characterized as having female-biased expression. Genomewide transcriptome analysis of 13,769 genes in adult flies by Graveley *et al.* (2011) determined that 7% of genes have female-biased expression and 17% of genes have male-biased expression. In contrast, 81% of EURD genes have female-biased expression (an 11-fold increase over the *Drosophila* transcriptome) and no EURD genes have male-biased expression (a substantial decrease over the *Drosophila* transcriptome) (Figure 4.1C). The extreme enrichment for female-biased genes and against male-biased genes was unique to EURD genes. Other sets of genes, of equal or greater number than the EURD set, were enriched or depleted for either female-biased genes or male-biased genes but none to the same extent as the EURD set.

Consistent with female-biased expression, EURD genes play key roles in germline-associated functions. To illustrate, *oskar* (*osk*) is required for assembly of the germ plasm, *zero population growth* (*zpg*) is required for germline stem cell differentiation, *piwi* and *nanos* (*nos*) are required for self-renewal of germline stem cells, and *ovarian tumor* (*otu*) is require for germline proliferation (Ephrussi *et al.* 1991; Markussen *et al.* 1995; Nagoshi *et al*. 1995; Rongo *et al*. 1995; Gilboa *et al.* 2003; Wang and Lin 2004; Aravin *et al*. 2007). Additionally, EURD

genes are involved in anterior-posterior specification in oocytes. These genes include *osk, nos, Bicaudal C (BicC), bicoid* (*bcd*), and regulators of *bcd* mRNA localization (*exuperantia* (*exu*), *swallow* (*swa*), *α-Tubulin at 67C (α-Tub67C*), and *γ-Tubulin at 37C (γ-Tub37C*)) (Pokrywka *et al*. 2004; Snee and MacDonald 2009; Chang *et al*. 2011). The prevalence of germline genes among the EURD set suggests that they function in the adult head to regulate an event that is characteristic of the germline, such as cell proliferation. Because many of the EURD genes are germline genes, hereafter we refer to them as germline genes.

Germline genes are expressed in glial cells

To determine the cellular expression pattern of germline genes in the adult brain, transgenic flies were obtained that have the *Green Fluorescent Protein* (*GFP*) gene expressed under control of the *piwi*, *otu*, or *exu* transcription regulatory sequences (Wang and Hazelrigg 1994; Glenn and Searles 2001; G. Hannon, personal communication). GFP reporter transgenes were crossed into the *Elav-GAL4* and *Elav-ATMi* genetic backgrounds and adult brains were analyzed by fluorescence microscopy. In both *Elav-GAL4* and *Elav-ATMi* flies, each reporter transgene was expressed in a subset of cells that were commonly located near the junction between the optic lobe and the central brain (Figure 4.3A-C and Figure 4.4A-C). Furthermore, staining for the Repo protein, a marker of glial cells, revealed that each reporter transgene was exclusively expressed in glial cells (Figure 4.3D-I and Figure 4.4D-I). These data indicate that germline genes perform a function in some glial cells under wild type conditions. Additionally, these data provide insight into how *ATM* knockdown in neurons and glial cells had opposite effects on the expression of germline genes (Figure 4.1B). Specifically, these data suggest that *ATM* knockdown in glial cells cell-autonomously causes the repression of germline gene expression, whereas *ATM* knockdown in neurons non-cell-autonomously signals the activation of

germline gene expression in glial cells. To our knowledge, this is the first evidence that germline genes are expressed in glial cells. Nanos and Piwi-interacting RNAs (piRNAs), which are bound by Piwi, are expressed in neurons, but their expression has not been directly examined in glial cells (Ye *et al*. 2004; Lee *et al*. 2011; Rajasethupathy *et al*. 2012).

Germline gene knockdown in glial cells causes neurodegeneration

Taken together, the data indicate that germline genes operate in glial cells to protect neurons from degeneration. Analyses for hallmarks of neurodegeneration in flies, such as holes in the brain, indicate that neurons survive in the presence of increased germline gene expression in *Elav-ATMi* flies but not in the presence of decreased germline gene expression in *Repo-ATMi* flies (Petersen *et al*. 2012). To determine the extent to which germline gene expression is required in glial cells to protect neurons from degeneration, we analyzed the brains of flies in which the expression of germline genes was knocked down by RNAi. The *Repo-GAL4* transgene was used to drive expression of UAS-transgenes that encode shRNAs for RNAi knockdown of *piwi*, *peroxinectin-like* (*pxt*), or *zpg*. In all cases, germline gene knockdown in glial cells resulted in increased neurodegeneration (Figure 4.5A-D). Repo-piwi RNAi flies had the highest level of neurodegeneration, with substantially more holes than age-matched *Repo-GAL4* flies. In contrast, knockdown of *piwi*, *pxt*, or *zpg* in neurons using the *Elav-GAL4* driver did not cause neurodegeneration, producing few or no holes in the brain (Figure 4.5E-H). Thus, germline gene expression specifically in glial cells protects neurons from degeneration.

Germline gene expression may promote glial cell proliferation to protect neurons from degeneration: a possible link between neurodegeneration and cancer

Our finding that germline gene expression in somatic glial cells affects the survival of neurons in the *Drosophila* adult brain is reminiscent of the finding that germline gene

misexpression affects the proliferation of somatic neuroepithelial cells in the *Drosophila* larval brain (Janic *et al*. 2010; Richter *et al*. 2011). In the study by Janic *et al.* (2010), germline genes were found to be overexpressed in tumors caused by mutation of the *lethal (3) malignant brain tumor* [*l(3)mbt*] gene. Of the 26 germline genes with increased expression in *l(3)mbt* larval brain tumors, a significant number, eight, overlapped with EURD genes ($p<0.001$) (Table 4.2). Two other genes *CG9925* and *giant nuclei* (*gnu*) were upregulated in *Elav-ATMi* flies but did not meet the significance cutoff for downregulation in *Repo-ATMi* flies. Intriguingly, the common genes includes all but one of the *l(3)mbt* germline genes that has female-biased expression. In the case of the *l(3)mbt* germline genes, 11 have female-biased expression, 7 have male-biased expression, and the remaining 8 have unbiased expression or were not detected in the Gravely *et al.* (2011) analysis. *Aubergine* (*aub*) is the only female-biased *l(3)mbt* gene that is not also an EURD gene; however, *aub* fulfills the characteristics of an EURD gene; it was upregulated in *Elav-ATMi* flies (1.53-fold), it was downregulated in *Repo-ATMi* flies (1.82 fold), and it had similar fold upregulation and downregulation. Thus, *ATM* knockdown and *l(3)mbt* mutation affect the expression of a common set of germline genes.

Germline gene misexpression is required for neuroepithelial cell proliferation in *l(3)mbt* flies (Janic *et al*. 2010). To illustrate, mutation of *piwi* or *nos* largely blocks tumor formation in *l(3)mbt* flies. In other animals, germline gene misexpression in somatic cells is also linked to cell proliferation. In *C. elegans*, germline gene misexpression in somatic cells results from mutations in many synMuv B genes, including the tumor suppressor gene *lin-35/retinoblastoma* (*Rb*) (Wu *et al*. 2012). In humans, >140 germline genes, collectively referred to as Cancer/Testis (CT) antigens, are overexpressed in somatic cells in a wide range of human cancers, including melanomas and several types of carcinomas (Cheng *et al*. 2011). These data suggest that altered

germline genes expression in *ATM* knockdown flies affects glial cell proliferation, a process that known to occur in the adult brain (Kato *et al*. 2009; von Trotha *et al*. 2009). Reduced germline gene expression in *Repo-ATMi* flies may inhibit proliferation, and increased germline gene expression in *Elav-ATMi* flies may promote proliferation (Figure 4.6).

A role for glial cell proliferation in neurodegeneration is supported by the finding that several EURD genes regulate the mitotic cell cycle. For example, *greatwall* (*gwl*) encodes a kinase that locks a cell into the mitotic cycle once the cell is committed to mitosis (Zhao *et al*. 2008; Boke and Hagen 2011), and *Cyclin B* (*CycB*) encodes the regulatory subunit of a cyclin dependent kinase involved in the mitotic G2-M transition (Duncan and Su 2004). Furthermore, in *Drosophila*, glial cell proliferation is induced as a result of activation of the programmed cell death (PCD) pathway in brain neurons (Kato *et al*. 2009; Kato *et al.* 2011). In line with this mechanism, the PCD activator gene *reaper* (*rpr*) was upregulated 2-fold in *Elav-ATMi* flies but was not affected in *Repo-ATMi* flies (Petersen *et al*. 2012). Thus, while obvious neurodegeneration was not detected in *Elav-ATMi* flies, it is possible that neurons with activated PCD or another stress response pathway are prevented from dying by their signals to glial cells that promote germline gene expression and cell proliferation (Figure 4.6).

A model for ATM-mediated regulation of germline gene transcription in glial cells

Data presented here suggest that an ATM signaling pathway functions cell autonomously in glial cells to promote germline gene transcription. This is reasonable, given that ATM phosphorylates transcription factors such as CREB and p53 to regulate transcription (Taylor and Stark 2001; Shi *et al*. 2004). One possibility is that ATM regulates the activity of the Myb-MuvB (MMB)/*Drosophila* RBF, E2F, and Myb (dREAM) transcription regulatory complex in glial cells. This evolutionarily conserved complex regulates the transcription of many genes and

can both activate and repress transcription (Lewis *et al*. 2004). Analyses in somatic *Drosophila* Kc cells identified direct transcription repression targets of MMB/dREAM, eight of which were EURD genes (Georlette *et al*. 2007) (Table 4.2). Furthermore, L(3)mbt is a sub-stoichiometric subunit of the MMB/dREAM complex (Lewis *et al*. 2004). L(3)mbt is also a component of the LINT complex that represses the transcription of germline genes (Meier *et al*. 2012). Thus, ATM may normally function to inhibit the transcription repression activity of L(3)mbt complexes in glial cells (Figure 4.6). Accordingly, *ATM* knockdown in glial cells removes the inhibition allowing the L(3)mbt complexes to more fully repress the transcription of germline genes.

A remaining puzzle is how *ATM* knockdown in neurons acts non-cell-autonomously to cause derepression of germline gene transcription in glial cells. In one possible scenario, *ATM* knockdown in neurons causes the activation of PCD in neurons, which signals glial cells to upregulate ATM activity leading to inhibition of MMB/dREAM, misexpression of germline genes, and cell proliferation (Figure 4.6). Aspects of this model are supported by evidence from other systems but lack direct experimental support in *Drosophila* A-T models. In particular, experimental support is lacking for the proposal that glial cell proliferation increases in *Elav-ATMi* flies and decreases in *Repo-ATMi* flies. Additionally, findings reported here raised a number of interesting questions, such as how would germline genes promote the proliferation of somatic glial cells, are particular glial subtypes affected by *ATM* knockdown, and what is the relationship between germline gene expression and innate immunity gene expression in glial cells, both of which affect neuron survival.

4.4 Materials and Methods

All flies were maintained on standard molasses medium at 25°C. *Elav-GAL4*, *Elav-ATMi*, *Repo-GAL4*, and *Repo-ATMi* flies are described in Petersen *et al.* (2012). Exu-GFP, osk-GFP, and piwi-GFP flies are described in Wang and Hazelrigg (1994), Glenn and Searles (2001), and G. Hannon (personal communication), respectively. Germline gene RNAi flies (piwi, nos, zpg, and pxt) were obtained from the Bloomington Stock Center. Microarray analysis, statistical analyses, quantitative RT-PCR, immunofluorescence microscopy, and paraffin sectioning were performed as described in Petersen *et al.* (2012).

4.5 Acknowledgments

We thank Clinton Morgan, Judith Kimble, Grace Boekhoff-Falk, Haifan Lin, Keith Hansen, Randy Tibbetts, Chiara Gamberi, and Melissa Harrison for their insights throughout the course of the research. This work was supported by a grant from the NIH (R01 NS059001 to D. A. W.) and a pre-doctoral fellowship from NIH training grant T32 GM08688 (to A. J. P.).

Table 4.1: Cell cycle genes upregulated in Elav-ATMi flies

CG number	Gene	Elav-ATMi[1]
CG8308	α-Tubulin at 67C (α-Tub67C)	3.9
CG14444	Anaphase promoting complex 7 (APC7)	2.9
CG6897	aurora borealis (bora)	2.7
CG4454	Borealin-related (Borr)	2.6
CG6392	CENP-meta (cmet)	2.1
CG5940	Cyclin A (CycA)	3.6
CG3510	Cyclin B (CycB)	9.1
CG5814	Cyclin B3 (CycB3)	2.5
CG8994	exuperantia (exu)	2.4
CG4274	fizzy (fzy)/Cdc20	3.2
CG17566	γ-Tubulin at 37C (γ-Tub37C)	2.5
CG5272	giant nuclei (gnu)	2.9
CG7719	greatwall (gwl)	6.1
CG12165	Inner centromere protein (Incenp)	4.1
CG9191	Kinesin-like protein at 61F (Klp61F)	2.7
CG9241	Minichromosome maintenance 10 (Mcm10)	3.1
CG12047	mushroom body defect (mud)/NuMA	2.6
CG17256	Nek2	2.6
CG4799	Pendulin (Pen)	5.0
CG5052	pimples (pim)	3.3
CG12306	polo	7.2
CG13345	RacGAP50C/tumbleweed (tum)	3.3
CG2092	scraps (scra)	-2.1
CG17286	spindle defective 2 (spd-2)	2.2
CG10522	sticky (sti)/citron	2.1
CG1395	string (stg)	2.2
CG12298	subito (sub)/mitotic kinesin-like protein 2 (MKLP2)	3.4
CG5785	three rows (thr)	2.0

[1] fold difference in expression between Elav-ATMi and Elav-GAL4 flies

Table 4.2: Elav-up/Repo-down (EURD) genes

CG number	Gene[1]	Elav-ATMi[2]	Repo-ATMi[3]	Bias[4]	l(3)mbt[5]	MMB[6]
CG4193	deadhead (dhd)	21.4	-25.0	F	X	
CG10125	zero population growth (zpg)	11.0	-11.1	F	X	X
CG3510	Cyclin B (CycB)	9.1	-4.3	F		X
CG1372	yolkless (yl)	8.5	-6.7	F		
CG7660	peroxinectin-like (pxt)	8.2	-8.3	F	X	X
CG10901	oskar (osk)	8.2	-5.6	F		
CG1058	ripped pocket (rpk)	8.0	-3.6	F		
CG7719	greatwall (gwl)	6.1	-2.6	F		
CG4824	Bicaudal C (BicC)	5.6	-5.0	U		
CG3429	swallow (swa)	5.1	-3.3	F	X	X
CG3509		4.4	-2.0	U		
CG5637	nanos (nos)	4.2	-5.3	F	X	X
CG11411	female sterile (1) Nasrat (fs(1)N)	4.1	-3.2	F		X
CG8308	α-Tubulin at 67C (α-Tub67C)	3.9	-4.3	F		
CG17018	[limkain b1 domain protein]	3.7	-4.5	F		
CG7014	Ribosomal protein S5b (RpS5b)	3.6	-2.1	F	X	
CG6122	piwi	3.5	-2.9	F	X	X
CG1034	bicoid (bcd)	3.1	-2.6	F		
CG12743	ovarian tumor (otu)	2.5	-3.4	F		
CG12047	mushroom body defective (mud)	2.5	-2.2	U		
CG17566	γ-Tubulin at 37C (γ-Tub37C)	2.5	-2.3	F	X	
CG8994	exuperantia (exu)	2.4	-2.1	U		
CG1759	caudal (cad)	2.4	-2.7	U		
CG18543	matrimony (mtrm)	2.4	-2.7	F		
CG6927		2.2	-5.3	F		X
CG31775		2.2	-2.6	-		
CG17286	spindle defective 2 (spd-2)	2.2	-2.9	F		
CG9925	[tudor domain protein]	4.1		F	X	
CG5272	giant nuclei (gnu)	2.9		F	X	

[1]gene name, parentheses indicate gene abbreviations, brackets indicate predicted protein domains
[2]fold difference in expression between Elav-ATMi and Elav-GAL4 flies
[3]fold difference in expression between Repo-ATMi and Repo-GAL4 flies
[4]F, female-biased expression; U, unbiased expression; -, expression below detection (Graveley *et al*. 2011)
[5]X's indicate germline genes that are misexpressed in *l(3)mbt* flies (Janic *et al*. 2010)
[6]X's indicate genes regulated by MMB/dREAM in *Drosophila* Kc cells (Georlette *et al*. 2007)

Figure 4.1. Characterization of EURD gene expression. (A) Shown is a Venn diagram that displays the number of genes that commonly or uniquely changed expression between *Elav-ATMi* and *Repo-ATMi* flies. (B) Graphed is the fold change in genes expression of the 27 EURD genes in *Elav-ATMi* flies compared to *Repo-ATMi* flies. The coefficient of determination (R^2) is 0.82. (C) Shown is the percentage of genes from panel A that have female-biased or male-biased expression (% female-% male) (Graveley *et al*. 2012). Genes that have unbiased expression or were not detected in the Graveley *et al.* (2012) study bring the total to 100%.

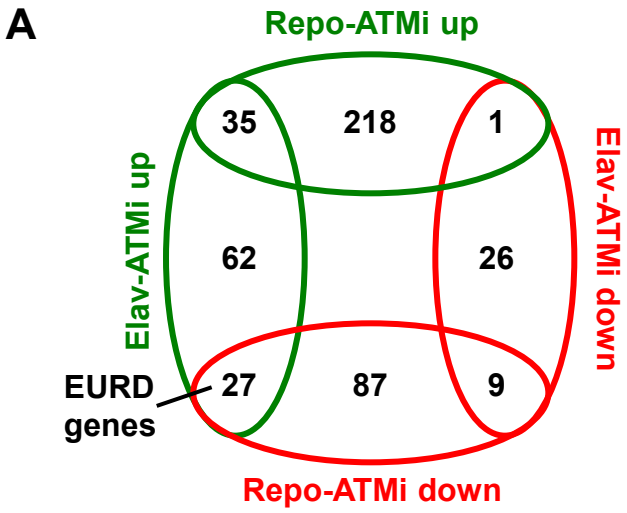
A
Repo-ATMi up
35
218
1
Elav-ATMi up
62
26
Elav-ATMi down
EURD genes
27
87
9
Repo-ATMi down

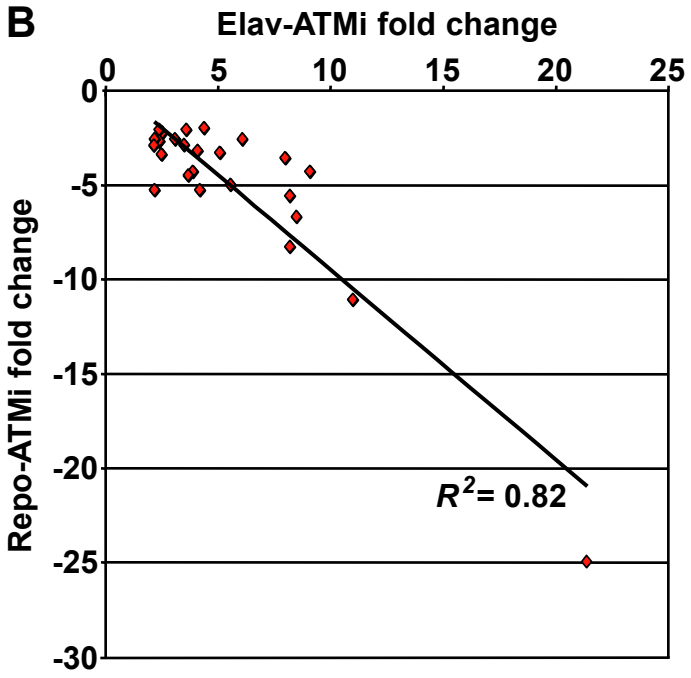
B
Elav-ATMi fold change
0
5
10
15
20
25
0
-5
-10
-15
-20
-25
-30
Repo-ATMi fold change
R^2= 0.82

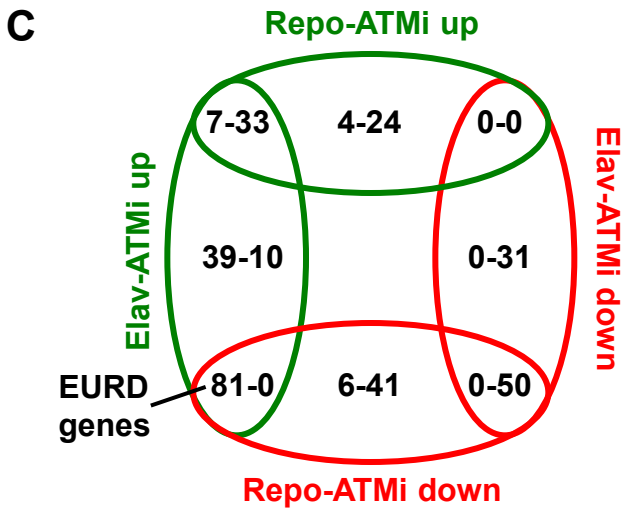
C
Repo-ATMi up
7-33
4-24
0-0
Elav-ATMi up
39-10
0-31
Elav-ATMi down
EURD genes
81-0
6-41
0-50
Repo-ATMi down

Figure 4.2. Germline genes were expressed in glial cells in *Elav-GAL4* flies. (A-C) GFP expression detected by immunofluorescence (green) in the adult brain of *Elav-GAL4* flies carrying piwi-GFP, otu-GFP, or exu-GFP transgenes, respectively. The GFP protein in piwi-GFP and otu-GFP flies was nuclear and the GFP protein in exu-GFP flies was cytoplasmic. (D-F) Nuclear Repo expression detected by immunofluorescence (red) in the samples shown in panels A-C. (G-I) Merged images of GFP and Repo immunofluorescence.

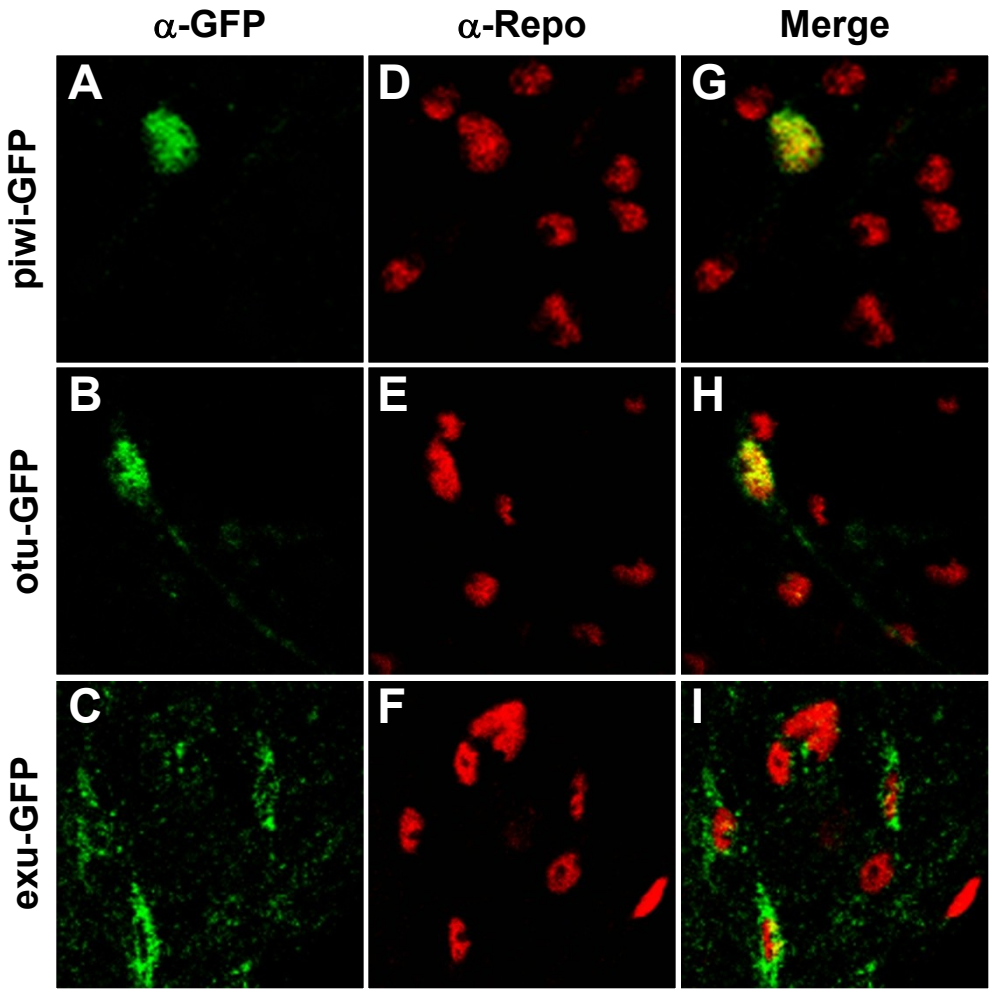
α-GFP
α-Repo
Merge
piwi-GFP
otu-GFP
exu-GFP
A
B
C
D
E
F
G
H
I

Figure 4.3. Germline genes were expressed in glial cells in *Elav-ATMi* flies. (A-C) GFP expression detected by immunofluorescence (green) in the adult brain of *Elav-ATMi* flies carrying piwi-GFP, otu-GFP, or exu-GFP transgenes, respectively. The GFP protein in piwi-GFP and otu-GFP flies was nuclear and the GFP protein in exu-GFP flies was cytoplasmic. (D-F) Nuclear Repo expression detected by immunofluorescence (red) in the samples shown in panels A-C. (G-I) Merged images of GFP and Repo immunofluorescence.

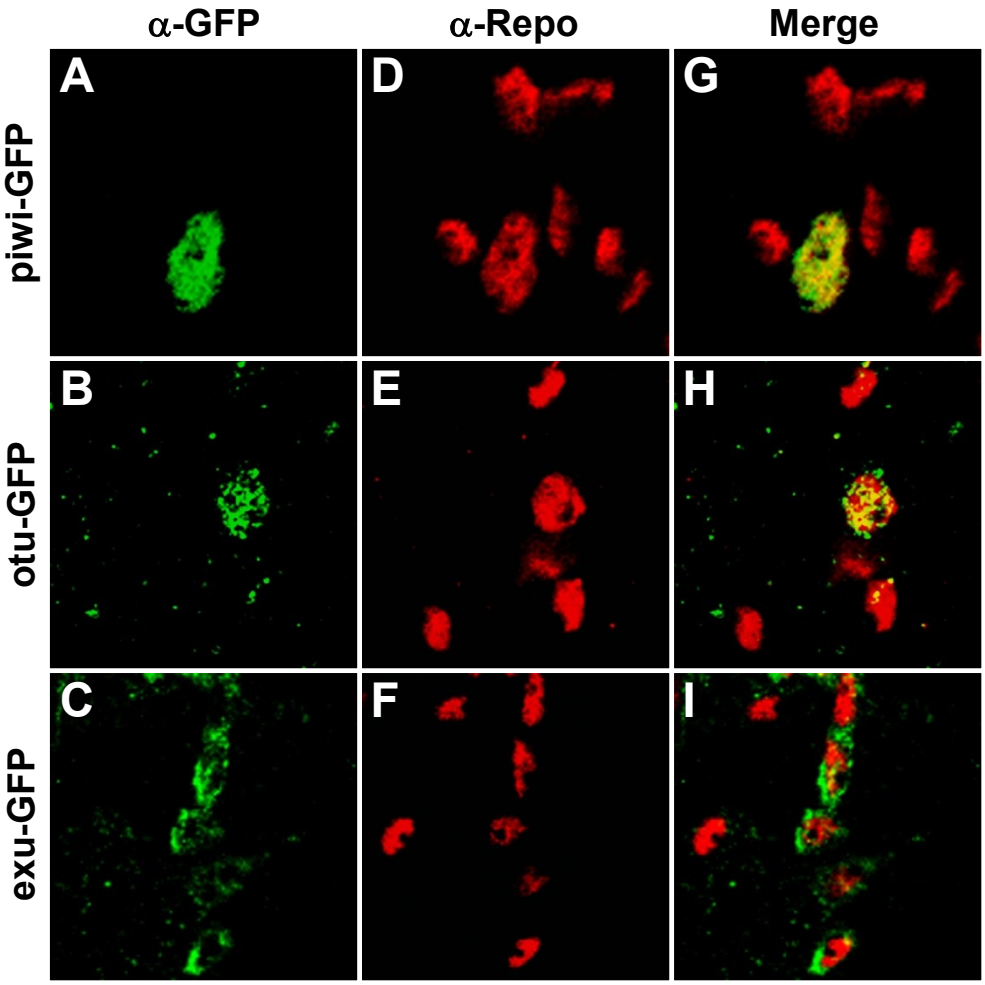
α-GFP
α-Repo
Merge
piwi-GFP
otu-GFP
exu-GFP
A
B
C
D
E
F
G
H
I

Figure 4.4. Knockdown of germline genes in glial cells caused neurodegeneration. Shown are paraffin sections of brains from 28-day old flies of the indicated genotypes. (A-D) Germline gene knockdown in glial cells. (E-H) Germline gene knockdown in neurons. Arrows indicate holes in the brain.

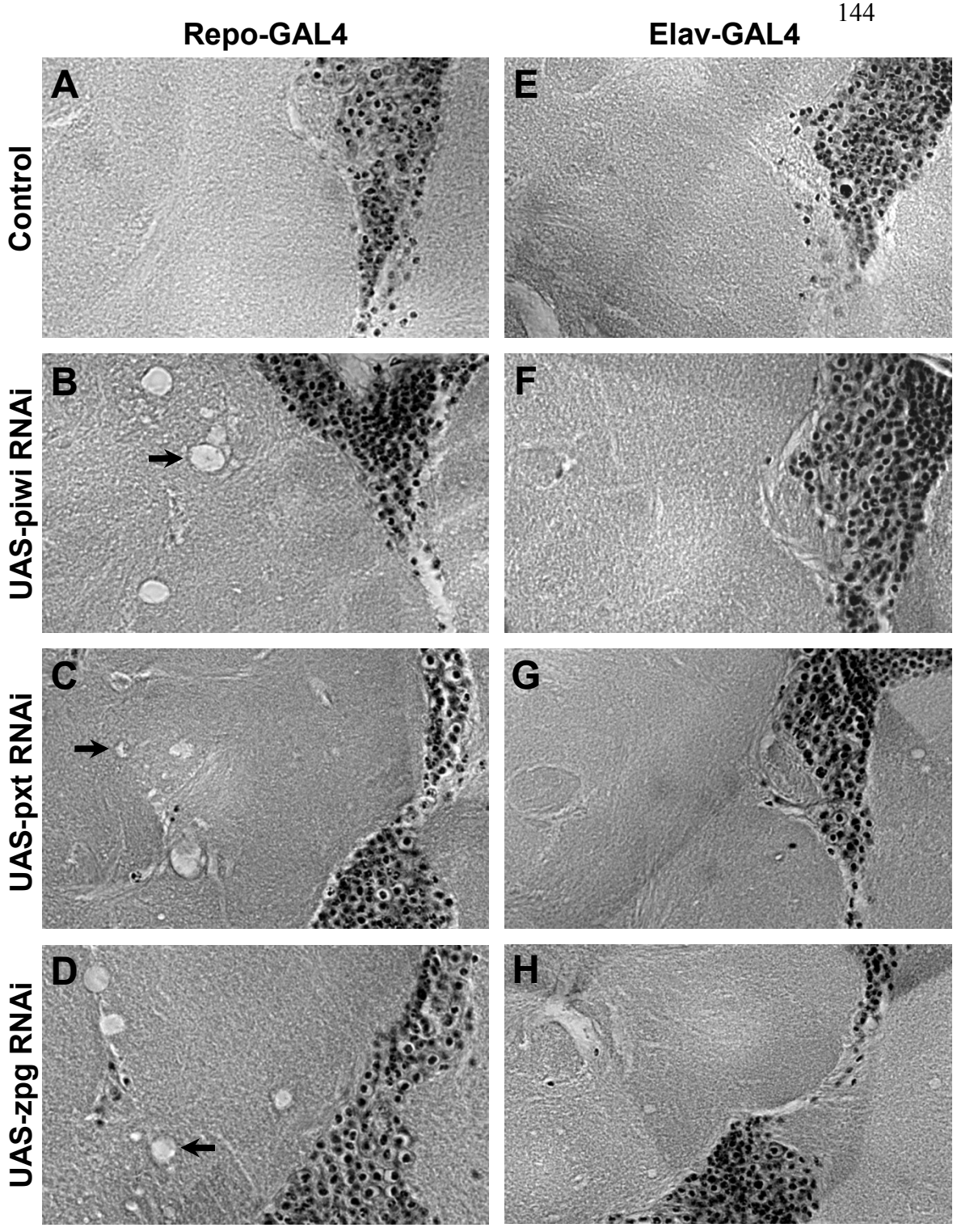
Repo-GAL4
Elav-GAL4
Control
UAS-piwi RNAi
UAS-pxt RNAi
UAS-zpg RNAi
A
B
C
D
E
F
G
H

Figure 4.5. A model for how ATM-mediated regulation of germline gene expression in glial cells may affect neuron survival. A toxic event or *ATM* knockdown in neurons may initiate a stress response that signals ATM activation in glial cells (1A) and/or neurodegeneration (1B). ATM activation in glial cells relieves L(3)mbt complex-mediated repression of germline gene transcription (2) resulting in glial cell proliferation, which through an unknown mechanism (3) blocks neurodegeneration. Events shown in blue typeset are supported by data presented in Figures 1-3 or in Petersen *et al.* (2012). Events shown in black typeset are supported by the literature and are described in more detail in the Results and Discussion section.

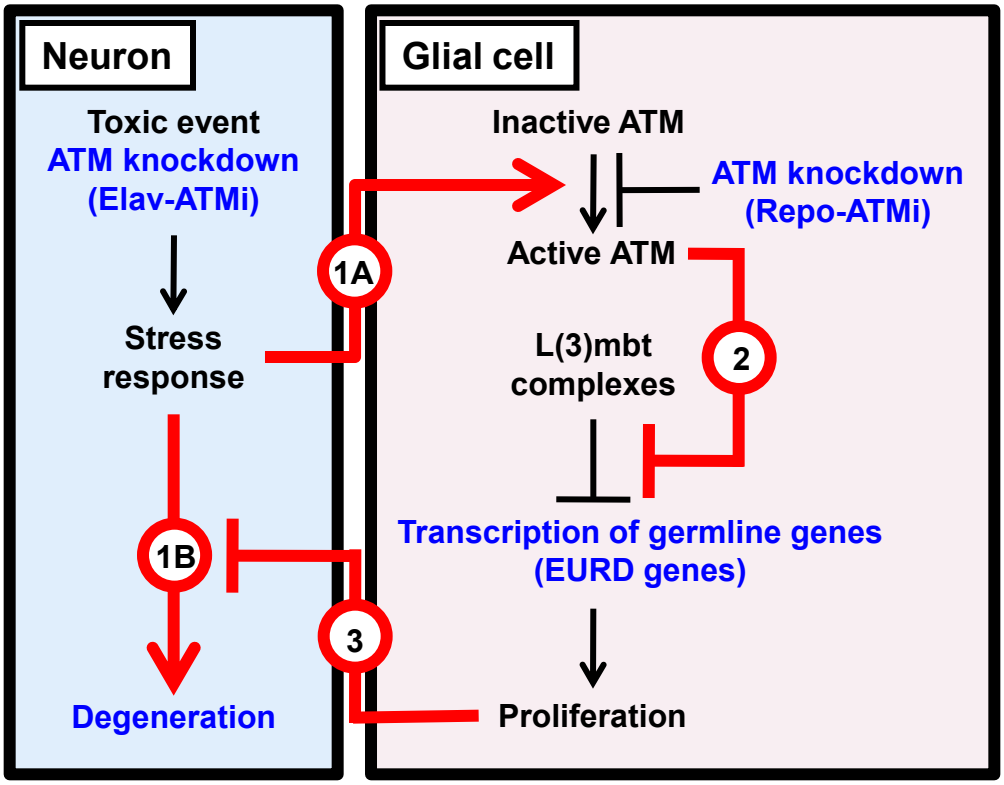
Neuron
Toxic event
ATM knockdown
(Elav-ATMi)
Stress
response
1A
1B
Degeneration
Glial cell
Inactive ATM
ATM knockdown
(Repo-ATMi)
Active ATM
L(3)mbt
complexes
2
Transcription of germline genes
(EURD genes)
3
Proliferation

Chapter 5

Summary of research and future directions

5.1 Summary of research

Activation of the innate immune response in glial cells occurs in response to cell-autonomous loss of ATM function and promotes neurodegeneration

My research has focused on identifying molecular events underlying neurodegeneration in *Drosophila* models of the human disease A-T. This disease is caused by mutations in the *ATM* gene, which encodes a kinase with a conserved function within the DNA damage response. To study loss of ATM function in the fly, I have used the temperature-sensitive ATM^{8} allele to eliminate ATM function in all cells in the adult, as well as *Elav-ATMi* and *Repo-ATMi* flies to selectively reduce ATM function via RNAi in neurons or glial cells, respectively (Rimkus *et al*. 2008; Pedersen *et al*. 2010; Petersen *et al*. 2012).

To assay for neurodegeneration, I have utilized four primary assays: longevity, climbing ability, histology via paraffin sectioning, and activated caspase 3 staining ($Casp^{Act}$). Deficiencies in these phenotypes are commonly associated with neurodegenerative models in *Drosophila* (Lessing and Bonini 2009). When compared to wildtype control flies, ATM^{8} flies exhibited shorter longevities, reduced climbing ability, increased neuropil lesions in paraffin sections, and increased levels of $Casp^{Act}$ staining (Chapter 2). These phenotypes indicated that ATM^{8} flies suffer from neurodegeneration. *Repo-ATMi* flies exhibited the same characteristic neurodegenerative phenotypes as ATM^{8}, whereas *Elav-ATMi* flies appear phenotypically normal in these assays. This result suggests that ATM function in glial cells, rather than neurons, is necessary for neuronal survival in the fly.

To identify molecular events that promote neurodegeneration in ATM^{8} and *Repo-ATMi* flies, I performed microarray analysis on the relevant genotypes to identify gene expression changes in these flies. Both ATM^{8} and *Repo-ATMi* flies upregulated many genes that function in

the *Drosophila* innate immune response. This response was found to occur in response to ATM loss cell-autonomously in glial cells, introducing the first published reference to a glial cell innate immune response in *Drosophila* (Chapter 2). In contrast, *Elav-ATMi* flies did not exhibit upregulation of innate immune response genes. Thus, these models indicate that ATM-deficient flies that suffer from neurodegeneration also activate the innate immune response.

To further link these two processes, ATM^{8} and *Repo-ATMi* flies were separated into three groups based on climbing ability (poor, moderate, and good climbers) (Chapter 3). Poor climbing flies exhibited shorter longevities and higher levels of $Casp^{Act}$ staining than good climbing flies, indicating that climbing ability correlates with neurodegeneration. Gene expression analysis in these flies revealed that poor climbing flies exhibit higher levels of innate immune response genes than good climbing flies, providing additional correlation between neurodegeneration and the innate immune response.

The innate immune response is a conserved mechanism between flies and humans, and signals through pathways utilizing NF-κB proteins. In *Drosophila*, activation of the Toll receptor facilitates signaling through the NF-κB protein Dif and activation of the Imd pathway promotes signaling through the NF-κB protein Relish (Rel). To determine if ATM-deficient flies initiate the innate immune response via these pathways, mutant alleles of *Dif* and *Rel* were introduced into ATM^{8} flies. These experiments proved that loss of ATM signals through Rel to produce the innate immune response since loss of Rel, but not loss of Dif, was sufficient to block innate immunity gene expression (Chapter 3). Additionally, mutations in the *Imd* gene, whose product functions upstream of Rel, were tested in ATM^{8} flies. Loss of Imd function affected gene expression in ATM^{8}/+ flies, but not ATM^{8} flies, suggesting that Imd may play a role in innate immunity gene expression but is not essential for it to occur.

Next, I sought to determine if this Rel-dependent innate immune response plays a causative role in neurodegeneration. I performed the four neurodegenerative assays in ATM^{8}, *Rel* double-mutant flies, as well as ATM^{8}, *Dif* and ATM^{8}, *Imd* double mutants as controls. These experiments revealed that blocking activation of the innate immune response suppressed the neurodegeneration observed in ATM^{8} flies, indicating that the innate immune response is necessary for neurodegeneration in this system (Chapter 3). A mutation in *Dif* did not affect neurodegeneration, but mutations in *Imd* had variable effects on neurodegeneration. At least one of the three *Imd* mutant alleles tested caused increased longevity and reduced $Casp^{Act}$ staining in ATM^{8} flies, suggesting that loss of Imd function prevents neurodegeneration. However, another *Imd* mutation also increased the severity of defects observed in ATM^{8} paraffin sections, suggesting loss of Imd promotes neurodegeneration (Chapter 3). Additional work in the future is needed to determine the necessity of Imd in Rel activation during neurodegeneration.

These experiments identified that Rel activation is necessary for neurodegeneration in ATM-deficient flies. Next, I wanted to determine if Rel activation alone is sufficient to produce neurodegeneration. To accomplish this, I expressed an active form of Rel, RelD, specifically in glial cells. In these flies, I observed upregulation of innate immune response genes and neuropil lesions indicative of neurodegeneration (Chapter 3). Thus, it appears that Rel activation in glial cells is sufficient to cause neurodegeneration, even in the absence of another defect.

Cumulatively, these experiments provide compelling evidence that loss of ATM in glial cells causes aberrant activation of an innate immune response that is necessary for neurodegeneration. Evidence from ATM-deficient mice, who exhibit glial cell activation in the brain, supports the implication that ATM deficiency in glial cells may play a role in A-T (Kuljis *et al*. 1997). Furthermore, numerous *Drosophila* models of neurodegenerative disease exhibit

upregulation of innate immunity genes, suggesting that innate immune response activation may function in several neurodegenerative disorders (Greene *et al*. 2005; Shieh and Bonini 2011; Chinchore *et al*. 2012). Finally, activation of the innate immune response in glial cells has been shown to occur during neurodegeneration in humans, notably in Alzheimer's disease and Parkinson's disease (Akiyama *et al*. 2000; Zhang *et al*. 2005). Since activation of the innate immune response appears to be necessary as well as sufficient to cause neurodegeneration, the ability to study this phenomenon in a genetically-tractable model organism such as *Drosophila* is critical to further delineate mechanisms by which to abrogate this signaling response and prevent disease progression in humans. Experiments that can be used to accomplish this task will be presented in the future directions.

Knockdown of ATM function in neurons and glial cells differentially alter the expression of germline genes in the brain

In *Elav-ATMi* flies, where ATM function is knocked down in neurons, two primary classes of genes were found to be upregulated via microarray analysis. One class of genes function within the cell cycle, suggesting that ATM-deficient neurons in the brain undergo cell cycle reentry (Chapter 4). This phenomenon is not new to the ATM field. Previous work in our lab showed that ATM deficient photoreceptor neurons undergo cell cycle reentry, a process that is partially necessary for neurodegeneration of these photoreceptors (Rimkus *et al*. 2008). Furthermore, studies on brain tissue from A-T patients revealed significant upregulation of cell cycle regulatory genes, suggesting that this phenomenon occurs in the disease as well (Yang and Herrup 2005). Since cell cycle genes were not altered in the *Repo-ATMi* microarray, this role of ATM in suppressing cell cycle reentry in the absence of overt DNA damage may represent a neuronal-specific function of ATM.

The second class of genes found to be upregulated in *Elav-ATMi* flies are genes that primarily function within the female germline. These genes function in numerous pathways, most notably in the anterior-posterior localization of mRNA in the developing embryo and germline stem cell maintenance (Aravin *et al*. 2007; Chang *et al*. 2011). An interesting feature of this set of genes is that almost all of them are similarly downregulated in *Repo-ATMi* flies (Chapter 4). Further analysis on these germline genes reveal that they are significantly female-biased relative to the general population of genes, confirming the ovary-specific expression for many of them.

Immunofluorescence analysis revealed that expression of at least a subset of these genes occurs naturally in *Drosophila* glial cells, as *exu* and *otu* GFP reporter constructs specifically stained within glial nuclei. Furthermore, knockdown of the germline genes *piwi*, *pxt*, or *zpg* in glial cells, but not neurons, produce neuropil lesions indicative of neurodegeneration. These results suggest that germline genes may function to promote the viability of glial cells. In flies lacking ATM function in neurons (*Elav-ATMi*), glial cells may upregulate these genes in order to provide additional support to the neurons or to proliferate in response to neuronal damage. A recent report supports this hypothesis, showing that misexpression of germline genes occurs in a *Drosophila* mutant that promotes brain tumor formation (Janic *et al*. 2010). This report links germline gene expression with cell proliferation, consistent with their function in germline cells of the ovary. In *Repo-ATMi* flies, downregulation of these genes may be due to active repression of their expression, underlying the neurodegeneration observed in these flies, or due to death of glial cells resulting in a lower baseline level of expression.

Future work on this project will analyze whether glial cells in *Elav-ATMi* flies exhibit proliferative capabilities, as well as whether restored levels of germline gene expression in *Repo-*

ATMi flies can reduce the severity of neurodegeneration. Additionally, the specific function of these genes in non-germline cells must be characterized in order to understand how their expression regulates neuronal viability. Specific experiments for this section will not be discussed in detail in the future directions section.

5.2 Future directions

My work has provided convincing data that activation of the innate immune response causes neurodegeneration in ATM-deficient flies. In order to fully implement these findings into a treatment for neurodegeneration in A-T, we must comprehensively characterize the events surrounding Rel activation in this phenomenon. This characterization comes in two parts: identification of what events lead to Rel activation in the absence of a pathogenic stimulus, and identification of transcriptional targets of Rel that promote neurodegeneration. Answers to these two questions will delineate a signaling pathway, from stimulus through to effector, that promotes neuronal death in the fly. This work may have impact reaching beyond A-T, as similar innate immune response events appear to play a role in numerous neurodegenerative diseases.

Another necessary step to relate my work to the human disease is to show that the same phenomenon occurs in mammalian systems and is amenable to pharmacological input. ATM knockout mice are unsuitable for studying neurodegeneration; however, conditional knockout of ATM function in specific cells like neurons or glia may provide a system to study loss of ATM function in the mouse brain while bypassing the phenotypes that cause early lethality such as cancer. Furthermore, screening the ability of drugs, such as non-steroidal anti-inflammatory drugs (NSAIDs) or TNF inhibitors, to prevent neurodegeneration in ATM-deficient flies, and possibly mice, may provide insight into how to treat neurodegeneration in A-T patients.

Identify the specific events underlying Rel activation in ATM-deficient glial cells

In order to identify how Rel becomes activated in ATM-deficient glial cells, systematic analysis using genetic mutations will be used to determine what components of canonical Rel signaling are capable of suppressing innate immunity gene expression. Starting with the furthest upstream components, this includes (in order): *PGRP-LC*, *Imd*, *dFADD*, *Dredd*, *Tak1*, *Ird5*, and *Kenny*.

If *PGRP-LC* is shown to affect innate immunity gene expression, it indicates that an extracellular stimulus initiates the innate immune response. This is the canonical method of activation for this pathway, typically by a pathogenic infection. However, my hypothesis would be that an endogenous molecule is responsible for this activation, similar to what is observed in mammalian systems where the innate immune response can be activated by DAMPs (danger-associated molecular patterns). This hypothesis could be tested by dissociating glial cells into culture and supplying various intracellular components to the media. Potential stimulatory factors include DNA, ATP, or glutamate – all factors shown to stimulate the innate immune response in mammals (Owens 2009).

If *PGRP-LC* does not affect innate immunity gene expression, it suggests that an intracellular mechanism underlies Rel activation in ATM-deficient flies. Since *Imd* mutations affected innate immune gene expression in ATM^{δ}/+ but not ATM^{δ} flies, there is a high likelihood that *PGRP-LC* mutants may behave the same way. Intracellular activation of Rel during neurodegeneration was proposed by Chinchore *et al*. (2012) in a model of retinal degeneration, since they saw suppression with *Rel* mutations but not *Imd*. By systematically testing the proteins involved in Rel activation, it can be determined at what level of the cascade full

suppression of the innate immune response occurs. This determination will be critical for determining how to inhibit this mechanism in humans to affect disease progression.

Identify the transcriptional targets of Rel in glial cells responsible for promoting neurodegeneration

Since my work and work by Chinchore *et al*. (2012) has identified that loss of Rel function suppresses neurodegeneration, a transcriptional target of Rel is likely responsible for causing neuronal death. In order to identify what target may be performing this role, a series of genome-wide analysis could be performed. First, I would perform a gene expression microarray comparison looking at ATM^{8} flies and ATM^{8}, *Rel* double-mutants (both compared back to control flies). These comparisons should identify genes with altered expression in ATM^{8} flies that are not altered in ATM^{8}, *Rel* that may function in neurodegeneration. Next, I would perform microarray analysis on flies overexpressing activated Rel in glial cells (*Repo-GAL4*, *UAS-RelD*). These flies also suffer from neurodegeneration, so whatever relevant Rel target genes are altered in flies of this genotype may cause neurodegeneration (Chapter 3).

Another potential method for determining the relevant Rel transcriptional targets is chromatin immunoprecipitation, or ChIP. For ChIP analysis, a transcription factor is cross-linked to DNA, DNA is cleaved into short fragments, and the resulting transcription factor-DNA fragment complex is purified using an antibody against the transcription factor of interest. This allows identification of the specific DNA sequences bound by the transcription factor, providing insight into what genes are regulated by the factor. For this experiment, I would isolate glial cells from the brain of ATM^{8} flies. I would then perform ChIP analysis on Rel from this group of cells to provide insight into what genes Rel is regulating in glial cells during neurodegeneration.

Next, I would compare this list of genes with the lists of genes from the microarray studies to identify genes potentially involved in neurodegeneration.

Once a list of potential genes is compiled, manipulation of the level of these genes will be performed to identify factors definitively involved in neurodegeneration. Loss-of-function mutants of these genes will determine their necessity for neurodegeneration in ATM^{8} flies, and gain-of-function expression will identify genes sufficient for neurodegeneration. When the important gene(s) is/are identified, mammalian homologs of the gene(s) of interest could serve as biomarkers for neurodegeneration or as pharmacological targets for treatment.

Identify whether loss of ATM in mammalian glial cells is sufficient to produce neurodegeneration and an innate immune response

To ultimately affect the lives of A-T patients, my work from *Drosophila* must be validated in a mammalian system. As outlined in Chapter 1, certain caveats exist for studying neurodegeneration in mice. To circumvent these problems, I propose creating a conditional ATM knockout only in neurons or glial cells of the mouse. A mouse line carrying *loxP* sites flanking exons 57 and 58 in the mouse *ATM* gene was made to allow conditional removal of these exons upon Cre recombinase expression, mimicking a known human mutation and causing loss of ATM function (Zha *et al*. 2008). By directing Cre recombinase expression to specific cell types, such as astrocytes, microglia, or specific neurons like Purkinje cells, the role of ATM loss in these cell types can be determined (Gong *et al*. 2007; Chow *et al*. 2008; Ros-Bernal *et al*. 2011). These conditional knockout mice would be monitored for development of neurodegeneration as they age, a phenotype that is potentially masked by early mortality in full *ATM* knockout mice. If neurodegeneration is observed, then there is essentially unlimited experiments that could be performed to learn more about this disease. Early hypotheses could be

based on the work in *Drosophila* implicating the innate immune response, but additional work could determine the role of neuronal cell cycle reentry, oxidative stress, or DNA damage in neurodegeneration.

Identify pharmacological methods that prevent neurodegeneration in *Drosophila* or mouse models of A-T.

The *Drosophila* models of A-T, combined with the conditional knockout mice (if neurodegeneration is observed), provide a means to identify drugs that may benefit A-T patients. Based on my findings from the fly, targeting the innate immune response through NSAIDs or anti-inflammatory drugs may provide a low-toxicity method for lessening the severity of disease symptoms. Additionally, more specific drugs such as TNFα inhibitors like enbrel may prove to be efficacious in treating neurodegeneration in diseases where the innate immune response is activated.

The use of *Drosophila* in drug development carries certain caveats but is far from impossible. These caveats include the lack of a circulatory system similar to mammals, differences in blood-brain barrier function, and differences in drug metabolism. As a mechanism to quickly screen efficacy of drugs for the ability to alter a specific phenotype, such as longevity or climbing ability for neurodegeneration, flies represent a cheap and tractable system. *Drosophila* has already provided insight into potential therapeutics for neurodegenerative diseases, including geldanamycin for the treatment of Parkinson's disease and histone deacetylase inhibitors for the treatment of polyQ aggregation disorders such as Huntington's disease (Steffan *et al*. 2001; Auluck and Bonini 2002; Celotto and Palladino 2005).

As a proof-of-principle experiment, preliminary experiments performed in our lab indicate that treatment of *Repo-ATMi* flies with aspirin increases their longevity, indicating that

aspirin treatment in A-T patients may slow down disease progression. Additional drugs that could be tested in this manner include TNFα inhibitors, such as enbrel, or any of the numerous NF-κB inhibitors including drugs or natural compounds (Peppel *et al*. 1991; Gupta *et al*. 2010; Paur *et al*. 2010) These drugs would be hypothesized to suppress innate immune response activation, and therefore neurodegeneration, based on our findings in the fly. Furthermore, any drugs showing efficacy in flies could be tested in conditional knockout mice which would validate their use in mammalian neurodegeneration. Implications of these studies reach far beyond the field of A-T. Since numerous neurodegenerative diseases appear to occur at least in part due to innate immune response activation, any drugs identified in this manner may show broad effects on neurodegenerative diseases in general.

Final comments

My work in *Drosophila* has provided novel insights into mechanisms underlying neurodegeneration in A-T. These findings identify that loss of ATM function in glial cells causes activation of the innate immune response and neurodegeneration. Both glial cell dysfunction and innate immune response activation are implicated in other neurodegenerative diseases like Alzheimer's and Parkinson's disease, suggesting a common mechanism underlying numerous neurodegenerative conditions. To understand how these problems manifest to cause neurodegeneration, *Drosophila* and its associated tools and methods will provide an important conduit for studying this phenomenon going forward.

In order to directly affect the lives of patients suffering from A-T or other neurodegenerative diseases, validation of the findings in our models must occur in mammals. For studying A-T, conditional ATM knockout mice can be generated that lack ATM function in particular neurons or glial cells. These mice will inform us whether loss of ATM function in a

specific type of cell is responsible for causing neurodegeneration. Furthermore, the *Drosophila* models and the conditional knockout mice provide systems in which to test pharmacological methods to prevent innate immune response-dependent neurodegeneration. Combined, this multi-organism approach could lead to a treatment for neurodegeneration in A-T through the basic observations from *Drosophila* and the specific observations from conditional knockout mice.

Appendix 1

The effect of ATM knockdown on ionizing radiation-induced neuronal cell cycle reentry in *Drosophila*

This appendix was published in:

Rimkus SA, Petersen AJ, Katzenberger RJ, and Wassarman DA. (2010) The effect of ATM knockdown on ionizing radiation-induced neuronal cell cycle reentry in Drosophila. *Cell Cycle* 9: 2686-7.

S.A.R., A.J.P., and R.J.K. performed the experiments for this appendix. S.A.R., A.J.P., and D.A.W. made the table and wrote the text.

Neuronal death in many neurodegenerative diseases is preceded by re-expression of cell cycle regulatory proteins and DNA synthesis (Herrup and Yang 2007). To illustrate, in post-mortem cerebella of individuals with Ataxia-telangiectasia (A-T), Purkinje neurons at risk for degeneration express proliferating cell nuclear antigen and Cyclin B, and in a mouse model of A-T, DNA replication accompanies expression of these proteins in at-risk neurons (Yang and Herrup 2005). A-T is a recessive genetic disease caused by mutation of the A-T mutated (ATM) gene (Lavin 2008). A link between cell cycle regulation and neurodegeneration in A-T is not unexpected because ATM regulates the cell cycle progression of cells that incur DNA damage (Reinhardt and Yaffe 2009). For example, in response to ionizing radiation (IR)-induced DNA damage, ATM promotes G1 phase cell cycle arrest through phosphorylation and stabilization of p53. Thus, ATM may function to maintain neurons in a quiescent or G0 state, and progressive neurodegeneration that occurs in the absence of ATM may result from cell cycle reentry triggered by the accumulation of DNA damage over time.

Our prior studies of a *Drosophila* model of A-T, in which ATM expression is knocked down by RNA interference (RNAi), indicate that cell cycle reentry not only correlates with neurodegeneration but also causes neurodegeneration (Rimkus *et al*. 2008). ATM knockdown results in reentry of post-mitotic neurons into S phase of the cell cycle prior to caspase-dependent apoptosis. Blocking apoptosis by expression of the baculovirus p35 caspase inhibitory protein results in accumulation of neurons in G2/M phase of the cell cycle. Moreover, blocking cell cycle reentry by mutation of the cell cycle activator Cdc25/String inhibits neurodegeneration. These data predict the existence of ATM-regulated events that continuously function to block signals that promote cell cycle reentry of post-mitotic neurons.

A key feature of the *Drosophila* studies was the use of a method that enabled cell cycle analysis of post-mitotic neurons *in vivo*. Other studies of the role ATM plays in neurodegeneration have utilized fixed tissue or neurons cultured *in vitro*, which likely lack cell-cell signaling events that influence the process of cell cycle reentry-mediated neurodegeneration in a whole animal. Indeed, in contrast to our finding that ATM knockdown induces cell cycle reentry of neurons *in vivo*, others have found that pharmacological inhibition of ATM activity does not induce cell cycle reentry of mammalian cortical neurons *in vitro* (Kruman *et al*. 2004; Rimkus *et al*. 2008).

The *Drosophila* method involves marking all post-mitotic neurons in flies by expression of green fluorescent protein (GFP) under control of the *embryonic lethal, abnormal vision* (*elav*) gene transcriptional regulatory sequences (Neufeld *et al*. 1998; Rimkus *et al*. 2008). In the third instar larval eye imaginal disc, the developmental precursor to the adult eye, *elav* expression marks cells that have exited the cell cycle and differentiated into photoreceptor neurons (Robinow and White 1999). Fluorescence activated cell sorting (FACS) is then used to determine the DNA content and, thus, the cell cycle status of individual GFP-positive cells produced by dissociation of eye imaginal discs with trypsin. Here we have used this method to test the hypothesis that DNA damage causes cell cycle reentry of post-mitotic neurons and to determine the extent to which ATM knockdown affects DNA damage-induced cell cycle reentry.

Fly larvae were either untreated or irradiated with 50 Gy of gamma rays and allowed to recover for either 0.5-2.5 h or 21 h prior to eye imaginal disc dissection and FACS analysis. Two fly genotypes were analyzed. Flies designated elav-GFP expressed GFP in post-mitotic neurons by means of the GAL4-UAS system; expression of the GAL4 transcription factor from an elav-GAL4 transgene drove expression of a UAS-GFP transgene in post-mitotic neurons.

Flies designated elav-GFP-ATMi expressed GFP in the same manner and had reduced ATM expression in post-mitotic neurons due to a UAS-ATMi transgene that expressed a short hairpin RNA that targeted ATM mRNA for degradation by RNAi. For each sample, ~20 pairs of eye imaginal discs were dissected from wandering third instar larvae, and the DNA content of 5,000 live, GFP-positive, single cells was determined using a Becton Dickinson LSRII flow cytometer.

Consistent with our prior study, a substantial percentage (~28%) of neurons in untreated elav-GFP eye imaginal discs were cycling (either in S or G2/M phase) (Table 1). Treatment with IR followed by 0.5-2.5 h of recovery resulted in a statistically significant 11.9% increase in cycling neurons ($P<0.001$), most of which were resident in S phase. Recovery for 21 h did not result in a further increase in cycling neurons (relative to 0.5-2.5 h of recovery); however, it did decrease the percentage of S phase neurons to that of untreated larvae and increase the percentage of G2/M phase neurons, suggesting that neurons continued to progress through the cell cycle during this recovery period. Thus, in the context of eye imaginal discs, IR-induced DNA damage can cause post-mitotic neurons to reenter the cell cycle and complete DNA replication.

A parallel study of elav-GFP-ATMi eye imaginal discs revealed that treatment with IR and recovery for 0.5-2.5 h did not significantly increase the percentage of cycling neurons over the ~14.8% increase caused by ATM knockdown ($P>0.05$) (Table 1). However, recovery for 21 h resulted in a statistically significant ~17.6% increase in cycling neurons ($P<0.001$), which had progressed into G2/M phase. Thus, ATM knockdown attenuates IR-induced neuron cell cycle reentry shortly (0.5-2.5 h) after IR treatment but not after a longer period of time (21 h). Attenuation of DNA damage-induced cell cycle reentry by ATM inhibition was also observed in a study of cortical neurons *in vitro*; however, in this case, subsequent cell cycle reentry was not

observed (Kruman *et al*. 2004). This difference may be due to environmental context (*in vivo* versus *in vitro*) or one of many differences between the experimental protocols.

In summary, IR-induced DNA damage is sufficient to cause post-mitotic neurons *in vivo* to reenter the cell cycle, and loss of ATM delays but does not block IR-induced neuronal cell cycle reentry. In other words, IR-induced DNA damage can cause neuronal cell cycle reentry through ATM-dependent and ATM-independent mechanisms. The demonstration of an ATM-independent mechanism provides support for the hypothesis that progressive neurodegeneration in A-T results from cell cycle reentry triggered by the accumulation of DNA damage over time.

Acknowledgements

We thank K. Schell and the UW-Madison Comprehensive Cancer Center FACS facility for assistance with flow cytometry and R. Tibbetts for insights that greatly improved this work. Funding support was provided by a grant from the NIH (R01 NS059001 to D.A.W.) and a pre-doctoral fellowship from NIH training grant T32 GM08688 (to A.J.P.).

Table 1 **Cell cycle profiles of wild type and ATM knockdown neurons in response to IR**

			Cell cycle phase*			
Genotype	**Recovery (h)**		**G1**	**S**	**G2/M**	**Replicates**
elav-GFP	No irradiation	Δ11.9% (P<0.001)	72.0 ± 1.2	17.6 ± 1.1	10.4 ± 1.0	n=18
elav-GFP	0.5-2.5	Δ15.4% (P<0.001)	60.1 ± 1.7	26.7 ± 2.6	13.2 ± 2.3	n=9
elav-GFP	21		56.6 ± 2.0	16.5 ± 1.5	26.9 ± 1.2	n=6
elav-GFP-ATMi	No irradiation	Δ4.8% (P>0.05)	57.2 ± 1.9	22.5 ± 2.7	20.3 ± 2.7	n=13
elav-GFP-ATMi	0.5-2.5	Δ17.6% (P<0.001)	52.4 ± 0.6	30.8 ± 2.4	16.8 ± 2.5	n=3
elav-GFP-ATMi	21		39.6 ± 2.5	12.0 ± 1.3	48.5 ± 3.1	n=8

*Data were analyzed using CellQuest (Becton Dickinson) and ModFit (Verify Software House) software. Indicated are the average percentage of photoreceptor neurons in each phase of the cell cycle and the standard error of the mean. P-values were calculated using one-way ANOVA and Tukey's multiple comparison post-test.

Appendix 2

Mitotic clones in the developing *Drosophila* eye disc reveals cell cycle reentry of ATM null photoreceptors

Introduction

Previous work in our lab identified that photoreceptor neurons with ATM levels knocked down via RNAi (*GMR-ATMi* or *Elav-ATMi*) reenter the cell cycle and replicate their DNA. This phenomenon has been observed in *ATM* null neurons in mice and humans (Yang and Herrup 2005). In order to determine if the same event occurs in *ATM* null tissue in the fly, clones of *ATM* were generated through mitotic recombination.

Clone generation utilizes the FLP/FRT recombination system to generate homozygous tissue from a heterozygous precursor cell via mitotic recombination (Chapter 1, Figure 1.3) (Xu and Rubin 1993). For my purposes, I utilized a null allele of *ATM*, ATM^{6}, to create *ATM* null tissue in the *Drosophila* eye disc, a precursor tissue to the adult compound eye. To promote recombination, the FLP transgene was expressed via the *eyeless* promoter. *Eyeless* expression occurs throughout development, with high expression in all developing cells of the eye disc, including the photoreceptor neurons. For the GFP construct, I used a membrane-bound GFP, allowing resolution of the individual ommatidia, which are sets of seven photoreceptors constituting the facets of the compound eye.

Results

To determine if ATM null tissue reentered the cell cycle, I stained eye discs containing *ATM* wild-type and *ATM* null clones for phosphorylated serine 10 on histone H3, a marker of DNA replication (Wei *et al*. 1998). Eye discs from third-instar wandering larvae were dissected and stained for PH3 and subjected to light microscopic analysis. Approximately half of the larvae exhibited clones in the eye, as detected by areas lacking GFP expression. Clones of wildtype *ATM* did not exhibit PH3 staining, indicating that photoreceptors with normal ATM function do not undergo cell cycle reentry (Figure A2.1A and B). In *ATM* null clones, on the

other hand, robust PH3 staining is observed in ATM-deficient photoreceptors, indicating that endogenous loss of ATM recapitulates the cell cycle reentry phenotype observed in ATM knockdown photoreceptors (Figure A2.1).

Materials and methods

Fly stocks for *ATM*^{6}, *eyFLP*, and GFP were obtained from the Bloomington Stock Center. Tissue dissection and staining protocols for PH3 were performed as in Rimkus *et al*. 2008.

Figure A2.1. ATM null clones exhibit cell cycle reentry of photoreceptor neurons. Shown are images of wandering third instar larval eye discs, with red staining depicting PH3 staining. Lack of GFP expression identifies tissue in which mitotic recombination has occurred to generate *ATM* wildtype tissue (A and B) or *ATM* null tissue (C and D). Yellow squares in A and C depict the regions expanded for B and D, respectively, and the dotted line in C indicates the border of the eye disc tissue.

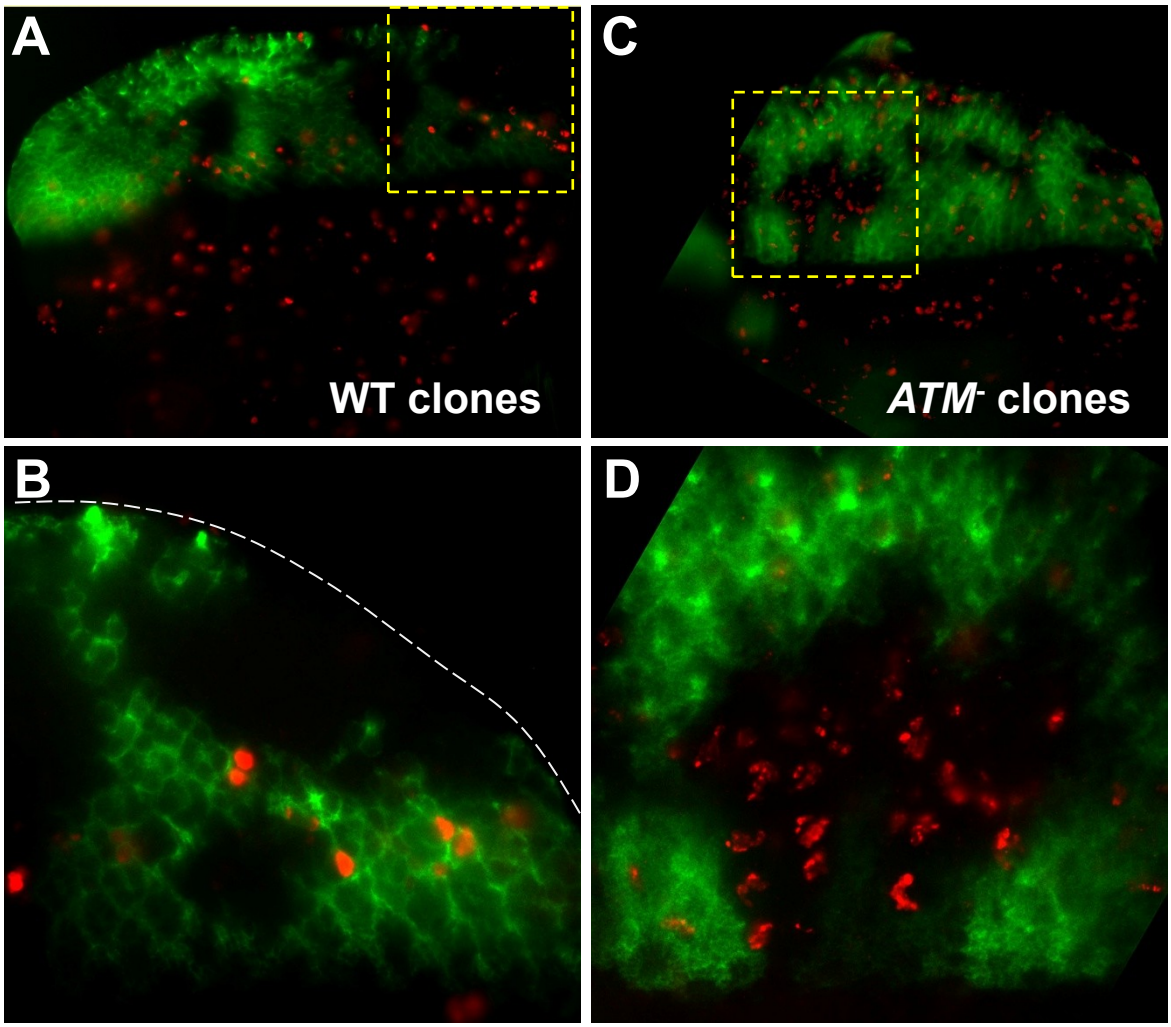
A
WT clones
C
ATM- clones
B
D

Appendix 3

Dominant suppressor effects of genes with altered expression in ATM-deficient microarrays on the GMR-ATMi rough eye phenotype

Introduction

Microarray analysis on ATM-deficient flies yielded a large number of genes whose expression level is altered in response to a reduction in ATM kinase function (Chapters 2 and 4; Appendix 4; Petersen *et al*. 2012). To determine whether many of these genes function in the neurodegenerative phenotype of ATM-deficient flies, a genetic screen was performed to determine whether mutations in these genes could dominantly affect the rough eye phenotype produced by knocking down ATM levels in the *Drosophila* compound eye (Rimkus *et al*. 2008). For this analysis, heterozygous mutant alleles of various proteins functioning within the cell cycle, germline processes, or innate immunity were acquired and crossed into the *GMR-ATMi* background.

Results and Discussion

To evaluate the relevance of the observed changes in gene expression to neurodegeneration, we examined the extent to which gene mutations modified the previously characterized rough eye and neurodegeneration phenotypes of *GMR-ATMi* flies (Rimkus *et al*. 2008). In *GMR-ATMi* flies, the *GMR-GAL4* driver directs expression of *pWIZ-ATM*^{T4} in all cells of the developing eye. The assumption was that the neurodegeneration pathways for brain neurons and photoreceptor neurons are conserved, as has been shown in other *Drosophila* models of human neurodegenerative diseases (Ghosh and Feany 2004). In support of this assumption, *stg* expression increased in both *Elav-ATMi* and *GMR-ATMi* adult heads, and *stg* mutants suppressed the *GMR-ATMi* rough eye phenotype. Furthermore, gene expression microarray analysis of *GMR-ATMi* adult heads revealed significant overlap with the genes that changed expression in the *Elav-ATMi*, *Repo-ATMi*, or *ATM*^{8} microarrays, especially mitotic cell cycle genes.

Mutants were obtained for 111 genes, including many genes that had increased expression in the *Elav-ATMi* array or select genes that had increased expression in other arrays (Figure A3.1). Mutant flies were crossed to *GMR-ATMi* flies, and progeny were scored for modification of the rough eye phenotype. Mutations in 38 genes were found to dominantly suppress the *GMR-ATMi* rough eye phenotype (highlighted yellow in Figure A3.1). In comparison, a prior screen of 643 random P-element mutants for modifiers of the *GMR-ATMi* rough eye phenotype only identified three suppressor genes (*stg*, *RAD50*, and *Rpd3*) (Rimkus *et al*. 2008). The 34% hit rate for genetic modifiers seen among the genes that changed expression in ATM inactivation flies is 68-fold higher than the 0.5% hit rate observed in the unbiased screen for modifiers of the *GMR-ATMi* rough eye phenotype, indicating that the microarray analysis was an efficient approach to identify genes involved in neurodegeneration.

For a subset of the microarray genes that suppressed the *GMR-ATMi* rough eye phenotype, transmission electron microscopy (TEM) of tangential eye sections was used to assess the extent of modification of photoreceptor neurodegeneration (Figure A3.2A-C). All of the gene mutants examined significantly reduced the level of photoreceptor neurodegeneration caused by *GMR-ATMi*, including genes involved in activation of the mitotic cell cycle (*aurora borealis*, *greatwall (gwl)*, and *stg*), activation of the SAC (*Anaphase promoting complex 7*), somatic cell to germ cell transformation (*cup*, *swallow*, *vas*, and *wisp*), and activation of the innate immune response (*Attacin-C* and *poor imd response upon knockin*) ($P<0.01$) (Figure A3.2D). Of particular note was a *greatwall* (*gwl*) mutant, which almost completely blocked neurodegeneration (Figure A3.2C). The high degree of suppression by *gwl* may be due to inhibition of multiple neurodegeneration-causing events. *Gwl* encodes a protein kinase that plays multiple roles in mitotic and meiotic cell cycle progression and may have roles in germ

cell-related processes, since, like many germ cell genes, its expression increased in *Elav-ATMi* flies and decreased in *Repo-ATMi* flies (Chapter 4) (Archambault *et al*. 2007). Thus, misexpression of genes involved in mitotic cell cycle activation, germ cell-related processes, SAC activation, and the innate immune response is likely a cause rather than a consequence of neurodegeneration.

Materials and Methods

The genetic screen was performed by crossing *GMR-GAL4/CyO; $pATM^{T4}$/$pATM^{T4}$* flies with mutant fly strains and screening for modifiers of the *GMR-GAL4/+; $pATM^{T4}$/+* rough eye phenotype. So as not to bias the analysis, stock numbers instead of genotypes were used as identifiers during the screen.

Adult heads were embedded, sectioned, and imaged by TEM as described in Rimkus *et al.* (2008). Three heads were sectioned for each genotype and degree of neurodegeneration was scored by counting the average number of normal photoreceptors per ommatidium in each genotype. Rhabdomere membranes were considered normal if they were not absent, condensed, fragmented, or split. Statistical analysis was performed using Prism 4.0c software (Graphpad), and one-way ANOVA with Dunnett's multiple comparison test was used to compare control *GMR-ATMi* flies to experimental *GMR-ATMi* flies that carried a heterozygous mutation in a gene identified by microarray analysis.

Acknowledgements

We thank Ben August for assistance with eye sectioning and TEM, Stacey Rimkus for assistance screening stocks, and Helen Salz for providing *deadhead* flies.

Figure A3.1. The complete list of gene mutants that were screened for modification of the *GMR-ATMi* rough eye phenotype. Mutation of genes highlighted in yellow suppressed the rough eye phenotype of *GMR-ATMi* flies. If multiple alleles of a gene were screened, the CG number and gene name are indicated for the first allele but not the alleles that immediately follow in the list.

CG number	Gene	Allele	GMR-ATMi
CG8308	α-Tubulin at 67C (α-Tub67C)	3	No change
		2	No change
		1	No change
CG14444	Anaphase Promoting Complex 7 (APC7)	EY11333	Suppressed
		EY02849	No change
CG4740	Attacin C (AttC)	MB05438	Suppressed
CG6897	aurora borealis (bora)	EY21751	Suppressed
CG4824	Bicaudal C (BicC)/GLD-3	4	No change
CG1759	caudal (cad)	2	No change
CG5363	cdc2/Cdk1	GT-000294	No change
		B47	No change
		E1-23	No change
CG1878	Cecropin B (CecB)	B193	No change
CG1373	Cecropin C (CecC)	MB01213	No change
CG6392	CENP-meta (cmet)	EY00718	Suppressed
		04431	No change
CG17604	crossover suppressor on 3 of Gowan (c(3)G)	1	Suppressed
CG11181	cup	1	Suppressed
		01355	No change
CG5494	Cuticular protein 92F (Cpr92F)	c03081	No change
CG5940	Cyclin A (CycA)	c05304	No change
		C8LR1	No change
CG3510	Cyclin B (CycB)	KG08886	No change
		KG00006	No change
		2	No change
CG9964	Cyp309a1	KG02086	No change
CG8540	Cyp316a1	MB06750	Suppressed
CG8687	Cyp6a14	KG00760	No change
CG14728	Cyp315a1/shadow (sad)	1	No change
CG4193	deadhead (dhd)	15	No change
CG6157	discontinuous actin hexagon (dah)	f04432	No change
		30	No change
CG5235	dopamine b-monooxygenase	EY02761	Suppressed
		KG02953	Suppressed
CG3723	Dynein heavy chain at 93AB (Dhc93AB)	MB05444	Suppressed
		MB04366	No change
CG5400	Eclosion hormone (Eh) RNAi	JF02143	No change
CG2914	Ets at 21C (Ets21C)	f03639	Suppressed
CG8994	exuperantia (exu)	DG04401	No change
CG11411	female sterile (1) Nasrat (fs(1)N)	4	Suppressed
		1	No change
CG4274	fizzy (fzy)/Cdc20	3	No change
		1	No change
CG17566	γ-Tubulin at 37C (γ-Tub37C)	1	Suppressed
		3	No change
CG5272	giant nuclei (gnu)	305	No change
CG4181	Glutathione S transferase D2 (GstD2)	f00583	Suppressed
CG12242	Glutathione S transferase D5 (GstD5)	1	No change
CG4423	Glutathione S transferase D6 (GstD6)	MB02663	Suppressed
CG7719	greatwall (gwl)	EP515	Suppressed
		3	No change
CG7756	Heat shock protein cognate 70-2 (Hsc70-2)	MB04273	No change
CG12165	Inner centromere protein (Incenp)	QA26	No change
CG9191	Kinesin-like protein 61F (Klp61F)	07012	No change
CG4178	Larval serum protein 1β (Lsp1β) RNAi	JF02368	Suppressed
CG18543	matrimony (mtrm)	KG08051	No change
CG17795	methuselah-like 2 (mthl2)	e01373	No change
CG4978	Mini chromosome maintenance 7 (Mcm7)	f03462	No change
CG9241	Mini chromosome maintenance 10 (Mcm10)	KG00233	Suppressed
CG12047	mushroom body defect (mud)/NuMA	4	Suppressed
		1	No change
CG10207	Na+-dependent inorganic phosphate transporter (NaPi-T)	e02874	No change
CG5637	nanos (nos)	L7	No change
CG17256	Nek2	EP1209	No change
CG31299	nocturnin	d05983	Suppressed
CG10901	oskar (osk)	6	No change
		7	No change
CG12743	ovarian tumor (otu)	14	No change
		7	No change
CG33105	p24-related-2 (p24-2)/emp24 protein	DG16306	Suppressed
CG4799	Pendulin (Pen)	DG08110	Suppressed
CG11765	Peroxiredoxin 2540 (Prx2540-2)	MB04531	No change
CG7059	phosphoglycerate mutase	MB01361	Suppressed
		f06779	Suppressed

CG number	Gene	Allele	GMR-ATMi
CG5052	pimples (pim)	IL	Suppressed
		A385	No change
CG12306	polo	KG03033	No change
		16-1	No change
CG15678	poor Imd response upon knockin (pirk)	EY00723	Suppressed
CG7660	pxt	EY03052	No change
CG13345	RacGAP50C/tumbleweed (tum)	347	No change
		DH15	No change
		AR2	No change
CG8606	RhoGEF4	G4106	No change
CG7361	Rieske iron-sulfur protein (RFeSP)	M73	No change
CG1058	ripped pocket (rpk) RNAi	JF01868	Suppressed
CG3827	scute (sc)	5	No change
		1	No change
CG30091	serine endopeptidase	G7521	Suppressed
CG6046	Sin3A-associated protein 18 (SAP18)	EP3462	Suppressed
CG34414	sprint (spri)	KG07279	Suppressed
CG10522	sticky (sti)/citron	KG01697	No change
CG1395	string (stg)	EY12388	Suppressed
CG10931	subito (sub)/mitotic kinesin-like protein 2 (MKLP2)	EP616	No change
		1	No change
CG3429	swallow (swa)	1	Suppressed
		6	Suppressed
CG11853	takeout (to)	c00632	No change
CG1389	torso (tor)	e00150	No change
		4	No change
CG17462	Trf4-2	EY05585	Suppressed
CG31509	Turandot A (TotA)	MB06977	Suppressed
CG31508	Turandot C (TotC)	f01700	No change
CG3524	v(2)k05816	EP695	Suppressed
CG3506	vasa (vas)	1	Suppressed
		RJ36	Suppressed
		KG01651	No change
CG12701	vielfaltig (vfl)/Zelda	G0353	No change
		G0427	No change
		G0120	No change
CG7670	Werner exonuclease (WRNexo)	e04496	No change
CG15737	wispy (wisp)/GLD-2	KG05287	Suppressed
CG1372	yolkless (yl)	15	No change
		13	No change
CG3994	Zinc transporter 35C (ZnT35C)	MB08945	No change
CG18729	zwilch	MB05212	No change
		c04101	No change
CG10073		MB02747	No change
CG10630		KG00804	No change
CG10934		EP538	No change
CG11052		DG02601	No change
CG11120		f02851	No change
CG13699		c04491	No change
CG14118		d06432	Suppressed
CG14545		MB09376	No change
CG14632		EP1498	No change
CG14752		MB00604	No change
CG14990		f07267	No change
CG15234		01094	No change
CG15530		C110	No change
CG17186		JF02425	No change
CG17322		KG04070	No change
CG18586		MB03855	No change
CG3119		G19432	Suppressed
		MB07697	Suppressed
CG31205		f05726	No change
CG31272		MB05128	No change
CG3679		MB02546	No change
CG42600		c04990	No change
CG5568		MB12106	No change
CG5873		c00427	No change
CG6347		e00490	No change
CG6783		KG06479	No change
CG6891		KG03306	No change
CG6927		JF01936	Suppressed
		BG01861	No change
CG9602		MB00748	No change
CG9925		KG01164	No change

Figure A3.2. Heterozygous mutation of genes that changed expression as a result of ATM inactivation suppressed photoreceptor neurodegeneration in *GMR-ATMi* flies. (A-C) Representative TEM images of eye sections used to quantitate photoreceptor degeneration. Photoreceptor neuron rhabdomeres are numbered in panel A, and ommatidial clusters are circled in panel B. Fly genotypes are indicated in the upper right of each panel. (D) Graphed is the average number of morphologically normal photoreceptors per ommatidium (± standard error of the means) for each of the indicated genes (n>100 ommatidia from at least two eyes). *GMR-GAL4* and *GMR-ATMi* serve as standards for comparison. Gene abbreviations are as follows: *APC7* (*Anaphase promoting complex 7*^{EY11333}), *bora* (*aurora borealis*^{EY21751}), *gwl* (*greatwall* ^{EP515}), *swa* (*swallow*^{1}), *AttC* (*Attacin-C*^{MB05438}), and *pirk* (*poor imd response upon knock-in*^{EY00723}).

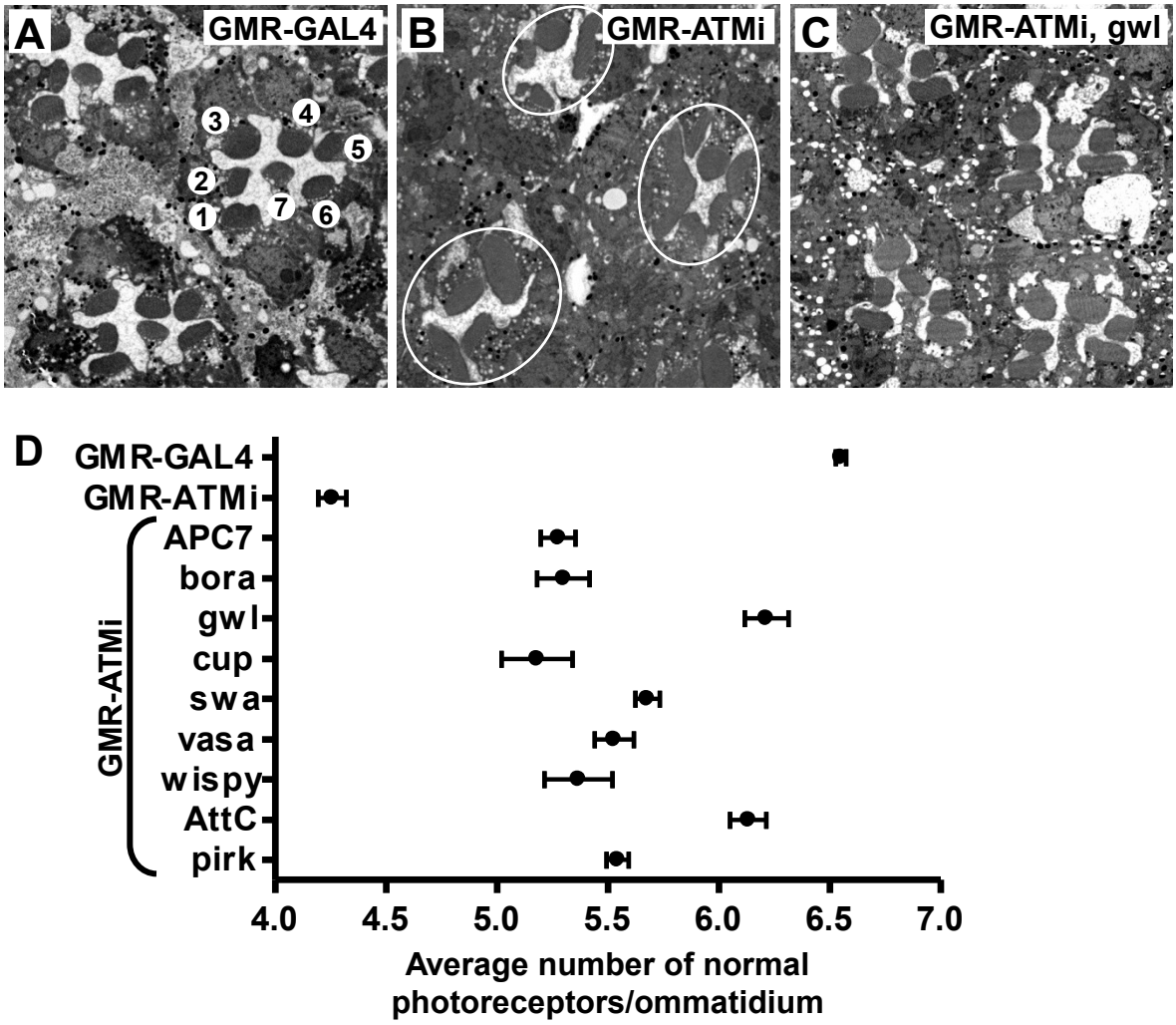
A
GMR-GAL4
1
2
3
4
5
6
7
B
GMR-ATMi
C
GMR-ATMi, gwl
D
GMR-GAL4
GMR-ATMi
GMR-ATMi
APC7
bora
gwl
cup
swa
vasa
wispy
AttC
pirk
4.0
4.5
5.0
5.5
6.0
6.5
7.0
Average number of normal
photoreceptors/ommatidium

Appendix 4

Summary of microarray studies on various ATM-deficient genotypes

Introduction

Previous sections in this thesis have dealt with microarray studies analyzing gene expression changes in response to loss of ATM in various tissues and cell types in the fly. Here, I provide a summary of all of the genotypes tested in this manner, the primary classes of genes observed to be differentially changed, and my confidence level that these genes represent the true gene expression changes in this condition. Table A4.1 provides a list of the microarrays summarized below. For all of the arrays, total RNA was isolated from the heads of approximately 200 flies per sample using TRI reagent (Sigma) and were analyzed using Nimblegen platforms and the ArrayStar analysis program. For all experiments, flies were collected 0-3 days post-eclosion and aged for an additional 3 days prior to RNA collection. For the ATM^{8} and $Elav^{C155}$-*ATMi* experiments, the initial 0-3 days occurred at 18°C and the final 3 days at 25°C. All other experiments were at 25°C for the duration.

***ATM*^{8}**

For this experiment, ATM^{8} homozygous flies were compared to ATM^{8}/+ flies. The majority of the genes found to be upregulated function within the innate immune response, and are characterized in Chapter 2. The findings from this array carry significant caveats, however. Initial expectations were that ATM^{8}/+ flies would exhibit a more wildtype phenotype than they do. Thus, using them as the control group drastically affected the number and type of genes that this experiment would identify. A feature of the innate immune response genes are that their expression is dramatically upregulated, sometimes upward of 100- to 1000-fold. In fact, comparison of ATM^{8} flies to true wildtype flies reveals upregulation of 50- to 150-fold for these genes, despite the microarray only producing a maximum difference of 8- to 10-fold. Thus, in

order for a gene to be identified with our 2-fold cutoff, its expression would theoretically have to increase approximately 20-fold between wildtype and ATM^{8}. Expectations based on other experiments suggest that genes identified in the other microarrays may be affected in ATM^{8} flies, and in fact germline gene expression is found to be downregulated in ATM^{8} compared to wildtype, similar to that seen for *Repo-ATMi* flies (Chapter 4).

Repo-ATMi

For this experiment, *Repo-ATMi* were compared to *Repo-GAL4* flies. Upregulated genes primarily belonged to the innate immune response and are covered in Chapter 2. Downregulated genes primarily belong to the germline class of genes and are covered in Chapter 4. Only two microarrays were performed for both control and experimental flies, but the consistency between them produced quality results and low P-values, indicating that the data is quite representative of what actually occurs in these flies.

Elav-ATMi

For this experiment, *Elav-ATMi* flies were compared to *Elav-GAL4*. Upregulated genes primarily function within the cell cycle and germline related processes and are covered in detail in Chapter 4. Four replicates of each of these genotypes were performed: two replicates on individual crosses between *Elav-GAL4* and either $pATM^{T4}$ or w^{1118} and two replicates on *Elav-Gal4* or *Elav-ATMi* stocks. The results were consistent regardless of how the arrays were performed, and thus P-values for this experiment are quite low and I am confident in the results.

Elav-ATMi, UAS-P35

For this experiment, *Elav-ATMi* flies were compared to *Elav-GAL4*, with both control and experimental flies expressing a *UAS-P35* construct to inhibit apoptotic cell death. While there were a large number of upregulated and downregulated genes, these genes did not fall within any

obvious gene ontology categories. One exception is that a portion of innate immunity genes are downregulated in these flies (*Def*, *DiptB*, *Mtk*, *drs4*, *GstE4*). Another observation reveals that the genes upregulated in *Elav-ATMi* flies are notably absent, specifically the cell cycle and germline genes. This would suggest that blocking apoptosis (or caspase activation) is sufficient to suppress cell cycle reentry and germline gene expression. One caveat for this conclusion is the nature of the experiment. Anecdotal evidence suggests that introducing a second UAS-containing construct into a UAS-RNAi experiment significantly affects the level of knockdown achieved. This has not been directly tested in these flies, raising the possibility that a sufficient level of knockdown of *ATM* may not have been achieved and lack of the subsequent changes in gene expression is due to this fact. Therefore, without extensive testing to show that *ATM* levels are reduced in this genotype, I would hesitate to make conclusions based on this data.

Elav-ATMi, Stg^{EY12388}

For this experiment, *Elav-ATMi* flies were compared to *Elav-GAL4*, with both control and experimental flies containing an EP-element allele of *Stg* to inhibit cell cycle progression. In this case, only a relatively small number of genes were differentially expressed, and these genes did not fall within any obvious gene ontology categories. As was the case for the *UAS-P35* array, the genes upregulated in *Elav-ATMi* flies are notably absent, specifically the cell cycle and germline genes. This would suggest that suppressing cell cycle activity is sufficient to suppress cell cycle reentry and germline gene expression. Once again, however, the EP-element used to generate this allele contains a UAS sequence, potentially reducing the level of *ATM* knockdown below the threshold required to generate the necessary effects on gene expression. Because of this, this data should only be believed if *ATM* levels are confirmed to be reduced in this genotype.

Elav^{C155}-ATMi

For this experiment, *Elav^{C155}-ATMi* flies were compared to *Elav^{C155}-GAL4*, and this experiment was performed by Dr. Stacey Rimkus. This GAL4 construct is inserted at the endogenous Elav locus, and is believed to produce stronger expression of GAL4 than the other *Elav-GAL4* used above. However, this has not been tested. For this experiment, no obvious class of genes was up or downregulated. A few genes that function in response to oxidative stress were upregulated, but this class was not identified as significant. A few explanations can explain why no significant effects were seen, and why this array does not overlap with the previous *Elav-ATMi* data set. Data for this set was collected by a different scientist in the laboratory, and the flies for this cross were raised at a lower temperature (18°C versus 25°C for the other arrays except *ATM^{8}*). This lower temperature was used due to the belief that raising them at 25°C would cause lethality. However, this has been shown not to be the case as *Elav^{C155}-ATMi* flies raised at 25°C yield at the expected rate and exhibit similar phenotypes to *Elav-ATMi* (Chapter 2). The major effect caused by raising these flies at 18°C is a reduction in the expression level of *GAL4*, and subsequent reduction in the knockdown of *ATM*. Thus, it is difficult to determine whether *ATM* levels were sufficiently reduced in this experiment to produce the effects on gene expression. Due to this, I would not be confident in concluding that these results are indicative of true *Elav^{C155}-ATMi* gene expression changes.

GMR-ATMi

For this experiment, *GMR-ATMi* flies were compared to *GMR-GAL4*. Obvious classes of genes did not appear to be upregulated or downregulated to a high extent in this experiment. However, subsets of genes did overlap with the other *ATM* knockdown arrays. This experiment showed a subset of overlapping cell cycle and potentially germline genes with the *Elav-ATMi*

array. Numerous genes overlapped between this experiment and *Elav*^{C155}*-ATMi* and *Repo-ATMi*, although the function of these genes is varied and does not follow an obvious trend. Since *GMR* is expressed in neurons and also potentially in glial cells in the eye, it is not surprising to see a subset of overlap between these arrays. In general, however, this overlap does not include genes with distinct functions. For these arrays, four replicates of each genotype were performed, so the numbers and P-values are quite strong and I believe the data to be accurate.

***Rh1-ATMi* (mRNA tagging)**

For this experiment, the *Rh1-GAL4* construct was used as the control for *ATM* knockdown in the photoreceptors of the eye. These flies additionally contained a UAS-polyA binding protein (PABP) construct to specifically isolate polyA mRNA from these photoreceptors. The idea for this experiment is based on a paper by Yang *et al*. (2005) who showed that it is possible via this method to isolate mRNA from a specific cell type. Unfortunately, this method was not fully worked out prior to their publication and provided numerous challenges. Eventually, I was able to generate enough mRNA for the experiment after a round of amplification using an RNA amplification kit (Ambion). However, the microarray did not reveal significant classes of genes due to low statistical relevance. The P-values derived from the two replicates were large and thus no conclusive determinations were able to be made. Furthermore, attempts to adapt this method to a more abundant cell type, such as neurons or glial cells, failed due to lethality of the PABP construct in these cell types.

***ATM* knockdown S2 cells**

For this array, RNA was isolated from cell types treated with dsRNA targeting *ATM* or untreated. This experiment was performed by Dr. Stacey Rimkus. The only gene found to be upregulated was *deadhead* at 2.2 fold, and the P-value for this gene would cause us to exclude it

(P=0.14). Thus, no genes were found to be significantly upregulated using our standard criteria. Similar results were observed for downregulated genes. Only one gene met our criteria of a >2.0 fold downregulation and a significant P-value. This gene is *tefu*, also known as *ATM*, and was the target of our RNAi knockdown. This is reassuring because it confirms that proper RNAi knockdown was achieved. However, it was only a 2-fold reduction in ATM levels and was not accompanied by any other gene expression changes. Therefore, either ATM levels are dispensable in S2 cells, or the level of knockdown was not sufficient to produce an effect.

References

Abraham RT. (2001) Cell cycle checkpoint signaling through ATM and ATR kinases. *Genes Dev* 15: 2177-96.

Abraham RT. (2004) PI 3-kinase related kinases: 'big' players in stress-induced signaling pathways. *DNA Repair* 3: 883-7.

Ahmed M and Rahman N. (2006) ATM and breast cancer susceptibility. *Oncogene* 25: 5906-11.

Akiyama H, Barger S, Barnum S, Bradt B, Bauer J, *et al*. (2000) Inflammation and Alzheimer's disease. *Neurobiol Aging* 21: 383-421.

Allen DM, van Praag H, Ray J, Weaver Z, Windrow CJ, *et al*. (2001) Ataxia telangiectasia mutated is essential during adult neurogenesis. *Genes Dev* 15: 554-66.

Alterman N, Fattal-Valevski A, Moyal L, Crawford TO, Lederman HM, *et al*. (2007) Ataxia-telangiectasia: mild neurological presentation despite null ATM mutation and severe cellular phenotype. *Am. J. Med. Genet* 143A: 1827-34.

al-Ubaidi MR, Hollyfield JG, Overbeck PA, and Baehr W. (1992) Photoreceptor degeneration induced by the expression of simian virus 40 large tumor antigen in the retina of transgenic mice. *Proc Natl Acad Sci U S A* 89: 1194-8.

Amor S, Puentes F, Baker D, and van der Valk P. (2010) Inflammation in neurodegenerative diseases. *Immunology* 129: 154-69.

Aravin AA, Hannon GJ, and Brennecke J. (2007) The Piwi-piRNA pathway provides an adaptive defense in the transposon arms race. *Science* 318: 761–4.

Archambault V, Zhao X, White-Cooper H, Carpenter ATC, and Glover DM. (2007) Mutations in Drosophila Greatwall/Scant reveal its roles in mitosis and meiosis and interdependence with Polo kinase. *PLoS Genet* 3: e200.

Arroyo DS, Soria JA, Gaviglio EA, Rodriguez-Galan MC, and Iribarren P. (2011) Toll-like receptors are key players in neurodegeneration. *Int Immunopharmacol* 11: 1415-21.

Asea A, Rehli M, Kabingu E, Boch JA, Baré O, *et al*. (2002) Novel signal transduction pathway utilized by extracellular HSP70. *J Biol Chem* 277: 15028-34.

Ashburner M, Ball CA, Blake JA, Botstein D, Butler H, *et al.*; The Gene Ontology Consortium. (2000) Gene ontology: tool for the unification of biology. *Nat Genet* 25: 25–9.

Auluck PK and Bonini NM. (2001) Pharmacological prevention of Parkinson disease in *Drosophila*. *Nat Med* 8: 1185-6.

Auluck PK, Chan HY, Trojanowski JQ, Lee VM, and Bonini NM. (2002) Chaperone suppression of alpha-synuclein toxicity in a Drosophila model for Parkinson's disease. *Science* 295: 865-8.

Bakkenist CJ and Kastan MB. (2003) DNA damage activates ATM through intermolecular autophosphorylation and dimer dissociation. *Nature* 421: 499-506.

Banin S, Moyal L, Sheih S, Taya Y, Anderson CW, *et al*. (1998) Enhanced phosphorylation of p53 by ATM in response to DNA damage. *Science* 281: 1674-7.

Barlow C, Hirotsune S, Paylor R, Liyanage M, Eckhaus M, *et al*. (1996) Atm-deficient mice: a paradigm of Ataxia Telangiectasia. *Cell* 86: 159-71.

Barlow C, Ribaut-Barassin C, Zwingman TA, Pope AJ, Brown KD, *et al*. (2000) ATM is a cytoplasmic protein in mouse brain required to prevent lysosomal accumulation. *Proc Natl Acad Sci U S A* 97: 871-6.

Bauer M, Katzenberger JD, Hamm AC, Bonaus M, Zinke I, *et al*. (2006) Purine and folate metabolism as a potential target of sex-specific nutrient allocation in *Drosophila* and its implication for lifespan-reproduction tradeoff. *Physiol Genomics* 25: 393-404.

Becher B, Fedorowicz V, and Antel JP (1996) Regulation of CD14 expression on human adult central nervous system-derived microglia. *J Neurosci Res* 45: 375-81.

Becker T, Loch G, Beyer M, Zinke I, Aschenbrenner AC, *et al*. (2010) FOXO-dependent regulation of innate immune homeostasis. *Nature* 463: 369-73.

Belvin MP, Jin Y, and Anderson KV. (1995) Cactus protein degradation mediates *Drosophila* dorsal-ventral signaling. *Genes Dev* 9: 783-93.

Benzer S. (1967) Behavioral mutants of *Drosophila* isolated by countercurrent distribution. *Proc Natl Acad Sci U S A* 58: 1112-9.

Bhatti S, Kozlov S, Farooqi AA, Naqi A, Lavin M, *et al.* (2011) ATM protein kinase: the linchpin of cellular defenses to stress. *Cell Mol Life Sci* 68: 2977-3006.

Bi X, Gong M, Srikanta D, and Rong YS. (2005) *Drosophila* ATM and MRE11 are essential for the G2/M checkpoint induced by low-dose radiation. *Genetics* 171: 845-7.

Biton S, Barzilai A, and Shiloh Y. (2008) The neurological phenotype of ataxia-telangiectasia: Solving a persistent puzzle. *DNA Repair (Amst)* 7: 1028-38.

Boder E. (1985) Ataxia-telangiectasia: an overview. *Kroc Found Ser* 19: 1-63.

Boder E and Sedgwick RP. (1957) Ataxia-telangiectasia. A familial syndrome of progressive cerebellar ataxia, oculocutaneous telangiectasia and frequent pulmonary infection. A

preliminary report on 7 children, an autopsy, and a case history. *Univ Soc Calif Med Bull* 9: 15-28.

Bodily KD, Morrison CM, Renden RB, and Brodie K (2001) A novel member of the Ig superfamily, *turtle*, is a CNS-specific protein required for coordinated motor control. *J Neurosci* 21: 3113-25.

Boke E and Hagan IM. (2011) Polo, greatwall, and protein phosphatase PP2A jostle for pole position. *PLoS Genet* 7: e1002213.

Bosotti R, Isacchi A, and Sonnhammer EL. (2000) FAT: A novel domain in PIK-related kinases. *Trends Biochem Sci* 25: 225-7.

Brand AH and Perrimon N. (1993) Targeted gene expression as a means of altering cell fates and generating dominant phenotypes. *Development* 118: 401-15.

Brodsky MH, Nordstrom W, Tsang G, Kwan E, Rubin GM, *et al*. (2000) *Drosophila* p53 binds a damage response element at the *reaper* locus. *Cell* 101: 103-13.

Brodsky MH, Weinert BT, Tsang G, Rong YS, McGinnis NM, *et al*. (2004) *Drosophila melanogaster* MNK/Chk2 and p53 regulate multiple DNA repair and apoptotic pathways following DNA damage. *Mol Cell Biol* 24: 1219-31.

Buchanan RL and Benzer S. (1993) Defective glia in the Drosophila brain degeneration mutant *drop-dead*. *Neuron* 10: 839-50.

Bundey S. (1994) Clinical and genetic features of ataxia-telangiectasia. *Int J Radiat Biol* 66: S23–9.

Burma S, Chen BP, Murphy M, Kurimasa A, and Chen DJ. (2001) ATM phosphorylates histone H2AX in response to DNA damage. *Science* 316: 42462-7.

Cabal-Hierro L and Lazo PS. (2012) Signal transduction by tumor necrosis factor receptors. *Cell Signal* 24: 1297-305.

Canman CE, Lim DS, Cimprich KA, Taya Y, Tamai K, *et al*. (1998) Activation of the ATM kinase by ionizing radiation and phosphorylation of p53. *Science* 281: 1677-9.

Cardona A, Saalfeld S, Preibisch S, Schmid B, Cheng A, *et al*. (2010) An integrated micro- and macroarchitectural analysis of the Drosophila brain by computer-assisted serial section electron microscopy. *PLoS Biol* 8: e1000502.

Carson CT, Schwartz RA, Stracker TH, Lilley CE, Lee DV, *et al*. (2003) The Mre11 complex is required for ATM activation and the G2/M checkpoint. *EMBO J* 15: 6610-20.

Cauchi RJ and van den Heuvel M. (2006) The fly as a model for neurodegenerative disease: is it worth the jump? *Neurodegenerative Dis* 3: 338-56.

Cavalieri S, Funaro A, Porcedda P, Turinetto V, Migone N, *et al*. (2006) ATM mutations in Italian families with ataxia telangiectasia include two distinct large genomic deletions. *Hum Mutat* 27: 1061.

Celotto AM and Palladino MJ. (2005) Drosophila: A "model" model system to study neurodegeneration. *Mol Interv* 5: 292-303.

Chakraborty S, Kaushik DK, Gupta M, and Basu A. (2010) Inflammasome signaling at the heart of central nervous system pathology. *J Neurosi Res* 88: 1615-31.

Chang CW, Nashchekin D, Wheatley L, Irion U, Dahlgaard K, *et al*. (2011) Anterior-posterion axis specification in *Drosophila* oocytes: identification of novel bicoid and oskar localization factors. *Genetics* 188: 883-96.

Chehab NH, Malikzay A, Stavridi ES, and Halazonetis TD. (1999) Phosphorylation of ser-20 mediates stabilization of human p53 in response to DNA damage. *Proc Natl Acad Sci U S A* 96: 13777-82.

Chen P, Peng C, Luff J, Spring K, Watters D, *et al*. (2003) Oxidative stress is responsible for deficient survival and dendritogenesis in purkinje neurons from ataxia-telangiectasia mutated mutant mice. *J Neurosci* 23: 11453-60.

Chen PC, Lavin MF, Kidson C, and Moss D. (1978) Identification of ataxia telangiectasia heterozygotes, a cancer prone population. *Nature* 274: 484-6.

Cheng YH, Wong EW, and Cheng CY. (2011) Cancer/testis (CT) antigens, carcinogenesis and spermatogenesis. *Spermatogenesis* 1: 209-20.

Chinchore Y, Gerber GF, and Dolph PJ. (2012) Alternative pathway of cell death in *Drosophila* mediated by NF-κB transcription factor Relish. *Proc Natl Acad Sci U S A* 109: E605-E612.

Chow LM, Zhang J, and Baker SJ. (2008) Inducible Cre recombinase activity in mouse mature astrocytes and adult neural precursor cells. *Transgenic Res* 17: 919-28.

Colton CA and Gilbert DL. (1987) Production of superoxide anions by a CNS macrophage, the microglia. *FEBS Lett* 223: 284-8.

Costa A, Jan E, Sarnow P, and Schneider D. (2009) The Imd pathway is involved in antiviral immune responses in *Drosophila*. *PloS One* 4: e7436.

Daniel JA, Pellegrini M, Lee BS, Guo Z, Filsuf D, *et al*. (2012) Loss of ATM kinase activity leads to embryonic lethality in mice. *J Cell Biol* 198: 295-304.

De Gregorio E, Han SJ, Lee WJ, Baek MJ, Osaki T, *et al*. (2002) An immune-responsive Serpin regulates the melanization cascade in *Drosophila*. *Dev Cell* 3: 581-92.

De Gregorio E, Spellman PT, Rubin GM, and Lemaitre B. (2001) Genome-wide analysis of the *Drosophila* innate response by using oligonucleotide microarrays. *Proc Natl Acad Sci U S A* 98: 12590-5.

De Gregorio E, Spellman PT, Tzou P, Rubin GM, and Lemaitre B. (2002) The Toll and Imd pathways are the major regulators of the immune response in Drosophila. *EMBO J* 21: 2568-79.

Derheimer FA and Kastan MB. (2010) Multiple roles of ATM in monitoring and maintaining DNA integrity. *FEBS Letters* 584: 3675-81.

DiAngelo JR, Bland ML, Bambina S, Cherry S, and Birnbaum MJ. (2009) The immune response attenuates growth and nutrient storage in *Drosophila* by reducing insulin signaling. *Proc Natl Acad Sci U S A* 106: 20853-8.

Doherty J, Logan MA, Taşdemir OE, and Freeman MR. (2009) Ensheathing glia function as phagocytes in the adult Drosophila brain. *J Neurosci* 29: 4768-81.

Duncan T and Su TT. (2004) Embryogenesis: coordinating cell division with gastrulation. *Curr Biol* 14: R305-7.

Dupre A, Boyer-Chatenet L, and Gautier J. (2006) Two-step activation of ATM by DNA and the Mre11-Rad50-Nbs1 complex. *Nat Struct Mol Biol* 13: 451-7.

Dushay MS, Asling B, and Hultmark D. (1996) Origins of immunity: Relish, a compound Rel-like gene in the antibacterial defense of Drosophila. *Proc Natl Acad Sci U S A* 93: 10343-7.

Elson A, Wang Y, Daugherty CJ, Morton CC, Zhou F, *et al*. (1996) Pleiotropic defects in ataxia-telangiectasia protein-deficient mice. *Proc Natl Acad Sci U S A* 93: 13084-9.

Ephrussi A, Dickinson LK, and Lehmann R. (1991) Oskar organizes the germ plasm and directs localization of the posterior determinant nanos. *Cell* 66: 37-50.

Falck J, Coates J, and Jackson SP. (2005) Conserved modes of recruitment of ATM, ATR and DNA-PKcs to sites of DNA damage. *Nature* 434: 605-11.

Fan Y and Bergmann A. (2010) The cleaved-Caspase-3 antibody is a marker of Caspase-9-like DRONC activity in *Drosophila. Cell Death Differ* 17: 534-9.

Feddersen RM, Ehlenfeldt R, Yunis WS, Clark HB, and Orr HT. (1992) Disrupted cerebellar cortical development and progressive degeneration of Purkinje cells in SV40 T antigen transgenic animals. *Neuron* 9: 955-66.

Fernandez NQ, Grosshans J, Goltz JS, and Stein D. (2001) Separable and redundant regulatory determinants in Cactus mediate its dorsal group dependent degradation. *Development* 128: 2963-74.

Fernandez-Funez P, Nino-Rosales M, de Gouyon B, She W-C, Luchak JM, *et al*. (2000) Identification of genes that modify ataxin-1-induced neurodegeneration. *Nature* 408: 101-6.

Ferrandon D, Jung AC, Criqui M, Lemaitre B, Uttenweiler-Joseph S, *et al*. (1998) A drosomycin-GFP reporter transgene reveals a local immune response in Drosophila that is not dependent on the Toll pathway. *EMBO J* 17: 1217-27.

Finelli A, Kelkar A, Song HJ, Yang H, and Konsolaki MA. (2004) A model for studying Alzheimer's Abeta42-induced toxicity in Drosophila melanogaster. *Mol Cell Neurosci* 26: 365-75.

Gatti RA, Berkel I, Boder E, Braedt G, Charmley P, *et al*. (1988) Localization of an ataxia telangiectasia gene to chromosome 11q22-23. *Nature* 336: 577-80.

Georgel P, Naitza S, Kappler C, Ferrandon D, Zachery D, *et al*. (2001) Drosophila immune deficiency (IMD) is a death domain protein that activates antibacterial defense and can promote apoptosis. *Dev Cell* 1: 503-14.

Georlette D, Ahn S, MacAlpine DM, Cheung E, Lewis PW, *et al*. (2007) Genomic profiling and expression studies reveal both positive and negative activities for the *Drosophila* Myb MuvB/dREAM complex in proliferating cells. *Genes Dev* 21: 2880-96.

Ghosh S and Feany MB. (2004) Comparison of pathways controlling toxicity in the eye and brain in Drosophila mutants of human neurodegenerative diseases. *Hum Mol Genet* 13: 2011-8.

Gilad S, Khosravi R, Shkedy D, Uziel T, Ziv Y, *et al*. (1996) Predominance of null mutations in ataxia telangiectasia. *Hum Mol Genet* 5: 433-9.

Gilboa L, Forbes A, Tazuke SI, Fuller MT, and Lehmann R. (2003) Germ line stem cell differentiation in *Drosophila* requires gap junctions and proceeds via an intermediate state. *Development* 130: 6625-34.

Glenn LE and Searles LL. (2001) Distinct domains mediate the early and late functions of the *Drosophila* ovarian tumor proteins. *Mech Dev* 102: 181-91.

Gong S, Doughty M, Harbaugh CR, Cummins A, Hatten ME, *et al*. (2007) Targeting Cre recombinase to specific neuron populations with bacterial artificial chromosome constructs. *J Neurosci* 27: 9817-23.

González-Scarano F and Baltuch G. (1999) Microglia as mediators of inflammatory and degenerative diseases. *Annu Rev Neurosci* 22: 219-40.

Goshima G, Wollman R, Goodwin SS, Zhang N, Scholey JM, *et al*. (2007) Genes required for mitotic spindle assembly in Drosophila S2 cells. *Science* 316: 417-21

Graveley BR, Brooks AN, Carlson JW, Duff MO, Landolin JM, *et al.* (2011) The developmental transcriptome of *Drosophila melanogaster. Nature* 471: 473-9.

Greene JC, Whitworth AJ, Kuo I, Andrews LA, Feany MB, *et al*. (2003) Mitochondrial pathology and apoptotic muscle degeneration in Drosophila parkin mutants. *Proc Natl Acad Sci U S A* 100: 4078-83.

Greene JC, Whitworth AJ, Andrews LA, Parker TJ, and Pallanck LJ. (2005) Genetic and genomic studies of Drosophila parkin mutants implicate oxidative stress and innate immune responses in pathogenesis. *Hum Mol Genet* 14: 799-811.

Greeve I, Kretzschmar D, Tschape JA, Beyn A, Brellinger C, *et al*. (2004) Age-dependent neurodegeneration and Alzheimer-amyloid plaque formation in trnasgenic Drosophila. *J Neurosci* 24: 3899-906.

Gumy-Pause F, Wacker P, and Sappino AP. (2004) *ATM* gene and lymphoid malignancies. *Leukemia* 18: 238-42.

Gupta SC, Sundaram C, Reuter S, and Aggarwal BB. (2010) Inhibiting NF-kB activation by small molecules as a therapeutic strategy. *Biochim Biophys Acta* 1799: 775-87.

Halle A, Hornung V, Petzold GC, Stewart CR, Monks BG, *et al*. (2008) The NALP3 inflammasome is involved in the innate immune response to amyloid-beta. *Nat Immunol* 9: 847-56.

Halliday GM and Stevens CH. (2011) Glia: intiators and progressors of pathology in Parkinson's disease. *Mov Disord* 26: 6-17.

Han SH, Ryu JH, Oh CT, Nam KB, Nam HJ, *et al.* (2004) The moleskin gene product is essential for Caudal-mediated constitutive antifungal Drosomycin gene expression in *Drosophila* epithelia. *Insect Mol Biol* 13: 323-7.

Hari KL, Santerre A, Sekelsky JJ, McKim KS, Boyd JB, *et al*. (1995) The mei-41 gene of D. melanogaster is a structural and functional homolog of the human ataxia telangiectasia gene. *Cell* 82: 815-21.

Hartenstein V. (2011) Morphological diversity and development of glia in *Drosophila*. *Glia* 59: 1237-52.

Hassin-Baer S, Bar-Shira A, Gilad S, Galanty Y, Khosravi R, *et al*. (1999) Absence of mutations in ATM, the gene responsible for ataxia telangiectasia in patients with cerebellar ataxia. *J Neurol* 246: 716-9.

Hedengren M, Asling B, Dushay MS, Ando I, Ekengren S, *et al.* (1999) Relish, a central factor in the control of humoral but not cellular immunity in *Drosophila*. *Mol Cell* 4: 827-37.

Herculano-Houzel S. (2009). The human brain in numbers: a linearly scaled-up primate brain. *Front Hum Neurosci* 3: 31.

Herrup K and Busser JC. (1995) The induction of multiple cell cycle events precedes target-related neuronal death. *Development* 121: 2385-95.

Herrup K and Yang Y. (2007) Cell cycle regulation in the postmitotic neuron: oxymoron or new biology? *Nat Rev Neurosci* 8: 368-78.

Hidalgo A, Kato K, Sutcliffe B, McIlroy G, Bishop S, *et al*. (2011) Trophic neuron-glia interactions and cell number adjustments in the fruit fly. *Glia* 59: 1296-303.

Hu X, Yagi Y, Tanji T, Zhou S, and Ip YT. (2004) Multimerization and interaction of Toll and Spätzle in Drosophila. *Proc Natl Acad Sci U S A* 101: 9369-74.

Ilieva H, Polymenidou M, and Cleveland DW. (2009) Non-cell autonomous toxicity in neurodegenerative disorders: ALS and beyond. *J Cell Biol* 187: 761-72.

Imler J-L and Bulet P. (2005) Antimicrobial peptides in Drosophila: structures, activities, and gene regulation. *Chem Immunol Allergy* 86: 1-21.

Ip YT, Reach M, Engstrom Y, Kadalayil L, Cai H, *et al*. (1993) *Dif*, a *dorsal*-related gene that mediates an immune response in *Drosophila*. *Cell* 75: 753-63.

Irving P, Troxler L, Heuer TS, Belvin M, Kopczynski C, *et al*. (2001) A genome-wide analysis of immune responses in *Drosophila*. *Proc Natl Acad Sci U S A* 98: 15119-24.

Jackson GR, Salecker I, Dong X, Yao X, Arnheim N, *et al*. (1998) Polyglutamine-expanded human huntingtin transgenes induce degeneration of *Drosophila* photoreceptor neurons. *Neuron* 21: 633-42.

Jackson SP. (2002) Sensing and repairing DNA double-strand breaks. *Carcinogenesis* 23: 687-96.

Janic A, Mendizabal L, Llamazares S, Rossell D, and Gonzalez C. (2010) Ectopic expression of germline genes drives malignant brain tumor growth in *Drosophila*. *Science* 330: 1824-7.

Jiang X, Sun Y, Chen S, Roy K, and Price BD. (2006) The FATC domains of PIKK proteins are functionally equivalent and participate in the Tip60-dependent activation of DNA-PKcs and ATM. *J Biol Chem* 281: 15741-6.

Jin JJ, Kim HD, Maxwell JA, Li L, and Fukuchi K. (2008) Toll-like receptor 4-dependent upregulation of cytokines in a transgenic mouse model of Alzheimer's disease. *J Neuroinflammation* 5: 23.

Joyce EF, Pedersen M, Tiong S, White-Brown SK, Paul A, *et al*. (2011) *Drosophila* ATM and ATR have distinct activities in the regulation of meiotic DNA damage and repair. *J Cell Biol* 195: 359-67.

Kamada S, Kikkawa U, Tsujimoto Y, and Hunter T. (2005) Nuclear translocation of caspase-3 is dependent on its proteolytic activation and recognition of a substrate-like protein(s). *J Biol Chem* 280: 857–60.

Kaneko T, Yano T, Aggarwal K, Lim JH, Ueda K, *et al*. (2006) PGRP-LC and PGRP-LE have essential yet distinct functions in the *Drosophila* immune response to monomeric DAP-type peptidoglycan. *Nat Immunol* 7: 715-23.

Kato K, Awasaki T, and Ito K. (2009) Neuronal programmed cell death induces glial cell division in the adult *Drosophila* brain. *Development* 136: 51-9.

Kato K, Forero MG, Fenton JC, and Hildago A. (2011) The glial regenerative response to central nervous system injury is enabled by pros-notch and pros-NFκB feedback. *PLoS Biol* 9: e1001133.

Katzenberger RJ, Marengo MS, and Wassarman DA. (2006) ATM and ATR pathways signal alternative splicing of Drosophila TAF1 pre-mRNA in response to DNA damage. *Mol Cell Biol* 26: 9256-67.

Kranenburg O, ven der Eb AJ, and Zantema A. (1996) Cyclin D, is an essential mediator of apoptotic neuronal cell death. *EMBO J* 15: 46-54.

Kretzschmar D, Hasan G, Sharma S, Heisenberg M, and Benzer S. (1997) The swiss cheese mutant causes glial hyperwrapping and brain degeneration in Drosophila. *J Neurosci* 17: 7425-32.

Kretzschmar D, Tschäpe J, Bettencourt Da Cruz A, Asan E, Poeck B, *et al*. (2004) Glial and neuronal expression of polyglutamine proteins induce behavioral changes and aggregate formation in *Drosophila*. *Glia* 49: 59-72.

Kuljis RO, Chen G, Lee EY, Aguila MC, and Xu Y. (1999) ATM immunolocalization in mouse neuronal endosomes: implications for ataxia-telangiectasia. *Brain Res* 842: 351-8.

Kuljis RO, Xu Y, Aguila MC, and Baltimore D. (1997) Degeneration of neurons, synapses, and neuropil and glial activation in a murine Atm knockout model of ataxia-telangiectasia. *Proc Natl Acad Sci U S A* 94: 12688-93.

Kruman IL, Wersto RP, Cardozo-Pelaez F, Smilenov, L, Chan SL, *et al*. (2004) Cell cycle activation linked to neuronal cell death initiated by DNA damage. *Neuron* 41: 549-61.

Landreth GE and Reed-Geaghan EG. (2009) Toll-like receptors in Alzheimer's disease. *Curr Top Microbiol Immunol* 336: 137-53.

Lavin MF. (2008) Ataxia-telangiectasia: from a rare disorder to a paradigm for cell signaling and cancer. *Nat Rev Mol Cell Biol* 9: 759-69.

Lavin MF, Delia D, and Chessa L. (2006) ATM and the DNA damage response. *EMBO Rep* 7: 154-60.

Lavin MF, Gueven N, Bottle S, and Gatti RA. (2007) Current and potential therapeutic strategies for the treatment of ataxia-telangiectasia. *Br Med Bull* 81 and 82: 129-47.

Lee LA, Van Hoewyk D, and Orr-Weaver TL. (2003) The *Drosophila* cell cycle kinase Pan Gu forms an active complex with Plutonium and Gnu to regulate embryonic divisions. *Genes Dev* 17: 2979-91.

Lee EJ, Banerjee S, Zhou H, Jammalamadaka A, Arcila M, *et al*. (2011) Identification of piRNAs in the central nervous system. *RNA* 17: 1090-9.

Lee JH and Paull TT. (2004) Direct activation of the ATM protein kinase by the Mre11/Rad50/Nbs1 complex. *Science* 304: 93-6.

Lee JH and Paull TT. (2005) ATM activation by DNA double-stranded breaks through the Mre11-Rad50-Nbs1 complex. *Science* 308: 551-4.

Lee SJ. (2008) Origins and effects of extracellular alpha-synuclein: implications in Parkinson's disease. *J Mol Neurosci* 34: 17-22.

Lee YS and Carthew RW. (2003) Making a better RNAi vector for Drosophila: use of intron spacers. *Methods* 30: 322-9.

Lefton-Greif MA, Crawford TO, Winkelstein JA, Loughlin GM, Koerner CB, *et al*. (2000) Oropharyngeal dysphagia and aspiration in patients with ataxia-telangiectasia. *J Pediatr* 136: 225-31.

Lemaitre B and Hoffmann J. (2007) The host defense of Drosophila melanogaster. *Annu Rev Immunol* 25: 697-743.

Lemaitre B, Kromer-Metzger E, Michaut L, Nicolas E, Meister M, *et al*. (1995) A recessive mutation, immune deficiency (imd), defines two distinct control pathways in the Drosophila host defense. *Proc Natl Acad Sci U S A* 92: 9465-9.

Lemaitre B, Nicolas E, Michaut L, Reichhart JM, and Hoffmann JA. (1996) The dorsoventral regulatory gene cassette spätzle/Toll/cactus controls the potent antifungal response in Drosophila adults. *Cell* 86: 973-83.

Lempiäinen H and Halazonetis TD. (2009) Emerging common themes in regulation of PIKKs and PI3Ks. *EMBO J* 28: 3067-73.

Lehnardt S. (2010) Innate immunity and neuroinflammation in the CNS: the role of microglia in Toll-like receptor-mediated neuronal injury. *Glia* 58: 253-63.

Lessing D and Bonini NM. (2009) Maintaining the brain: insight into human neurodegeneration from *Drosophila melanogaster* mutants. *Nat Rev Genet* 10: 359-70.

Leulier F, Rodriguez A, Khush RS, Abrams JM, and Lemaitre B. (2000) The *Drosophila* caspase Dredd is required to resist Gram-negative bacterial infection. *EMBO Rep* 1: 353-8.

Levashina EA, Ohresser S, Lemaitre B, and Imler JL. (1998) Two distinct pathways can control expression of the gene encoding the Drosophila antimicrobial peptide methnikowin. *J Mol Biol* 278: 515-27.

Lewis PW, Beall EL, Fleischer TC, Georlette D, Link AJ, *et al*. (2004) Identification of a *Drosophila* myb-E2F2/RBF transcription repressor complex. *Genes Dev* 18: 2929-40.

Liu B, Gao HM, Wang JY, Jeohn GH, Cooper CL, *et al*. (2002) Role of nitric oxide in inflammation-mediated neurodegeneration. *Ann N Y Acad Sci* 962: 318-31.

Liu N, Stoica G, Yan M, Scofield VL, Qiang W, *et al*. (2005) ATM deficiency induces oxidative stress and endoplasmic reticulum stress in astrocytes. *Lab Invest* 85: 1471-80.

Lu Y, Wu LP, and Anderson KV. (2001) The anti-bacterial arm of the Drosophia innate immune response requires an IkB kinase. *Genes Dev* 15: 104-10.

Lucin KM and Wyss-Coray T. (2009) Immune activation in brain aging and neurodegeneration: too much or too little? *Neuron* 64: 110-22.

Luo L, Liao YJ, Jan LY, and Jan YN. (1994) Distinct morphogenetic functions of similar small GTPases: *Drosophila* Drac1 is involved in axonal outgrowth and myoblast fusion. *Genes Dev* 8: 1787-802.

Maezawa I, Zimin PI, Wulff H, and Jin LW. (2011) Amyloid-beta protein oligomer at low nanomolar concentrations activates microglia and induces microglial toxicity. *J Biol Chem* 286: 3693-706.

Markussen FH, Michon AM, Breitwieser W, and Ephrussi A. (1995) Translational control of oskar generates short OSK, the isoform that induces pole plasma assembly. *Development* 121: 3723-32.

Martinon F and Tschopp J. (2004) Inflammatory caspases: linking an intracellular innate immune system to auto-inflammatory diseases. *Cell* 117: 561-74.

Matsuoka S, Rotman G, Ogawa A, Shiloh Y, Tamai K, *et al*. (2000) Ataxia telangiectasia-mutated phosphorylates Chk2 *in vivo* and *in vitro*. *Proc Natl Acad Sci* 97: 10389-94.

Matsuoka S, Ballif BA, Smogorzewska A, McDonald ER 3rd, Hurov KE, *et al.* (2007) ATM and ATR substrate analysis reveals extensive protein networks responsive to DNA damage. *Science* 316: 1160-6.

McConville CM, Stankovic T, Byrd PJ, McGuire GM, Yao Q, *et al*. (1996) Mutations associated with variant phenotypes in ataxia-telangiectasia. *Am J Hum Genet* 59: 320-30.

McDonald MJ and Roshbash M. (2001) Microarray analysis and organization of circadian gene expression in *Drosophila*. *Cell* 107: 567-78.

McGrath-Morrow SA, Gower WA, Rothblum-Oviatt C, Brody AS, Langston C, *et al*. (2010) Elevated serum IL-8 levels in ataxia telangiectasia. *J Pediatr* 156: 682-4.

McKinnon PJ. (2004) ATM and ataxia telangiectasia. *EMBO Rep* 5: 772-6.

McKinnon PJ. (2012) ATM and the molecular pathogenesis of ataxia telangiectasia. *Ann Rev Pathol Mech Dis* 7: 303-21.

Meier K, Mathieu EL, Finkernagel F, Reuter LM, Scharfe M, *et al*. (2012) LINT, a novel dL(3)mbt-containing complex, represses malignant brain tumour signature genes. *PLoS Genet* 8: e1002676.

Metcalfe JA, Parkhill J, Campbell L, Stacey M, Biggs P, *et al*. (1996) Accelerated telomere shortening in ataxia telangiectasia. *Nat Genet* 20: 203-6.

Miller RL, James-Kracke M, Sun GY, and Sun AY. (2009) Oxidative and inflammatory pathways in Parkinson's disease. *Neurochem Res* 34: 55-65.

Miyamoto S. (2011) Nuclear initiated NF-κB signaling: NEMO and ATM take center stage. *Cell Res* 21: 116-30.

Möller T. (2010) Neuroinflammation in Huntington's disease. *J Neural Transm* 117: 1001-8.

Morales I, Farias G, and Maccioni RB. (2010) Neuroimmunomodulation in the pathogenesis of Alzheimer's disease. *Neuroimmunomodulation* 17: 202-4.

Musacchio A and Salmon ED. (2007) The spindle-assembly checkpoint in space and time. *Nat Rev Mol Cell Biol* 8: 379-93

Mutsuddi M, Marshall CM, Benzow KA, Koob MD, and Rebay I. (2004) The spinocerebellar ataxia 8 noncoding RNA causes neurodegeneration and associates with staufen in Drosophila. *Curr Biol* 14: 302-8.

Nagoshi RN, Patton JS, Bae E, and Geyer PK. (1995) The somatic sex determines the requirement for ovarian tumor gene activity in the proliferation of the *Drosophila* germline. *Development* 121: 579-87.

Neufeld TP, de la Cruz AF, Johnston LA, and Edgar BA. (1998) Coordination of growth and division in the Drosophila wing. *Cell* 93: 1183-93.

Nowak-Wegrzyn A, Crawford TO, Winkelstein JA, Carson KA, and Lederman HM. (2004) Immunodeficiency and infections in ataxia-telangiectasia. *J Pediatr* 144: 505-11.

Oikemus SR, McGinnis N, Queiroz-Machado J, Tukachinsky H, Saeko T, *et al*. (2004) *Drosophila atm*/*telomere fusion* is required for telomeric localization of HP1 and telomere position effect. *Genes Dev* 18: 1850-61.

Oka A and Takashima S. (1998) Expression of the ataxia-telangiectasia gene (*ATM*) product in in human cerebellar neurons during development. *Neurosci Lett* 252: 195-8.

Ollmann M, Young LM, DiComo CJ, Karim F, Belvin M, *et al*. (2000*) Drosophila* p53 is a structural and functional homolog of the tumor suppressor p53. *Cell* 101: 91-101.

Owens T. (2009) Toll-like receptors in neurodegeneration. *Curr Top Microbiol Immunol* 336: 105-20.

Pandey UB and Nichols CD. (2011) Human disease models in *Drosophila melanogaster* and the role of the fly in therapeutic drug discovery. *Pharmacol Rev* 63: 411-36.

Pandita TK. (2002) ATM function and telomere stability. *Oncogene* 21: 611-8.

Pandita TK, Pathak S, and Geard CR (1995) Chromosome end associations, telomeres and telomerase activity in ataxia telangiectasia cells. *Cytogenet Cell Genet* 71: 86-93.

Parkhurst CN and Gan WB. (2010) Microglia dynamics and function in the CNS. *Curr Opin Neurobiol* 20: 595-600.

Paur I, Balstad TR, Kolberg M, Pedersen MK, Austenaa LM, *et al*. (2010) Extract of oregano, coffee, thyme, clove, and walnuts inhibits NF-kB in monocytes and in transgenic reporter mice. *Cancer Prev Res* 3: 653-63.

Pedersen M, Tiong S, and Campbell SD. (2010) Molecular genetic characterization of Drosophila ATM conserved functional domains. *Genome* 53: 778-86.

Peng J, Zipperlen P, and Kubli E. (2005) *Drosophila* sex peptide stimulates female innate immune system after mating via the Toll and Imd pathways. *Curr Biol* 15: 1690-4.

Peppel K, Crawford D, and Beutler B. (1991) A tumor necrosis factor (TNF) receptor-IgG heavy chain chimeric protein as a bivalent antagonist of TNF activity. *J Exp Med* 174: 1483-9.

Pereanu W, Kumar A, Jennett A, Reichert H, and Hartenstein V. (2010) Development-based compartmentalization of the Drosophila central brain. *J Comp Neurol* 518: 2996-3023.

Petersen AJ, Rimkus SA, and Wassarman DA. (2012) ATM kinase inhibition in glial cells activates the innate immune response and causes neurodegeneration in *Drosophila. Proc Natl Acad Sci* 109: E656-64.

Petersen AJ and Wassarman DA. (2012) *Drosophila* innate immune response pathways moonlight in neurodegeneration. *Fly* 6: 169-72.

Philips T and Robberecht W. (2011) Neuroinflammation in amyotrophic lateral sclerosis: role of glial activation in motor neuron disease. *Lancet Neurol* 10: 253-63.

Plun-Favreau H, Lewis PA, Hardy J, Martins LM, and Wood NW. (2010) Cancer and neurodegeneration: Between the devil and the deep blue sea. *PLoS Genet* 6: e1001257.

Pokrywka NJ, Meng L, Debiec K, and Stephenson EC. (2004) Identification of hypomorphic and null alleles of swallow via molecular and phenotypic analyses. *Dev Genes Evol* 214: 185-92.

Rajasethupathy P, Antonov I, Sherian R, Frey S, Sander C, *et al*. (2012) A role for neuronal piRNAs in the Epigenetic control of memory-related synaptic plasticity. *Cell* 149: 693-707.

Ransohoff RM and Brown MA. (2012) Innate immunity in the central nervous system. *J Clin Invest* 122: 1164-71.

Reinhardt HC and Yaffe MB. (2009) Kinases that control the cell cycle in response to DNA damage: Chk1, Chk2, and MK2. *Curr Opin Cell Biol* 21: 245-55.

Reiter LT, Potocki L, Chien S, Gribskov M, and Bier E. (2001) A systematic analysis of human disease-associated gene sequences in *Drosophila melanogaster Genome Res* 11: 1114-25.

Reynolds AD, Kadiu I, Garg SK, Glanzer JG, Nordgren T, *et al*. (2008) Nitrated alpha-synuclein and microglial neuroregulatory activities. *J Neuroimmune Pharmacol* 3: 59-74.

Richard KL, Filali M, Prefontaine P, and Rivest S. (2008) Toll-like receptor 2 acts as a natural innate immune receptor to clear amyloid beta 1-42 and delay the cognitive deline in a mouse model of Alzheimer's disease. *J Neurosci* 28: 5784-93.

Richter C, Oktaba K, Steinmann J, Müller J, and Knoblich JA. (2011) The tumour suppressor L(3)mbt inhibits neuroepithelial proliferation and acts on insulator elements. *Nat Cell Biol* 13: 1029-39.

Rimkus SA, Katzenberger RJ, Trinh AT, Dodson GE, Tibbetts RS, *et al*. (2008) Mutations in String/CDC25 inhibit cell cycle re-entry and neurodegeneration in a Drosophila model of Ataxia telangiectasia. *Genes Dev* 22: 1205-20.

Rimkus SA, Petersen AJ, Katzenberger RJ, and Wassarman DA. (2010) The effect of ATM knockdown on ionizing radiation-induced neuronal cell cycle reentry in *Drosophila*. *Cell Cycle* 9:1-2.

Rivera-Calzada A, Maman JD, Spagnolo L, Pearl LH, and Llorca O. (2005) Three-dimensional structure and regulation of the DNA-dependent protein kinase catalytic subunit (DNA-PKcs). *Structure* 13: 243-55.

Robinow S and White K. (1999) Characterization and spatial distribution of the ELAV protein during Drosophila melanogaster development. *J Neurobiol* 22: 443-61.

Rogakou EP, Pilch DR, Orr AH, Ivanova VS, and Bonner WM. (1998) DNA double-stranded breaks induce histone H2AX phosphorylation on serine 139. *J Biol Chem* 273: 5858-68.

Rongo C, Gavis ER, and Lehmann R. (1995) Localization of *oskar* RNA regulates oskar translation and requires Oskar protein. *Development* 121: 2737-46.

Roodveldt C, Christodoulou J, and Dobson CM. (2008) Immunological features of alpha-synuclein in Parkinson's disease. *J Cell Mol Med* 12: 1820-9.

Ros-Bernal F, Hunot S, Herrero MT, Parnadeau S, Corvol JC, *et al*. (2011) Microglial glucocorticoid receptors play a pivotal role in regulating dopaminergic neurodegeneartion in parkinsonism. *Proc Natl Acad Sci U S A* 108: 6632-7.

Rubin GM and Spradling AC. (1982) Genetic transformation of *Drosophila* with transposable element vectors. *Science* 218: 348-53.

Rutschmann S, Jung AC, Hetru C, Reichhart JM, Hoffmann JA, *et al.* (2000a) The Rel protein DIF mediates the antifungal but not the antibacterial host defense in *Drosophila*. *Immunity* 12: 569-80.

Rutschmann S, Jung AC, Zhou R, Silverman N, Hoffmann JA, *et al*. (2000b) Role of Drosophila IKK gamma in a toll-independent antibacterial immune response. *Nat Immunol* 1: 342-7.

Ryu JH, Nam KB, Oh CT, Nam HJ, Kim SH, *et al.* (2004) The homeobox gene *Caudal* regulates constitutive local expression of antimicrobial peptide genes in *Drosophila* epithelia. *Mol Cell Biol* 24: 172-85.

Sackton TB, Lazzaro BP, Schlenke TA, Evans JD, Hultmark D, *et al*. (2007) Dynamic evolution of the innate immune system in *Drosophila*. *Nat Genet* 39: 1461-68.

Salminen A, Ojala J, Kauppinen A, Kaarniranta K, and Suuronen T. (2009) Inflammation in Alzheimer's disease: amyloid-beta oligomers trigger innate immunity defence via pattern recognition receptors. *Prog Neurobiol* 87: 181-94.

Salminen A, Ojala J, Suuronen T, Kaarinaranta K, and Kauppinen A. (2008) Amyloid-beta oligomers set fire to inflammasomes and induce Alzheimer's pathology. *J Cell Mol Med* 12: 2255-62.

Satterfield TF, Jackson SM, and Pallanck LJ. (2002) A Drosophila homolog of the polyglutamine disease gene SCA2 is a dosage-sensitive regulator of actin filament formation. *Genetics* 162: 1687-702.

Savitsky K, Bar-Shira A, Gilad S, Rotman G, Ziv Y, *et al*. (1995) A single ataxia telangiectasia gene with a product similar to PI-3 kinase. *Science* 268: 1749-53.

Sedgwick RP and Boder E. (1960) Progressive ataxia in childhood with particular reference to ataxia-telangiectasia. *Neurology* 10: 705–15.

Sekelsky JJ, Brodsky MH, and Burtis KC. (2000) DNA repair in Drosophila: insights from the Drosophila genome sequence. *J Cell Biol* 150: F31-6.

Senger K, Harris K, and Levine M. (2006) GATA factors participate in tissue-specific immune responses in Drosophila larvae. *Proc Natl Acad Sci U S A* 103: 15957-62.

Sepp KJ, Schulte J, and Auld VJ. (2001) Peripheral glia direct axon guidance across the CNS/PNS transition zone. *Dev Biol* 238: 47-63.

Shi Y, Venkataraman SL, Dodson GE, Mabb AM, LeBlanc S, *et al*. (2004) Direct regulation of CREB transcriptional activity by ATM in response to genotoxic stress. *Proc Natl Acad Sci* 101: 5898-903.

Shieh SY and Bonini NM. (2011) Genes and pathways affected by CAG-repeat RNA-based toxicity in *Drosophila*. *Hum Mol Genet* 20: 4810-21.

Shiloh Y. (2003) ATM and related protein kinases: safeguarding genome integrity. *Nat Rev Genet* 3: 155-68.

Silva E, Tiong S, Pederson M, Homola E, Royou A, *et al*. (2004) ATM is required for telomere maintenance and chromosomal stability during *Drosophila* development. *Curr Biol* 14: 1341-7.

Silverman N, Zhou R, Erlich RL, Hunter M, Bernstein E, *et al*. (2003) Immune activation of NF-κB and JNK requires *Drosophila* TAK1. *J Biol Chem* 278: 48928-34.

Silverman N, Zhou R, Stöven S, Pandey N, Hultmark D, *et al*. (2000) A *Drosophila* IκB kinase complex required for Relish cleavage and antibacterial immunity. *Genes Dev* 14: 2461-71.

Snee MJ and Macdonald PM. (2009) Bicaudal C and trailer hitch have similar roles in gurken mRNA localization and cytoskeletal organization. *Dev Biol* 328: 434-44.

Soller M and White K. (2004) ELAV. *Curr Biol* 14: R53.

Somma MP, Ceprani F, Bucciarelli E, Naim V, De Arcangelis V, *et al*. (2008) Identification of Drosophila mitotic genes by combining co-expression analysis and RNA interference. *PLoS Genet* 4: e1000126

Song Y-H, Mirey G, Betson M, Haber DA, and Settleman J. (2004) The *Drosophila* ATM ortholog, dATM, mediates the response to ionizing radiation and to spontaneous DNA damage during development. *Curr Biol* 14: 1354-9.

Spring K, Cross S, Li C, Watters D, Ben-Senior L, *et al.* (2001) Atm knock-in mice harbor an in-frame deletion corresponding to the human *ATM 7636del9* common mutation exhibit a variant phenotype. *Cancer Res* 61: 4561-8.

Steffan JS, Bodai L, Pallos J, Poelman M, McCampbell A, *et al*. (2001) Histone deacetylase inhibitors arrest polyglutamine-dependent neurodegeneration in *Drosophila*. *Nature* 413: 739-43.

Stewart GS, Maser RS, Stankovic T, Bressan DA, Kaplan MI, *et al*. (1999) The DNA double-strand break repair gene hMRE11 is mutated in individuals with an ataxia-telangiectasia-like disorder. *Cell* 99: 577-87.

Stork T, Bernardos R, and Freeman MR. (2012) Analysis of glial cell development and function in *Drosophila*. *Cold Spring Harbor Protoc* 1: 1-17.

Stöven S, Ando I, Kadalayil L, Engström Y, and Hultmark D. (2000) Activation of the Drosophila NF-kappaB factor Relish by rapid endoproteolytic cleavage. *EMBO Rep* 1: 347-52.

Stöven S, Silverman N, Junell A, Hedengren-Olcott M, Erturk D, *et al*. (2003) Caspase-mediated processing of the *Drosophila* NF-κB factor Relish. *Proc Natl Acad Sci U S A* 100: 5991-6.

Stutz A, Golenbock DT, and Latz E. (2009) Inflammasomes: too big to miss. *J Clin Invest* 119: 3502-11.

Sun H, Bristow BN, Qu G, and Wasserman SA. (2002) A heterotrimeric death domain complex in Toll signaling. *Proc Natl Acad Sci U S A* 99: 12871-6.

Sun SC, Ganchi PA, Ballard DW, and Greene WC. (1993) NF-kappa B controls expression of inhibitor I kappa B alpha: evidence for an inducible autoregulatory pathway. *Science* 259: 1912-5.

Syllaba K and Henner K. (1926) Contribution a l'independence de l'athetose double idiopathique et congenitale. Atteinte familiale, syndrome dystrophique, signe de reseau vasculaire conjonctival, integrite psychique. *Rev Neurol* 1: 541-62. (in French)

Tamura T, Sone M, Yamashita M, Wanker E, and Okazawa H. (2009) Glial cell lineage expression of mutant Ataxin-1 and Huntingtin induces developmental and late-onset neuronal pathologies in *Drosophila* models. *PLoS One* 1: e4262.

Tan L, Schedl P, Song HJ, Garza D, and Konsolaki M. (2008) The Toll-->NFkappaB signaling pathway mediates the neuropathological effects of the human Alzheimer's Abeta42 polypeptide in Drosophila. *PLoS One* 3: e3966.

Tauchi H, Matsuura S, Kobayashi J, Sakamoto S, and Komatsu K. (2002) Nijmegen breakage syndrome gene, NBS1, and molecular links to factors for genome stability. *Oncogene* 21: 8967-80.

Tauszig-Delamasure S, Bilak H, Capovilla M, Hoffmann JA, and Imler JL. (2002) *Drosophila* MyD88 is required for the response to fungal and Gram-positive bacterial infections. *Nat Immunol* 3: 91-7.

Taylor K and Kimbrell DA. (2007) Host immune response and differential survival of the sexes in *Drosophila*. *Fly* 1: 197-204.

Taylor WR and Stark GR. (2001) Regulation of the G2/M transition by p53. *Oncogene* 20: 1803-15.

Telatar M, Teraoka S, Wang Z, Chun HH, Liang T, *et al*. (1998) Ataxia-telangiectasia: identification and detection of founder-effect mutations in the ATM gene in ethnic populations. *Am J Hum Genet* 62: 86-97.

Ten RM, Paya CV, Israël N, Le Bail O, Mattei MG, *et al*. (1992) The characterization of the promoter of the gene encoding the p50 subunit of NF-kappa B indicates that it participates in its own regulation. *EMBO J* 11: 195-203.

Tzou P, Ohresser S, Ferrandon D, Capovilla M, Reichhart JM, *et al*. (2000) Tissue-specific inducible expression of antimicrobial peptide genes in Drosophila surface epithelia. *Immunity* 13: 737-48.

van der Bosch M, Bree RT, and Lowndes NF. (2003) The MRN complex: coordinating and mediating the response to broken chromosomes. *EMBO Rep* 4: 844-9.

von Trotha JW, Egger B, and Brand AH. (2009) Cell proliferation in the adult *Drosophila* adult brain revealed by clonal analysis and bromodeoxyuridine labeling. *Neural Dev* 4: 9.

Wang S and Hazelrigg T. (1994) Implications for bcd mRNA localization from spatial distribution of exu protein in *Drosophila* oogenesis. *Nature* 369: 400-3.

Wang Z and Lin H. (2004) Nanos maintains germline stem cell self-renewal by preventing differentiation. *Science* 303: 2016-9.

Warrick JM, Paulson HL, Gray-Board GL, Bui QT, Fischbeck KH, *et al*. (1998) Expanded polyglutamine protein forms nuclear inclusions and causes neural degeneration in *Drosophila. Cell* 93: 939-49.

Weber AN, Tauszig-Delamasure S, Hoffmann JA, Lelievre E, Gascan H, *et al*. (2003)Binding of the *Drosophila* cytokine Spätzle to Toll is direct and establishes signaling. *Nat Immunol* 4: 794-800.

Wei Y, Mizzen CA, Cook RG, Gorovsky MA, and Allis CD (1998) Phosphorylation of histone H3 at serine 10 is correlated with chromosome condensation during mitosis and meiosis in *Tetrahymena*. *Proc Natl Acad Sci U S A* 95: 7480–4.

Werner T, Liu G, Kang D, Ekengren S, Steiner H, *et al*. (2000) A family of peptidoglycan reconition proteins in the fruit fly Drosophila melanogaster. *Proc Natl Acad Sci U S A* 97: 13772-7.

Westbrook AM and Schiestl RH. (2010) Atm-deficient mice exhibit increased sensitivity to dextran sulfate sodium-induced colitis characterized by elevated DNA damage and persistent immune activation. *Cancer Res* 70: 1875-84.

White JE, Southgate E, Thomson JN, and Brenner S. (1986) The structure of the nervous system of the nematode *Caenorhabditis elegans*. *Phil Trans R Soc Lond B* 314:1–340.

Wiklund M-L, Steinert S, Junell A, Hultmark D, and Stöven S. (2009) The N-terminal half of the *Drosophila* Rel/NF-kappaB factor Relish, REL-68, constitutively activates transcription of specific Relish target genes. *Dev Comp Immunol* 33: 690–6.

Wittmann CW, Wszolek MF, Shulman JM, Salvaterra PM, Lewis J, *et al*. (2001) Tauopathy in *Drosophila*: neurodegeneration without neurofibrillary tangles. *Science* 293: 711-4.

Wu X, Shi Z, Cui M, Han M, and Ruvkun G. (2012) Repression of germline RNAi pathways in somatic cells by retinoblastoma pathway chromatin complexes. *PLoS Genet* 3: e1002542.

Xiong WC, Okano H, Patel NH, Blendy JA, and Montell C. (1994) repo encodes a glial-specific homeodomain protein required in the Drosophila nervous system. *Genes Dev* 8: 981-94.

Xu J, Xin S, and Du W. (2001) *Drosophila* Chk2 is required for DNA damage-mediated cell cycle arrest and apoptosis. *FEBS Lett* 508: 394-8.

Xu T and Rubin GM. (1993) Analysis of genetic mosaics in developing and adult Drosophila tissues. *Development* 117: 1223-37.

Xu Y, Ashley T, Brainerd EE, Bronson RT, Meyn MS, and Baltimore D. (1996) Targeted destruction of ATM leads to growth retardation, chromosomal fragmentation during meiosis, immune defects, and thymic lymphoma. *Genes Dev* 10: 2411-22.

Yamamoto K, Wang Y, Jiang W, Liu X, Dubois RL, *et al*. (2012) Kinase-dead ATM protein causes genomic instability and early embryonic lethality in mice. *J Cell Biol* 198: 305-13.

Yang Y and Herrup K. (2005) Loss of neuronal cell cycle control in ataxia-telangiectasia: a unified disease mechanism. *J Neurosci* 25: 2522-9.

Yang Z, Edenberg HJ, and Davis RL. (2005) Isolation of mRNA from specific tissues of *Drosophila* by mRNA tagging. *Nucleic Acids Res* 33: e148.

Yang Y, Gehrke S, Imai Y, Huang Z, Ouyang Y, *et al*. (2006) Mitochondrial pathology and muscle and domapinergic neuron degeneration caused by inactivation of Drosophila Pink1 is rescued by Parkin. *Proc Natl Acad Sci U S A* 103: 10793-8.

Yao KM and White K (1994) Neural specificity of elav expression: defining a Drosophila promoter for directing expression to the nervous system. *J Neurochem* 63: 41-51.

Ye B, Petritsch C, Clark IE, Gavis ER, Jan LY, *et al*. (2004) Nanos and Pumilio are essential for dendrite morphogenesis in Drosophila peripheral neurons. *Curr Biol* 14: 314-321.

You Z, Chahwan C, Bailis J, Hunter T, and Russell P. (2005) ATM activation and its recruitment to damaged DNA requires binding to the C-terminus of Nbs1. *Mol Cell Biol* 25: 5363-74.

Zaiou M. (2007) Multifunctional antimicrobial peptides: therapeutic targets in several human diseases. *J Mol Med* 85: 317-29.

Zha S, Sekiguchi J, Brush JW, Bassing CH, and Alt FW. (2008) Complementary functions of ATM and H2AX in development and suppresion of genomic instability. *Proc Natl Acad Sci U S A* 105: 9302-6.

Zhang Q, Raoof M, Chen Y, Sumi Y, Sursal T, *et al*. (2010) Circulating mitochondrial DAMPs cause inflammatory responses to injury. *Nature* 464: 104-7.

Zhang W, Wang T, Pei Z, Miller DS, Wu X, *et al*. (2005) Aggregated alpha-synuclein activates microglia: a process leading to disease progression in Parkinson's disease. *FASEB J* 19: 533-42.

Zhao Y, Haccard O, Wang R, Yu J, Kuang J, *et al*. (2008) Roles of the greatwall kinase in the regulation of cdc25 phosphatase. *Mol Biol Cell* 19: 1317-27.

Zimmerman JE, Rizzo W, Shockley KR, Raizen DM, Naidoo N, *et al*. (2006) Multiple mechanisms limit the duration of wakefulness in *Drosophila* brain. *Physiol Genomics* 27: 337-50.